



Search for the Higgs boson produced in association with a vector boson and decaying into two spin-zero particles in the $H \rightarrow aa \rightarrow 4b$ channel in pp collisions at $\sqrt{s} = 13$ TeV with the ATLAS detector

The ATLAS Collaboration

A search for exotic decays of the Higgs boson into a pair of spin-zero particles, $H \rightarrow aa$, where the a -boson decays into b -quarks promptly or with a mean proper lifetime $c\tau_a$ up to 6 mm and has a mass in the range of 20–60 GeV, is presented. The search is performed in events where the Higgs boson is produced in association with a W or Z boson, giving rise to a signature of one or two charged leptons (electrons or muons) and multiple jets from b -quark decays. The analysis is based on the dataset of proton–proton collisions at $\sqrt{s} = 13$ TeV recorded in 2015 and 2016 by the ATLAS detector at the CERN Large Hadron Collider, corresponding to an integrated luminosity of 36.1 fb^{-1} . No significant excess of events above the Standard Model background prediction is observed, and 95% confidence-level upper limits are derived for the production cross-sections for $pp \rightarrow WH$, ZH and their combination, times the branching ratio of the decay chain $H \rightarrow aa \rightarrow 4b$. For a -bosons which decay promptly, the upper limit on the combination of cross-sections for WH and ZH times the branching ratio of $H \rightarrow aa \rightarrow 4b$ ranges from 3.0 pb for $m_a = 20$ GeV to 1.3 pb for $m_a = 60$ GeV, assuming that the ratio of WH to ZH cross-sections follows the Standard Model prediction. For a -bosons with longer proper lifetimes, the most stringent limits are 1.8 pb and 0.68 pb, respectively, at $c\tau_a \sim 0.4$ mm.

1 Introduction

The discovery of the Higgs boson by the ATLAS and CMS collaborations [1, 2] at the Large Hadron Collider (LHC) has been a major achievement for the Standard Model (SM). A comprehensive programme to explore the properties of this particle is underway, including measurements of the branching ratios to SM particles and searches for decays into “exotic” or non-SM particles. Exotic Higgs boson decays are a powerful probe for physics beyond the SM (BSM). The Higgs boson has a very narrow decay width, so even a small coupling to a non-SM particle could open up a sizeable decay mode. Measurements at the LHC are in agreement with SM predictions, constraining the non-SM branching ratio of the Higgs boson to less than approximately 30% at 95% confidence level (CL) using the 7 and 8 TeV datasets [3–5]. Despite this experimental triumph, there is still ample room for exotic Higgs boson decays compatible with observations to date.

The Higgs boson has been proposed as a possible “portal” for hidden-sector particles to interact with SM particles [6–8]. Exotic decays in particular are predicted by many BSM theories [9], including those with an extended Higgs sector such as the Next-to-Minimal Supersymmetric Standard Model (NMSSM) [10–14], models with a first-order electroweak phase transition [15, 16], models with neutral naturalness [17–19] and models of dark matter [20–24].

The decay of the Higgs boson into a pair of spin-zero particles a , which in turn decay into a pair of SM particles, arises in several scenarios of new physics [9]. In particular, if the a -boson mixes with the Higgs boson and inherits its Yukawa couplings, decays of the type $a \rightarrow b\bar{b}$ are expected to be dominant for $m_a > 2m_b$. Models of this type have been used to explain the observations of a gamma-ray excess from the galactic centre by the Fermi Large Area Telescope (FermiLAT) [25, 26]. In models of neutral naturalness, the a -boson could have mean proper lifetimes ($c\tau_a$) ranging from about $10 \mu\text{m}$ to $\mathcal{O}(\text{km})$ [19]. Lifetimes smaller than $10 \mu\text{m}$ are referred to as “prompt”.

This paper considers the decay mode $H \rightarrow aa$ with the subsequent decay $a \rightarrow b\bar{b}$, building on the previous work of ref. [27], in which a similar analysis was reported with a subset of the data considered here. The previous result set an upper limit on the production cross-section $\sigma(WH)$ times the branching ratio for $H \rightarrow aa \rightarrow 4b$ ranging from 6.2 pb for an a -boson mass of $m_a = 20 \text{ GeV}$ to 1.5 pb for $m_a = 60 \text{ GeV}$, compared with the SM cross-section $\sigma_{\text{SM}}(WH) = 1.37 \text{ pb}$. This paper includes ten times more data, adds the ZH channel and an improved analysis technique.

This search focuses on the WH and ZH processes, with $W \rightarrow \ell\nu$, $Z \rightarrow \ell\ell$ ($\ell = e, \mu$) and $H \rightarrow aa \rightarrow 4b$, as shown in figure 1. The a -boson can be either a scalar or a pseudoscalar under parity transformations, since the decay mode considered in this search is not sensitive to the difference in coupling. The a -boson signals considered have masses in the range $20 \text{ GeV} \leq m_a \leq 60 \text{ GeV}$ and mean proper lifetimes, $c\tau_a$, up to 6 mm.

The resulting signature has a single lepton or two leptons accompanied by a high multiplicity of jets originating from b -quarks (b -jets). Since four b -jets are produced from the decay of the Higgs boson, they tend to have a low transverse momentum (p_T) compared with m_H and can overlap, especially for light a -bosons. Events with one or two electrons or muons, including those produced via leptonically decaying τ -leptons, are considered. The WH and ZH processes are chosen for this search because the presence of at least one charged lepton in the final state provides a powerful signature for triggering and for suppressing background from the high cross-section strong-interaction production of four b -jets.

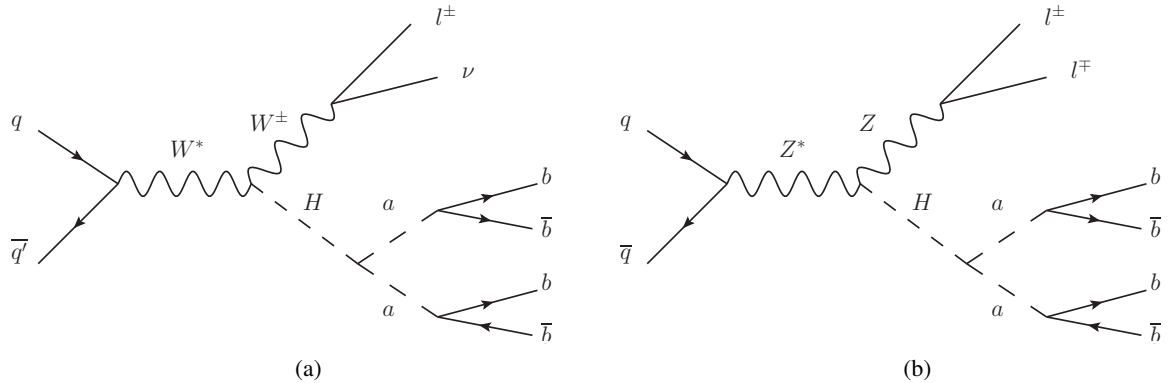


Figure 1: Representative tree-level Feynman diagrams for the (a) WH and (b) ZH production processes with the subsequent decays $W \rightarrow \ell\nu$, $Z \rightarrow \ell\bar{\ell}$ ($\ell = e, \mu$) and $H \rightarrow aa \rightarrow 4b$.

Several kinematic variables, including the reconstructed masses in the decay $H \rightarrow aa \rightarrow 4b$, are combined to identify signal events. The background estimation techniques, systematic uncertainties and statistical treatment closely follow those used in other ATLAS searches with similar signatures [28–32].

2 ATLAS detector

The ATLAS experiment [33] is a multipurpose particle physics detector with forward–backward symmetric cylindrical geometry and nearly 4π coverage in solid angle.¹ The interaction point is surrounded by an inner detector (ID) tracking system, a calorimeter system, and a muon spectrometer (MS). The ID covers $|\eta| < 2.5$ and consists of a silicon pixel detector, a silicon microstrip detector, and a transition radiation tracker. The ID includes the insertable B-layer [34], a pixel layer close to the interaction point, which provides high-resolution measurements at small radius to improve the tracking performance. A thin superconducting solenoid surrounds the ID and provides a 2 T axial magnetic field. The calorimeter system features a high-granularity lead/liquid-argon sampling calorimeter that measures the energy and the position of electromagnetic showers within $|\eta| < 4.9$. Liquid-argon sampling calorimeters are also used to measure hadronic showers in the endcap ($1.5 < |\eta| < 3.2$) and forward ($3.1 < |\eta| < 4.9$) regions, while a steel/scintillator tile calorimeter measures hadronic showers in the central region ($|\eta| < 1.7$). The MS surrounds the calorimeters and consists of three large superconducting air-core toroid magnets, each with eight coils, a system of precision tracking chambers ($|\eta| < 2.7$), and fast trigger chambers ($|\eta| < 2.4$). For Run 2, the ATLAS detector has a two-level trigger system. The first-level trigger is implemented in hardware and uses a subset of the detector information to reduce the rate of accepted events to 100

¹ ATLAS uses a right-handed coordinate system with its origin at the nominal interaction point (IP) in the centre of the detector and the z -axis along the beam pipe. The x -axis points from the IP to the centre of the LHC ring, and the y -axis points upward. Cylindrical coordinates (r, ϕ) are used in the transverse plane, ϕ being the azimuthal angle around the z -axis. The pseudorapidity is defined in terms of the polar angle θ as $\eta = -\ln \tan(\theta/2)$. The transverse momentum p_T and other transverse variables are defined by projecting these variables into the x - y plane, and the transverse energy E_T is defined as $\sqrt{m^2 + p_T^2}$, where m represents the mass of a considered object. The distance in the pseudorapidity–azimuthal-angle space is defined as $\Delta R = \sqrt{(\Delta\eta)^2 + (\Delta\phi)^2}$.

kHz. This is followed by the software-based high-level trigger that reduces the rate of recorded events to 1 kHz.

3 Event and object selection

Events are selected from proton–proton (pp) collisions collected by the ATLAS detector at the LHC at $\sqrt{s} = 13$ TeV in 2015 and 2016. The dataset corresponds to an integrated luminosity of $3.2 \pm 0.1 \text{ fb}^{-1}$ recorded in 2015 and $32.9 \pm 0.7 \text{ fb}^{-1}$ recorded in 2016, for a total of $36.1 \pm 0.8 \text{ fb}^{-1}$ [35]. The data used for this search were collected using the single-electron or single-muon triggers with the lowest p_T thresholds available, 20 (26) GeV for muons and 24 (26) GeV for electrons in 2015 (2016) [36].

Electrons are reconstructed from energy deposits (clusters) in the electromagnetic calorimeter matched to tracks in the ID [37] and are required to have $p_T > 15$ GeV and $|\eta| < 2.47$. Candidates in the transition region between the barrel and endcap calorimeters, $1.37 < |\eta| < 1.52$, are excluded. Electrons must satisfy the “tight” identification criterion based on a likelihood discriminant [38]. Muons are reconstructed by combining matching tracks in the ID and the MS, and are required to have $p_T > 10$ GeV and $|\eta| < 2.4$. Muon candidates must satisfy the “medium” identification criterion [39].

In order to distinguish leptons produced in the decays of W and Z bosons from those produced in the decays of heavy-flavour hadrons, all lepton candidates are required to originate from the primary interaction vertex, chosen as the vertex with the highest sum of the p_T^2 of its associated tracks. Furthermore, since lepton candidates arising from background sources, such as decays of hadrons, are typically embedded in jets, all lepton candidates are required to be isolated from other particles in the event. This is achieved by imposing a maximal allowed value on the energy deposited in the calorimeter and/or the momentum of ID tracks within a cone around the direction of the lepton candidate, according to the gradient isolation criteria [38, 39].

Jets are reconstructed from three-dimensional topological energy clusters [40] in the calorimeter using the anti- k_r jet algorithm [41] implemented in the FastJet package [42] with a radius parameter of 0.4. Jets are calibrated using energy- and η -dependent corrections [43] and are required to have $p_T > 20$ GeV and $|\eta| < 2.5$. Events containing jets arising from non-collision sources or detector noise are removed [44]. Finally, a track-based veto, the Jet Vertex Tagger (JVT), is used to reduce contributions from jets arising from additional pp interactions (pile-up) [45].

Jets including b -hadrons, referred as b -jets, are identified using information from a multivariate b -tagging algorithm that combines information from an impact-parameter-based algorithm, from the explicit reconstruction of an inclusive secondary vertex and from a multi-vertex fitter that attempts to reconstruct the b - to c -hadron decay chain [46, 47]. This b -tagging algorithm defines a set of “ b -tagged” jets. The working point used provides an efficiency to identify jets with b -hadrons from the primary vertex of approximately 77%. The rejection factors are 134 against light-quark and gluon jets, about 6 against jets originating from c -quarks, and about 22 against hadronically decaying τ -leptons, as determined in a simulated sample of top-quark pair ($t\bar{t}$) events [46, 47]. This b -tagging discriminant is used to categorize selected events as discussed in section 5. The b -tagging algorithm is also efficient in identifying jets containing b -hadrons that do not originate from the primary vertex. The efficiency is largest for proper lifetimes of $c\tau_a \sim 0.5$ mm and decreases for longer lifetimes.

The missing transverse momentum, E_T^{miss} , is defined as the magnitude of the transverse momentum imbalance \vec{E}_T^{miss} , the negative vector sum of the transverse momenta of calibrated selected objects, such as electrons, muons and jets. The transverse momenta of charged-particle tracks compatible with the primary vertex and not matched to any of those objects are also included in \vec{E}_T^{miss} [48].

Events are required to have at least one reconstructed electron or muon with $p_T > 27$ GeV which is matched within a cone of size $\Delta R = 0.15$ to the lepton candidate reconstructed by the trigger algorithms. Two event categories (single lepton and dilepton) are used to probe WH and ZH , respectively. Events with exactly one lepton are required to satisfy $E_T^{\text{miss}} > 25$ GeV and the transverse mass² must fulfil $m_T^W > 50$ GeV, in order to be consistent with W boson decays. Events in the dilepton channel must have exactly two leptons with the same flavour and opposite electric charges. In the ee and $\mu\mu$ channels, the dilepton invariant mass must be consistent with the Z boson mass window 85–100 GeV. Events in the $e\mu$ channel (different flavour) are also used in the analysis to study backgrounds. Finally, events must have at least three jets, of which at least two must be b -tagged. The selection requirements are summarized in table 1.

Table 1: Summary of requirements for the single-lepton and dilepton channels. Here $m_{\ell\ell}$ is the dilepton invariant mass in the ee and $\mu\mu$ channels.

Requirement	Single lepton	Dilepton
Trigger	single-lepton triggers	
Leptons	1 isolated	2 isolated, opposite-charge
Jets	≥ 3	
b -tagged jets	≥ 2	
Other	$E_T^{\text{miss}} > 25$ GeV, $m_T^W > 50$ GeV	$85 \text{ GeV} < m_{\ell\ell} < 100 \text{ GeV}$

4 Signal and background modelling

Simulated event samples are used to study the characteristics of the signal and to calculate its acceptance, as well as for most aspects of the background estimation. Monte Carlo (MC) samples were produced using the full ATLAS detector simulation [49] based on GEANT 4 [50]. A faster simulation, where the full GEANT 4 simulation of the calorimeter response is replaced by a detailed parameterization of the shower shapes [51], was adopted for some of the samples. To simulate the effects of pile-up, additional interactions were generated using PYTHIA 8.186 [52] with the A2 set of tuned parameters [53] and the MSTW2008LO [54] parton distribution function (PDF) set, and overlaid on the simulated hard-scatter event. Simulated events were reweighted to match the pile-up conditions observed in the data. All simulated events are processed through the same reconstruction algorithms and analysis chain as the data. In the simulation, the top-quark mass is assumed to be $m_t = 172.5$ GeV. Decays of b - and c -hadrons were performed by EVTGEN v1.2.0 [55], except in samples simulated with the SHERPA event generator [56].

Signal samples of associated Higgs boson production with a W or Z boson, $pp \rightarrow WH$ or ZH , were generated with POWHEG v2 [57–60] using the CT10 PDF set [61] at next-to-leading order (NLO). The Higgs boson mass is assumed to be $m_H = 125$ GeV. The Higgs boson decay into two spin-zero a -bosons

² The transverse mass is defined as $m_T^W \equiv \sqrt{2E_T^{\text{miss}} p_T^\ell (1 - \cos \Delta\phi)}$, where p_T^ℓ is the transverse momentum of the lepton and $\Delta\phi$ is the azimuthal angle between the lepton and \vec{E}_T^{miss} directions.

and the subsequent decay of each a -boson into a pair of b -quarks were simulated with PYTHIA 8.186. The a -boson decay was performed in the narrow-width approximation and the coupling to the b -quarks is assumed to be that of a pseudoscalar. However, since the polarization of the quarks is not observable, this search is insensitive to the chosen parity hypothesis for the a -boson. PYTHIA 8.186 was also used for the showering, hadronization, and underlying-event (UE) simulation with the A14 tune [62]. The mass of the a -boson was varied for different signal hypotheses in the range $20 \text{ GeV} \leq m_a \leq 60 \text{ GeV}$, in 10 GeV mass steps.

Signal samples with long-lived a -bosons were generated with MADGRAPH5_aMC@NLO [63] at leading order (LO) using the NNPDF2.3LO [64] PDF set and showered with PYTHIA 8.186. The model used is the SM with an additional dark sector that includes a dark vector boson and a dark Higgs boson [9, 65, 66]. In this model, the dark Higgs boson, which plays the role of the a -boson, is a scalar under parity transformation and decays promptly. Therefore, the lifetimes of the a -bosons were replaced with values sampled randomly from an exponentially falling distribution with the desired mean value. Signal MC samples were produced for a -boson mean proper lifetimes of 0.1, 1, and 10 mm. Intermediate a -boson lifetimes can be obtained by reweighting these samples. The masses of the a -boson are 20, 30, and 60 GeV. The uneven spacing of a -boson masses is motivated by the fact that the signal kinematics (and therefore acceptance) change significantly between 20 and 30 GeV, but are quite similar from 30 to 60 GeV. The ATLAS fast detector simulation was used for samples of long-lived a -bosons, after verifying that it correctly reproduces the GEANT 4-based simulation for the range of a -boson lifetimes under consideration.

The sample used to model the $t\bar{t}$ background was generated using the POWHEG v2 event generator [67], with the NNPDF3.0NLO PDF set. The POWHEG model parameter h_{damp} , which controls matrix element (ME) to parton shower (PS) matching and effectively regulates the high- p_T radiation, was set to $h_{\text{damp}} = 1.5m_t$ [68]. The PS and the hadronization were modelled by PYTHIA 8.210 [69] with the A14 tune. The renormalization and factorization scales were set to the transverse mass of the top quark, defined as $m_{T,t} = \sqrt{m_t^2 + p_{T,t}^2}$, where $p_{T,t}$ is the transverse momentum of the top quark in the $t\bar{t}$ centre-of-mass reference frame. The $t\bar{t}$ sample is normalized to the next-to-next-to-leading-order (NNLO) theoretical cross-section of 832_{-51}^{+46} pb, obtained with TOP++ 2.0 [70]. Alternative $t\bar{t}$ samples used to derive systematic uncertainties are described in section 7.

The simulated $t\bar{t}$ events are categorized depending on the parton-level flavour content of particle jets³ not originating from the decay of the $t\bar{t}$ system, using the procedure described in refs. [28, 29]. Events containing at least one particle jet matched to a b -hadron are labelled as $t\bar{t} + b\bar{b}$. Events containing at least one particle jet matched to a c -hadron and no b -hadron are labelled as $t\bar{t} + c\bar{c}$. The $t\bar{t} + b\bar{b}$ and $t\bar{t} + c\bar{c}$ categories are generically referred to as $t\bar{t}$ +HF events (with HF standing for ‘‘heavy flavour’’). Remaining events are labelled as $t\bar{t}$ + light-jets (referred to as $t\bar{t}$ + light) and also include events with no additional particle jets.

To model the dominant $t\bar{t} + b\bar{b}$ background with the highest available precision, the relative contributions of the different heavy-flavour categories in the $t\bar{t}$ sample described above are scaled to match the predictions of an NLO $t\bar{t} + b\bar{b}$ sample including parton showering and hadronization [71], generated with SHERPA+OPENLOOPS [56, 72], using the procedure described in ref [29]. The sample was produced with SHERPA 2.2.1 and the CT10 four-flavour (4F) scheme PDF set [73, 74]. The renormalization scale for this sample was chosen to be $\mu_R = \prod_{i=t,\bar{t},b,\bar{b}} E_{T,i}^{1/4}$ using the CMMPS prescription [71], while the factorization

³ Particle jets are reconstructed by clustering stable particles, excluding muons and neutrinos, using the anti- k_t algorithm with a radius parameter $R = 0.4$.

scale is set to $\mu_F = \frac{1}{2} \sum_{i=t,\bar{t},b,\bar{b}} E_{T,i}$. The resummation scale μ_Q , which sets an upper bound for the hardness of the PS emissions, was also set to $\frac{1}{2} \sum_{i=t,\bar{t},b,\bar{b}} E_{T,i}$.

The production of W and Z bosons in association with jets was simulated with SHERPA 2.2.1 [56] using the NNPDF3.0NNLO PDF set for both the ME calculation and the dedicated PS tuning developed by the SHERPA authors [75]. The ME calculation was performed with COMIX [76] and OPENLOOPS [72], and was matched to the SHERPA PS using the MEPS@NLO prescription [77]. The MEs were calculated for up to two additional partons at NLO and for three and four partons at LO in QCD. The W/Z + jets samples are normalized to the NNLO cross-sections [78, 79].

The diboson + jets samples were generated using SHERPA 2.1.1 as described in ref. [80]. Samples of $t\bar{t}W$ and $t\bar{t}Z$ ($t\bar{t}V$) events were generated with an NLO ME using MADGRAPH5_aMC@NLO interfaced to PYTHIA 8.210 with the NNPDF3.0NNLO PDF set and the A14 tune.

Samples of Wt and s -channel single-top-quark backgrounds were generated with POWHEG v1 at NLO accuracy using the CT10 PDF set. Overlap between the $t\bar{t}$ and Wt final states was resolved using the “diagram removal” scheme [81]. The t -channel single-top-quark events were generated using the POWHEG v1 event generator at NLO accuracy with the CT10 4F scheme PDF set. For this process, top quarks were decayed using MADSPIN. All single-top-quark samples were interfaced to PYTHIA 6.428 [82] with the Perugia 2012 tune [83]. The single-top quark t - and s -channel samples are normalized to the NLO theoretical cross-sections [84, 85], while the Wt channel is normalized to the approximate NNLO prediction [86, 87].

Higgs boson production in association with a single top quark is a rare process in the SM, but is included in the analysis and is treated as a background. Samples of single top quarks produced in association with a W boson and a Higgs boson, tWH , were produced with MADGRAPH5_aMC@NLO interfaced to HERWIG++ [88] with the CTEQ6L1 PDF set. The other Higgs boson production modes are found to be negligible and are not considered. The production of four top quarks ($t\bar{t}t\bar{t}$) as well as $t\bar{t}WW$ events were generated with MADGRAPH5_aMC@NLO with LO accuracy and interfaced to PYTHIA 8.186. The tZW production process was also generated with MADGRAPH5_aMC@NLO interfaced to PYTHIA 8.186, but at NLO accuracy.

In the single-lepton channel, the background from events with a jet or a photon misidentified as a lepton or with non-prompt leptons from hadron decays (hereafter referred to as a fake or non-prompt lepton) is estimated directly from data using a matrix method [89]. A data sample enhanced in fake and non-prompt leptons is selected by removing the lepton isolation requirements and, for electrons, loosening the identification criteria. The efficiency for these “loose” leptons to satisfy the nominal selection (“tight”) criteria is measured in data, separately for real prompt leptons and for fake or non-prompt leptons. For real prompt leptons, the efficiency is measured in Z boson events, while for fake and non-prompt leptons, it is estimated from events with low E_T^{miss} and low values of m_T^W .

The number of fake or non-prompt leptons satisfying the tight criteria can then be calculated by inverting the matrix defined by the two equations:

$$N^l = N_r^l + N_f^l, \quad N^t = \varepsilon_r N_r^l + \varepsilon_f N_f^l,$$

where N^l (N^t) is the number of events in data satisfying the loose (tight) lepton selection, N_r^l (N_f^l) is the number of events with a real prompt (fake or non-prompt) lepton in the loose lepton sample, and ε_r (ε_f) is the efficiency for these events to fulfil the tight lepton selection. By generalizing the resulting formula to extract $\varepsilon_f N_f^l$, a weight is assigned to each event selected in the loose lepton data sample,

providing a prediction for both the yields and the kinematic distributions of the fake and non-prompt lepton background.

When applying the matrix method in the case of high jet and b -tagged jet multiplicities, the number of events in data satisfying the loose and tight lepton selections is significantly reduced, leading to large fluctuations in the background predictions. In order to mitigate this problem, instead of tagging the jets by applying the b -tagging algorithm, their probabilities to be b -tagged are parameterized as a function of the jet p_T . This allows all events in the sample before b -tagging is applied to be used in predicting the normalization and shape of the background from fake or non-prompt leptons after b -tagging. The tagging probabilities are derived using an inclusive sample of fake or non-prompt leptons and the resulting predictions of this background estimate are in agreement with those obtained by applying the b -tagging algorithm and have greatly reduced statistical uncertainties.

In the dilepton channel, the background contribution from fake or non-prompt leptons is very small and is estimated from simulation and normalized to data in a control region with two same-charge leptons.

5 Event categorization

Events satisfying the object selection are categorized into analysis regions according to the number of leptons, jets and b -tagged jets. The regions enhanced in signal $H \rightarrow aa \rightarrow 4b$ events relative to the backgrounds are referred to as signal regions (SRs). The other regions, referred to as control regions (CRs), are used to constrain the background predictions and related systematic uncertainties (see section 7) through a profile likelihood fit to the data (see section 8). The signal and backgrounds are derived consistently in the signal and control regions in a combined fit. The discrimination of signal from background is further enhanced in the signal regions by using multivariate techniques, as described in section 6.

The $H \rightarrow aa \rightarrow 4b$ decay chain is expected to have multiple b -tagged jets, often three or four, satisfying the object selection. The dominant background arises from $t\bar{t}$ events in the single-lepton channel and Z + jets events in the dilepton channel, which can also have different jet and b -tagged jet multiplicities or leptons of different flavour in the case of the dilepton channel. The regions are referred to as (n_ℓ, n_j, n_b) indicating n_ℓ leptons, n_j selected jets and n_b b -tagged jets. The SRs contain at least three b -tagged jets and are $(1\ell, 3j, 3b)$, $(1\ell, 4j, 3b)$ and $(1\ell, 4j, 4b)$ for single-lepton events, and $(2\ell, 3j, 3b)$, $(2\ell, \geq 4j, 3b)$ and $(2\ell, \geq 4j, \geq 4b)$ for same-flavour dilepton events. The CRs are $(1\ell, 3j, 2b)$, $(1\ell, 4j, 2b)$, $(1\ell, \geq 5j, 3b)$ and $(1\ell, \geq 5j, \geq 4b)$ for single-lepton events, $(2\ell, \geq 3j, 2b)$ for same-flavour dilepton events, and $(2\ell, \geq 3j, 3b)$ and $(2\ell, \geq 4j, \geq 4b)$ for different-flavour dilepton events. The signal and control regions are summarized in figure 2, indicating the main background sources probed in the CRs. Figure 3 summarizes the background composition in the signal and control regions.

In the single-lepton signal regions, background $t\bar{t}$ events can only satisfy the selection criteria if accompanied by additional b -tagged jets. The $t\bar{t}$ + light background is dominant in the sample of events with exactly two or three b -tagged jets. The background processes $t\bar{t} + c\bar{c}$ and $t\bar{t} + b\bar{b}$ become more important as the jet and b -tagged-jet multiplicities increase. In particular, the $t\bar{t} + b\bar{b}$ background dominates for events with ≥ 5 jets and ≥ 4 b -tagged jets. In the case of $(1\ell, 3j, 3b)$ or $(1\ell, 4j, 3b)$, the main sources of $t\bar{t}$ background are events with jets mistagged as b -tagged jets, particularly from $W \rightarrow cs$ decays, where the c -jet is misidentified, and from $W \rightarrow \tau\nu$, where the τ -lepton decays hadronically and is likewise

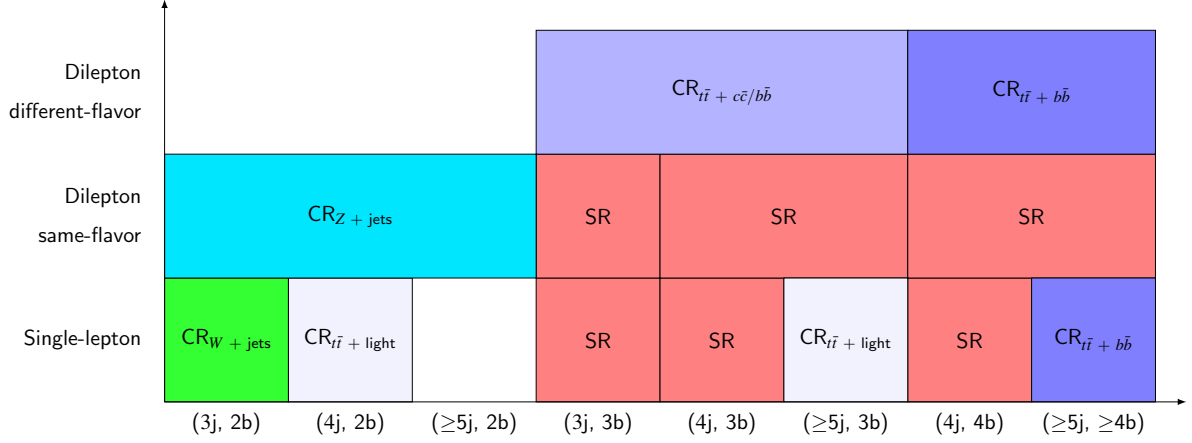


Figure 2: Definition of the signal and control regions (SR and CR, respectively) in the single-lepton and dilepton channels. The main background component probed with the CR is indicated. The vertical axis shows the lepton selection, while the horizontal axis shows the jet and b -tagged jet multiplicities.

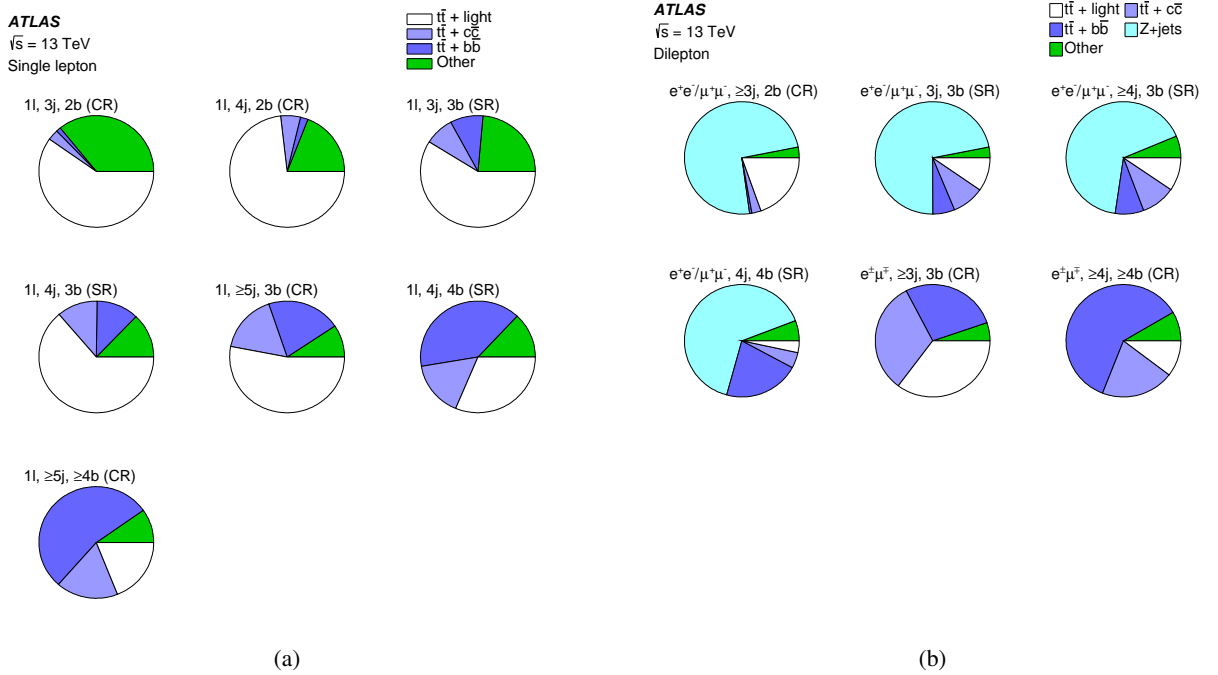


Figure 3: Fractional contributions of the various backgrounds to the total background prediction in the (a) single-lepton and (b) dilepton signal and control regions. The predictions for the various background contributions are obtained through the simulation and the data-driven estimates described in section 4. The $t\bar{t}$ background categories are also defined in section 4.

mistagged. In the case of $(1\ell, 4j, 4b)$, the $t\bar{t}$ background includes more events with genuine b -quarks from gluon splitting to $b\bar{b}$ pairs.

In the dilepton channel, the background is mainly composed of $t\bar{t}$ and $Z + \text{jets}$ events. In the case of the $t\bar{t}$ background, most events contain two prompt leptons from the leptonic decays of the two W bosons, and two b -jets from the top-quark decays. Additional jets arise from gluon splitting into $b\bar{b}$ and $c\bar{c}$ and from jets from initial-state radiation and pile-up. In each of these cases, the third and fourth b -tags in the event are from additional b -tagged jets, or from the mistag of additional c - or light-jets. In the samples with exactly three or four jets and exactly three b -tagged jets, the contributions of each of these sources is similar. In the case of the sample with exactly four jets and exactly four b -tagged jets, the contribution from events with real additional b -tagged jets, such as from gluon splitting into $b\bar{b}$, dominates.

In the case of the $Z + \text{jets}$ background, the dominant contribution is from Z bosons produced in association with multiple heavy-flavour jets, for example from gluon splitting into $b\bar{b}$. In particular, for events with exactly three jets and three b -tagged jets or exactly four jets and four b -tagged jets, about half of the events are from $Z + b\bar{b}$ with a mistagged light-flavoured jet and half are from $Z + b\bar{b}c$ with a mistagged c -jet. In the case of the events with exactly four jets and three b -tagged jets, approximately a third of the events are from $Z + b\bar{b}$ with a mistagged light-flavoured jet, a third are from $Z + b\bar{b}c$ with a mistagged c -jet and a third are from $Z + b\bar{b}b$.

In the dilepton channel, the control regions are designed to be populated by the two main background processes: $t\bar{t}$ and $Z + \text{jets}$. The control region with two same-flavour leptons, ($2\ell, \geq 3j$, 2b), is populated by $Z + \text{jets}$ and $t\bar{t} + \text{light}$. The control regions with two different-flavour leptons but with the same jet and b -tagged jet multiplicities as the signal regions, ($2\ell, \geq 3j$, 3b) and ($2\ell, \geq 4j, \geq 4b$), are enhanced in $t\bar{t} + c\bar{c}$ and $t\bar{t} + b\bar{b}$ processes.

6 Analysis strategy

In each of the six signal regions, a boosted decision tree (BDT) discriminant that combines information from several variables provides additional discrimination between signal and background. In the control regions, kinematic variables are used to provide additional discrimination between distinct sources of background. The distribution of H_T , defined as the scalar sum of the p_T of the jets, is used in the control regions with two b -tagged jets, while the invariant mass of the b -tagged jets is used in the control regions with three or four b -tagged jets. A statistical analysis based on a binned likelihood function constructed as a product of Poisson probability terms over all regions and all bins considered in the search is used to derive the background predictions and uncertainties, and to test for the presence of signal. The statistical procedure and the results are described in section 8.

The toolkit for multivariate analysis (TMVA) [90] is used to train the BDT discriminant. In the single-lepton channel, dedicated BDTs are trained to discriminate each of the signals with a -boson masses of 20, 30 and 50 GeV from $t\bar{t}$ events. The discriminant trained at 50 GeV is found to have good sensitivity for the a -boson mass range 40–60 GeV. In the dilepton channel, dedicated BDTs are trained to discriminate each of the signals from both the $t\bar{t}$ and $Z + \text{jets}$ events. The discriminant trained at 30 GeV is found to have good sensitivity over the full mass range (20–60 GeV) for each of the signal regions.

The choice of inputs used in the BDT discriminants was based on the following considerations. Signal events are characterized by the presence of a resonance resulting from the Higgs boson decay $H \rightarrow aa \rightarrow 4b$. Several variables are used to reconstruct the particles from the signal decay chain. The first is the reconstructed invariant mass of the b -tagged jets, m_{bbb} or m_{bbbb} , defined for events with three or four b -tagged jets respectively, which peaks around the Higgs boson mass for signal events. In the case of three

b -tagged jets, the peak is due to events where two b -quarks are merged in a single jet or one of the b -quarks is very soft in an asymmetric decay and has a small impact on the kinematics. In the case of events with four b -tagged jets, the invariant masses of the two b -tagged jet pairs are discriminating variables between signal and background. The pairings are chosen to minimize the difference between the invariant masses of the b -tagged jet pairs, and are labelled m_{bb1} and m_{bb2} , such that $m_{bb1} > m_{bb2}$.

Additional kinematic variables exhibit differences between signal and background. In both channels, the average angular separation between b -tagged jets, referred to as average $\Delta R(b,b)$, is typically larger for background events where the b -tagged jets originate from the decays of different particles, such as the two top quarks in $t\bar{t}$ events. In the single-lepton channel, several additional kinematic variables are included in the BDT discriminant. The H_T variable is a measure of the total hadronic energy in the event, which is typically larger for $t\bar{t}$ than for WH events. The transverse momentum of the W boson, p_T^W , constructed from the vector sum of the \vec{E}_T^{miss} and the lepton \vec{p}_T , is slightly higher for signal WH events, where the W boson recoils against the Higgs boson, than for background $t\bar{t}$ events.

Finally, two other variables are used to identify particles from the dominant $t\bar{t}$ background decay chain in the single-lepton channel. The first variable is used in the (1 ℓ , 4j, 3b) channel to select $t\bar{t}$ events with two b -tagged jets from the top-quark decays and a third b -tagged jet from a misidentified c - or light-jet from the hadronically decaying W boson. This variable is the invariant mass of two b -tagged jets (selected as the pair with the smallest ΔR separation) and the non- b -tagged jet, m_{bbj} , which reconstructs the hadronically decaying top quark, peaking around the top-quark mass for these background events. The second variable is an m_{T2} observable, defined as the minimum ‘‘mother’’ particle mass compatible with all transverse momenta and mass-shell constraints [91], that identifies events with several invisible particles. In the case of the $t\bar{t}$ background events, in addition to the E_T^{miss} from the neutrino from a leptonic W boson decay, invisible particles may arise from a τ -lepton decay or from a lost jet from a W boson. In these cases, m_{T2} has an endpoint at the top-quark mass, which is not the case for the signal.

For the dilepton channel, two variables are sensitive to the signal topology of a Z boson recoiling against a Higgs boson: the separation between the two leptons in the event, $\Delta R(\ell,\ell)$, and the separation between the Z boson, constructed from the two leptons, and the Higgs boson, constructed from the b -tagged jets, $\Delta R(Z,H)$. Another discriminating variable that carries information about the signal production mechanism is the cosine of the polar angle of the Higgs boson in the reference frame of the parent process $Z^* \rightarrow ZH$, referred to as $\cos \theta^*$, which is sensitive to the spin of the parent particle. Finally, the E_T^{miss} variable is used to discriminate against background $t\bar{t}$ events that include the presence of multiple neutrinos.

Table 2 summarizes the variables used to train each of the BDT discriminants for the six signal regions. Figures 4 and 5 show the expected distributions of the kinematical variables inclusively in number of jets and b -tagged jets. The jets with the largest values of the b -tagging discriminant are used to define the variables shown. The distributions are obtained ‘‘post-fit’’, after accounting for the systematic uncertainties and applying the statistical procedure described in sections 7 and 8, respectively.

Table 2: List of variables used to train the BDT multivariate discriminant for each signal region.

Variable	(1 ℓ , 3j, 3b)	(1 ℓ , 4j, 3b)	(1 ℓ , 4j, 4b)	(2 ℓ , 3j, 3b)	(2 ℓ , \geq 4j, 3b)	(2 ℓ , \geq 4j, \geq 4b)
m_{bbb}	✓	✓		✓	✓	
m_{bbbb}			✓			✓
m_{bb1}			✓			✓
m_{bb2}			✓			✓
Average $\Delta R(b,b)$	✓	✓	✓	✓	✓	✓
H_T	✓	✓	✓			
p_T^W	✓					
m_{bbj}		✓				
m_{T2}	✓	✓	✓			
$\Delta R(\ell,\ell)$				✓	✓	✓
$\Delta R(Z,H)$				✓	✓	
$\cos \theta^*$						✓
E_T^{miss}				✓	✓	✓

7 Systematic uncertainties

Many sources of systematic uncertainties affect this search, including those related to the integrated luminosity, to the reconstruction and identification of leptons and jets, and to the modelling of signal and background processes. Some uncertainties affect only the overall normalization of the samples, while others also impact the shapes of the distributions used to categorize events and build the final discriminants.

A single nuisance parameter is assigned to each source of systematic uncertainty, as described in section 8. Some of the systematic uncertainties, in particular most of the experimental uncertainties, are decomposed into several independent sources, as specified in the following. Each individual source then has a correlated effect across all channels, analysis categories, signal and background samples. For modelling uncertainties, especially the $t\bar{t}$ and Z + jets modelling, additional nuisance parameters are included to split some uncertainties into several sources affecting different subcomponents of a particular process independently.

The uncertainty of the combined integrated luminosity for 2015 and 2016 is 2.1%. It is determined using a methodology similar to that detailed in ref. [35]. Uncertainties in the modelling of pile-up are also estimated, and cover the differences between the predicted and measured inelastic cross-sections [92].

Uncertainties associated with leptons arise from the trigger, reconstruction, identification, and isolation efficiencies, as well as the momentum scale and resolution. These are measured in data using leptons in $Z \rightarrow \ell^+\ell^-$, $J/\psi \rightarrow \ell^+\ell^-$ and $W \rightarrow e\nu$ events [38, 39] and have only a small impact on the result.

Uncertainties associated with jets arise from their reconstruction and identification efficiencies. These are due to the uncertainty in the jet energy scale (JES), resolution and the efficiency of the JVT requirement that is meant to remove jets from pile-up. The JES and its uncertainty are derived by combining information from test-beam data, LHC collision data and simulation [43]. Additional uncertainties are also considered, associated with the jet flavour and pile-up corrections. The total per-jet uncertainties are 1–6%, although the effects are amplified by the large number of jets in the final state.

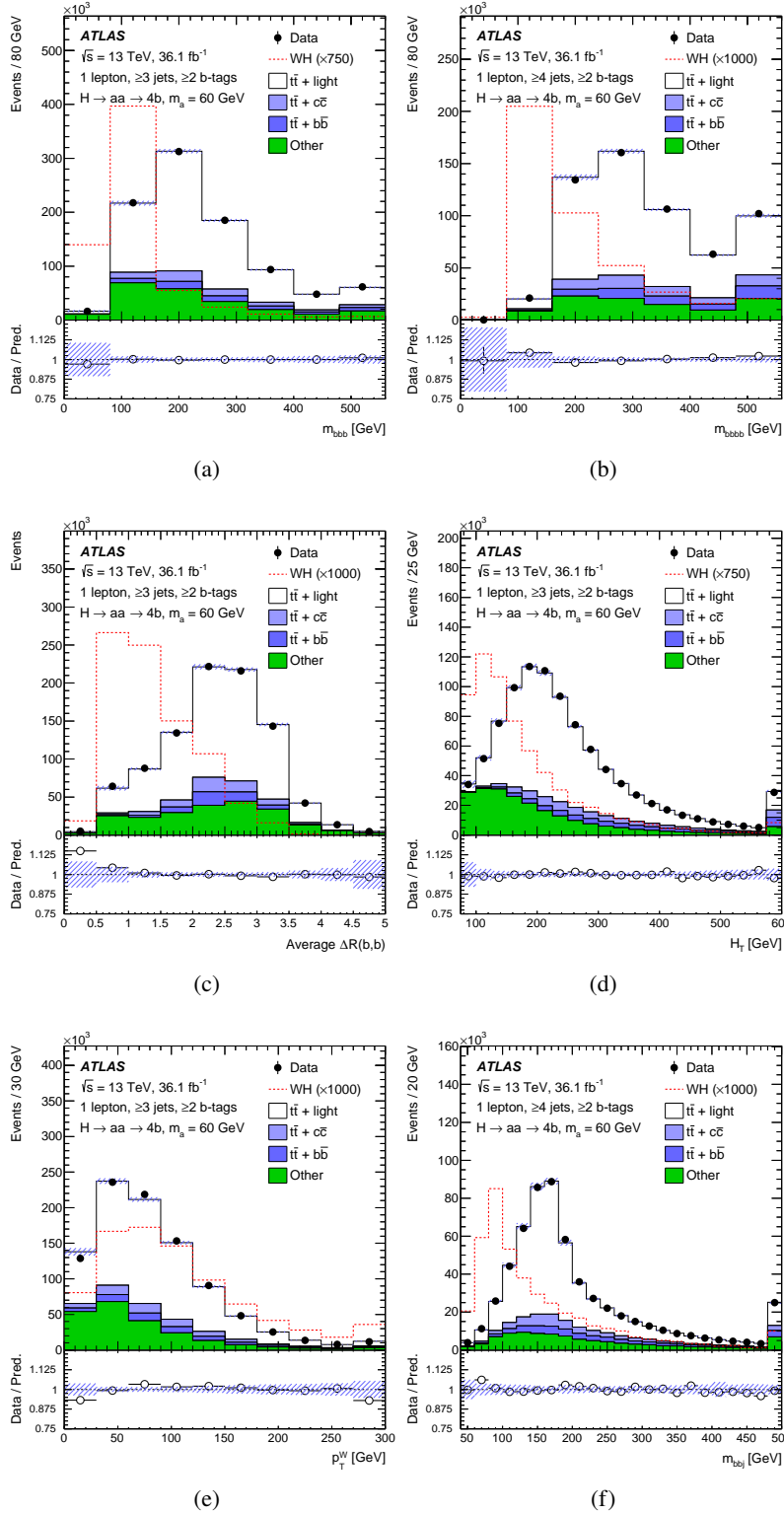


Figure 4: Comparison of data with the post-fit background estimates for (a) m_{bbb} , (b) m_{bbbb} , (c) average $\Delta R(b,b)$, (d) H_T , (e) p_T^W and (f) m_{bbj} in the single-lepton sample inclusive in number of jets and b -tagged jets. Comparisons use events with ≥ 3 jets, except when ≥ 4 jets are necessary to define the variable, in which case events with ≥ 4 jets are used. Distributions for the signal model ($WH, H \rightarrow aa \rightarrow 4b$), with $m_a = 60$ GeV, normalized to the SM $pp \rightarrow WH$ cross-section, assuming $\mathcal{B}(H \rightarrow aa \rightarrow 4b) = 1$ and scaled by a factor as indicated in the figure, are overlaid. The hashed area represents the total uncertainty in the background. The last bin contains the overflow.

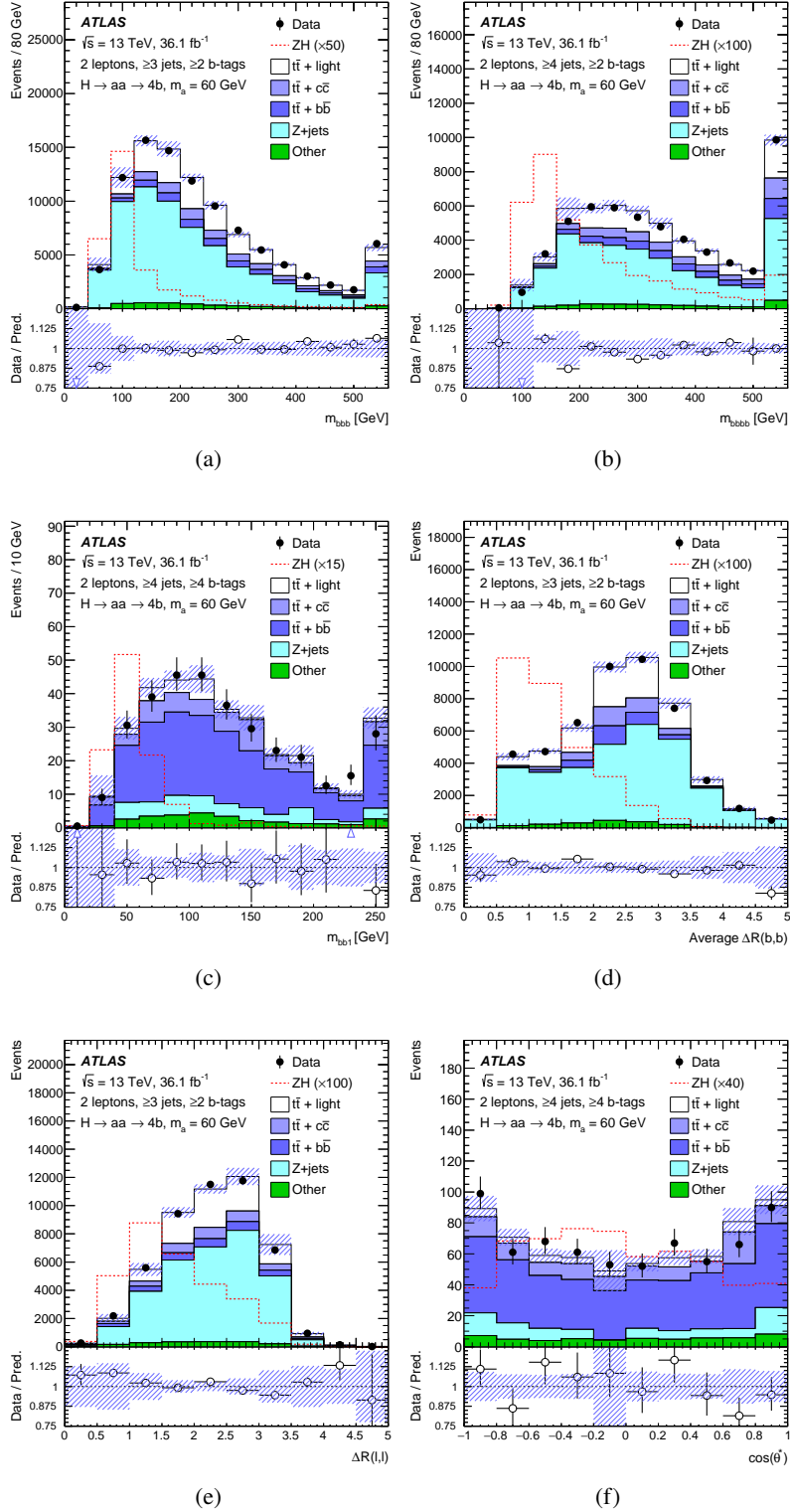


Figure 5: Comparison of data with the post-fit background estimates for (a) m_{bbb} , (b) m_{bbbb} , (c) m_{bbb1} , (d) average $\Delta R(b,b)$, (e) $\Delta R(\ell,\ell)$ and (f) $\cos \theta^*$ in the dilepton sample inclusive in number of jets and b -tagged jets. Comparisons use events with ≥ 3 jets, except when ≥ 4 jets are necessary to define the variable, in which case events with ≥ 4 jets are used. Distributions for the signal model (ZH , $H \rightarrow aa \rightarrow 4b$), with $m_a = 60$ GeV, normalized to the SM $pp \rightarrow ZH$ cross-section, assuming $\mathcal{B}(H \rightarrow aa \rightarrow 4b) = 1$ and scaled by a factor as indicated in the figure, are overlaid. The hashed area represents the total uncertainty in the background. The last bin contains the overflow.

The efficiency to correctly tag b -jets is measured in data using dilepton $t\bar{t}$ events [93]. The mistag rate for c -jets is measured in events with W bosons decays into $q\bar{q}$. For light jets, it is measured in multi-jet events using jets containing secondary vertices and tracks with impact parameters consistent with a negative lifetime [46]. The uncertainty associated with the b -tagging efficiency ranges between 2% and 10% depending on the jet p_T . The size of the uncertainties associated with the mistag rates is 5–20% for c -jets depending on the jet p_T and 10–50% for light jets depending on the jet p_T and η .

For the long-lived a -boson signals, the secondary vertices of b -jets are, on average, further displaced from the primary vertex than those of b -jets from $t\bar{t}$ events. An additional “displaced b -tagging” systematic uncertainty is applied to long-lived signal samples to account for a displacement-dependent mismodelling of the b -tagging efficiency. The uncertainty is determined using the “adjusted MC” method [94], which was originally developed for the calibration of the mistag rate for light-flavour jets. The resulting uncertainty increases approximately linearly with the a -boson proper lifetime, from $\sim 2\%$ for prompt a -bosons to $\sim 10\%$ for proper lifetimes of 10 mm. It is applied in addition to the standard b -tagging uncertainties.

Uncertainties associated with energy scales and resolutions of leptons and jets are propagated to E_T^{miss} . An uncertainty in the contribution from charged-particle tracks not associated with reconstructed leptons and jets is also included in the E_T^{miss} uncertainty [48].

Several sources of systematic uncertainty affecting the modelling of the main backgrounds, $t\bar{t}$ and Z + jets are considered. For the $t\bar{t}$ background, the procedure closely follows that described in ref. [28]. An uncertainty of 6% is assumed for the $t\bar{t}$ production cross-section [70], including contributions from variations of the factorization and renormalization scales, and uncertainties arising from the PDFs, α_S , and the top-quark mass.

Systematic uncertainties affecting the shape of the $t\bar{t}$ background account for the choice of generator, the choice of PS and hadronization models, and the effects of initial- and final-state radiation. The uncertainties are derived from comparisons between the nominal simulation (POWHEG+PYTHIA) and alternative samples produced with SHERPA+OPENLOOPS (varying the NLO event generator, PS and hadronization models) or POWHEG+HERWIG 7 [95] (varying only the PS and hadronization models).

Additional uncertainties are evaluated to account for the use of SHERPA+OPENLOOPS NLO to model the $t\bar{t} + b\bar{b}$ and $t\bar{t} + c\bar{c}$ backgrounds. Uncertainties are also assessed for the choice of scheme to treat massive quarks and the choice of PDF sets, as well as the choice of shower recoil model and scale. Uncertainties are also included to account for differences in the relative contributions of the $t\bar{t} + b\bar{b}$, $t\bar{t} + c\bar{c}$ and $t\bar{t} + \text{light}$ processes. All uncertainties are treated as uncorrelated across the $t\bar{t}$ flavour components. The normalization of the $t\bar{t} + b\bar{b}$ process is included as an independent free-floating factor, while the $t\bar{t} + c\bar{c}$ component is assigned a 50% normalization uncertainty, derived from studies of alternative background samples [29].

In the case of the W + jets and Z + jets backgrounds, all normalizations are included as independent free-floating factors. In the case of the Z + jets background in the dilepton channel, a separate normalization factor is considered for each jet and b -tagged jet multiplicity bin: $(2\ell, \geq 3j, 2b)$, $(2\ell, 3j, 3b)$, $(2\ell, \geq 4j, 3b)$ and $(2\ell, \geq 4j, \geq 4b)$. Additional assigned uncertainties are based on variations of the factorization and renormalization scales and of the matching parameters in the SHERPA simulation.

A cross-section uncertainty of $^{+5\%}_{-4\%}$ is assigned to the three single-top-quark production modes [86, 96, 97]. For the Wt and t -channel production modes, uncertainties associated with the choice of PS and hadronization model and with initial- and final-state radiation are evaluated by using a set of alternative samples. The uncertainty in modelling of the interference between Wt and $t\bar{t}$ production at NLO is

assessed by comparing the default simulation to an alternative one that resolves the interference at the cross-section level (“diagram subtraction” scheme) instead of the amplitude level (“diagram removal” scheme) [81].

A 50% normalization uncertainty in the diboson background is assumed, which includes uncertainties in the inclusive cross-section and the production of additional jets [80]. The uncertainties in the $t\bar{t}W$ and $t\bar{t}Z$ NLO cross-section predictions are 13% and 12%, respectively [66, 98], due to PDF and scale uncertainties, and are treated as uncorrelated between the two processes. An additional modelling uncertainty for $t\bar{t}W$ and $t\bar{t}Z$, related to the choice of event generator, PS and hadronization models, is derived from comparisons of the nominal samples with alternative ones generated with SHERPA.

In the single-lepton channel, uncertainties in the estimation of the background with fake or non-prompt leptons come from the limited number of events in the data sample without the lepton isolation requirement and from uncertainties in the measured non-prompt and prompt lepton efficiencies. The normalization uncertainty assigned to this background is 50%, as derived by comparing the background prediction with data in control regions obtained by inverting the requirements on E_T^{miss} and on m_T^W . An uncertainty in the shape of the predicted background distribution covers the difference between the prediction obtained using an inclusive sample before b -tagging is applied and the prediction after b -tagging. In the dilepton channel, the simulated non-prompt lepton background is assigned a 25% uncertainty, correlated across lepton flavours and all analysis categories.

Several sources of systematic uncertainty affect the theoretical modelling of the signal. Uncertainties originate from the choice of PDFs, the factorization and renormalization scales, and the PS, hadronization and UE models.

8 Results

The distributions of the discriminant for each of the analysis categories are combined in a profile likelihood fit to test for the presence of signal, while simultaneously determining the normalizations and constraining the differential distributions of the most important background components. As described in section 6, in the signal regions, the output of the BDT classifier is used as the discriminant, while H_T or the invariant mass of the b -jets is used in the control regions.

The likelihood function, $\mathcal{L}(\mu, \theta)$, is constructed as a product of Poisson probability terms over all bins in each distribution. The Poisson probability depends on the predicted number of events in each bin, which in turn is a function of the signal-strength parameter $\mu = \sigma \times \mathcal{B}(H \rightarrow aa \rightarrow 4b)$, where σ are the $pp \rightarrow WH$ and ZH cross-sections. The nuisance parameters, θ , encode the effects of systematic uncertainties. The nuisance parameters are implemented in the likelihood function as Gaussian, log-normal or Poisson priors. The statistical uncertainty of the prediction, which incorporates the statistical uncertainty of the simulated events and of the data-driven fake and non-prompt lepton background estimate, is included in the likelihood as a nuisance parameter for each bin.

The likelihood function depends on six free-floating normalization factors for $t\bar{t} + b\bar{b}$, Z + jets for the four jet and b -tagged jet multiplicities and W + jets. No prior knowledge from theory or subsidiary measurements is assumed for the normalization factors, hence they are only constrained by the profile likelihood fit to the data. As shown in table 3, the normalization factors are compatible with SM expectations within the uncertainties. The other main background components, particularly $t\bar{t}$ + light and $t\bar{t}$ + $c\bar{c}$, are also compatible with SM expectations within the uncertainties described in section 7. In the combination of

the single-lepton and dilepton channels, the ratio of WH to ZH cross-sections is assumed to follow the SM prediction.

Table 3: Normalization factors included as independent free-floating factors in the likelihood fit. The uncertainties include statistical and systematic components.

Sample	Normalization factor		
	Single-lepton	Dilepton	Combination
$t\bar{t} + b\bar{b}$	1.5 ± 0.5	0.9 ± 0.3	1.1 ± 0.3
$W + \text{jets}$	0.7 ± 0.3	–	0.7 ± 0.3
$Z + \text{jets} (2\ell, \geq 3j, 2b)$	–	1.0 ± 0.1	1.1 ± 0.1
$Z + \text{jets} (2\ell, 3j, 3b)$	–	1.2 ± 0.2	1.1 ± 0.2
$Z + \text{jets} (2\ell, \geq 4j, 3b)$	–	1.1 ± 0.2	1.1 ± 0.1
$Z + \text{jets} (2\ell, \geq 4j, \geq 4b)$	–	1.4 ± 0.5	1.4 ± 0.5

The test statistic t_μ is defined as the profile likelihood ratio: $t_\mu = -2 \ln(\mathcal{L}(\mu, \hat{\theta}_\mu) / \mathcal{L}(\hat{\mu}, \hat{\theta}))$, where $\hat{\mu}$ and $\hat{\theta}$ are the values of the parameters which maximize the likelihood function, and $\hat{\theta}_\mu$ are the values of the nuisance parameters which maximize the likelihood function for a given value of μ . This test statistic is used to measure the probability that the observed data is compatible with the signal+background hypothesis, and to perform statistical inferences about μ , such as upper limits using the CL_s method [99–101]. The uncertainty of the best-fit value of the signal strength, $\hat{\mu}$, is obtained when varying t_μ by one unit.

After performing the fit, the leading sources of systematic uncertainty are the modelling of the $t\bar{t}$ and $Z + \text{jets}$ backgrounds and the b -, c - and light-jet-tagging efficiencies. Table 4 summarizes the main systematic uncertainties by indicating their impact on the normalization of the main backgrounds and the signal ($\hat{\mu}$) with $m_a = 60$ GeV in the most sensitive signal regions ($1\ell, 4j, 4b$) and ($2\ell, \geq 4j, \geq 4b$). The uncertainties in the normalization are obtained by varying the parameter corresponding to the source of uncertainty under consideration up and down by one standard deviation, while keeping the other nuisance parameters fixed at their central value.

Figures 6 and 7 show the distributions in the control regions of the single-lepton and dilepton channels, respectively, after performing the likelihood fit of these distributions to data assuming $\mu = 0$. The fit produces better agreement between the data and the background predictions, and it reduces the uncertainties as a result of the nuisance-parameter constraints and the correlations generated by the fit. Figure 8 shows the post-fit background distributions for the signal regions of the dilepton and single-lepton channels. Table 5 compares the observed event yield with the SM background prediction in each signal region, as well as the expected number of signal events for a few representative values of m_a . The overall acceptance times efficiency for signal is approximately 0.2% and 0.4% for the signal regions ($1\ell, 4j, 4b$) and ($2\ell, \geq 4j, \geq 4b$), respectively.

No significant deviations from the SM predictions are found and upper limits are set on $\sigma \times \mathcal{B}(H \rightarrow aa \rightarrow 4b)$ for a mass hypothesis m_a tested in steps of 10 GeV between 20 and 60 GeV, as shown in figure 9. The observed (expected) upper limits on μ for the single-lepton channel range from 2.9 (2.4) pb, for $m_a = 20$ GeV, to 1.6 (0.94) pb, for $m_a = 60$ GeV. For the dilepton channel they range from 1.6 (1.2) pb, for $m_a = 20$ GeV, to 0.54 (0.39) pb for $m_a = 60$ GeV. For comparison, the SM NNLO cross-sections for $pp \rightarrow WH$ and ZH are $\sigma_{\text{SM}}(WH) = 1.37$ pb and $\sigma_{\text{SM}}(ZH) = 0.88$ pb, respectively [102]. Upper limits are derived for the combination of the single-lepton and dilepton channels assuming that the ratio of WH

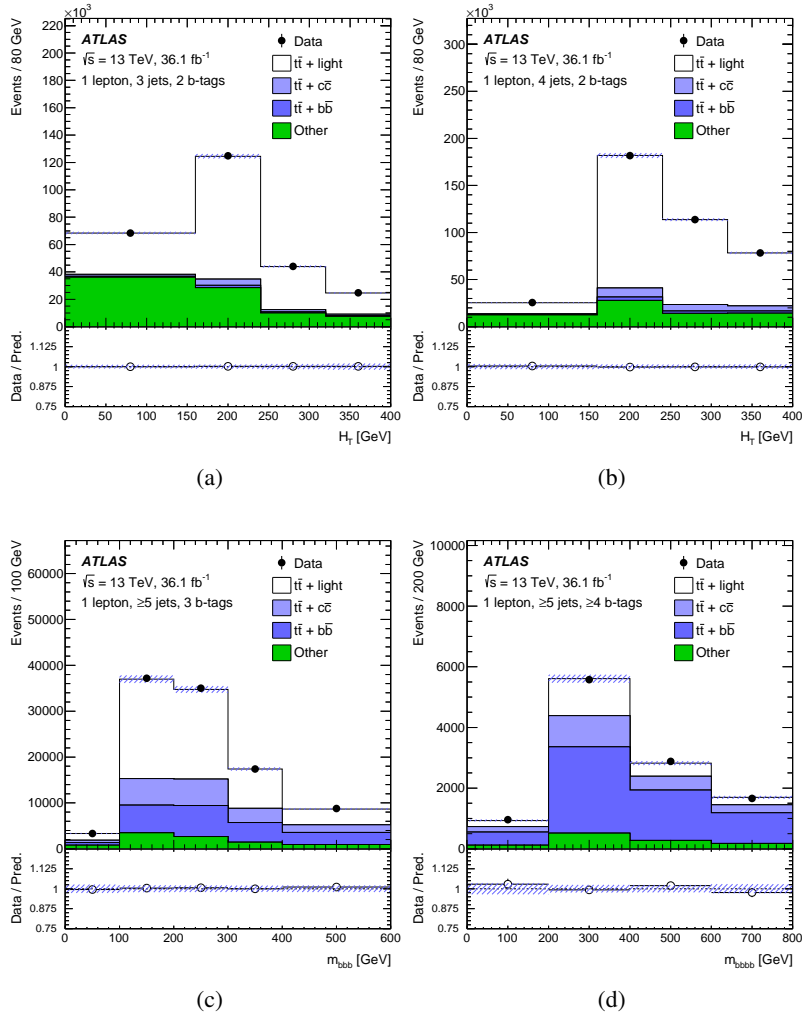


Figure 6: Comparison between data and prediction in the single-lepton control regions of the H_T variable for (a) (1 ℓ , 3j, 2b) and (b) (1 ℓ , 4j, 2b) and the invariant mass of b -tagged jets for (c) (1 ℓ , ≥ 5 j, 3b) and (d) (1 ℓ , ≥ 5 j, ≥ 4 b), after the combined single-lepton and dilepton fit to the data. The last bin contains the overflow.

Table 4: Summary of the impact of the considered systematic uncertainties (in %) on the yields for the main backgrounds and the signal ($m_a = 60$ GeV) for the single-lepton and dilepton regions (1ℓ , $4j$, $4b$) and (2ℓ , $\geq 4j$, $\geq 4b$) after the fit. The total uncertainty can differ from the sum in quadrature of individual sources due to correlations.

Systematic uncertainty	Impact on yield [%]						
	Single lepton				Dilepton		
	WH signal	$t\bar{t}$ + light	$t\bar{t}$ + $c\bar{c}$	$t\bar{t}$ + $b\bar{b}$	ZH signal	$t\bar{t}$ + $b\bar{b}$	Z + jets
Luminosity	2	2	2	2	2	2	2
Lepton efficiencies	1	1	1	1	1	1	1
Jet efficiencies	1	1	1	1	1	1	2
Jet energy resolution	5	4	4	1	7	5	6
Jet energy scale	4	2	3	2	4	4	7
b -tagging efficiency	16	5	4	9	20	14	17
c -tagging efficiency	1	5	9	3	7	1	1
Light-jet-tagging efficiency	2	16	5	2	1	3	1
Theoretical cross-sections	–	5	5	5	–	8	–
$t\bar{t}$: modelling	–	5	35	45	–	19	–
$t\bar{t}$ +HF: normalization	–	–	31	33	–	38	–
$t\bar{t}$ +HF: modelling	–	–	10	5	–	7	–
Z + jets: normalization	–	–	–	–	–	–	38
Signal modelling	7	–	–	–	10	–	–
Displaced b -tagging	5–8	–	–	–	5–8	–	–
Total	33–34	32	75	58	30–31	32	36

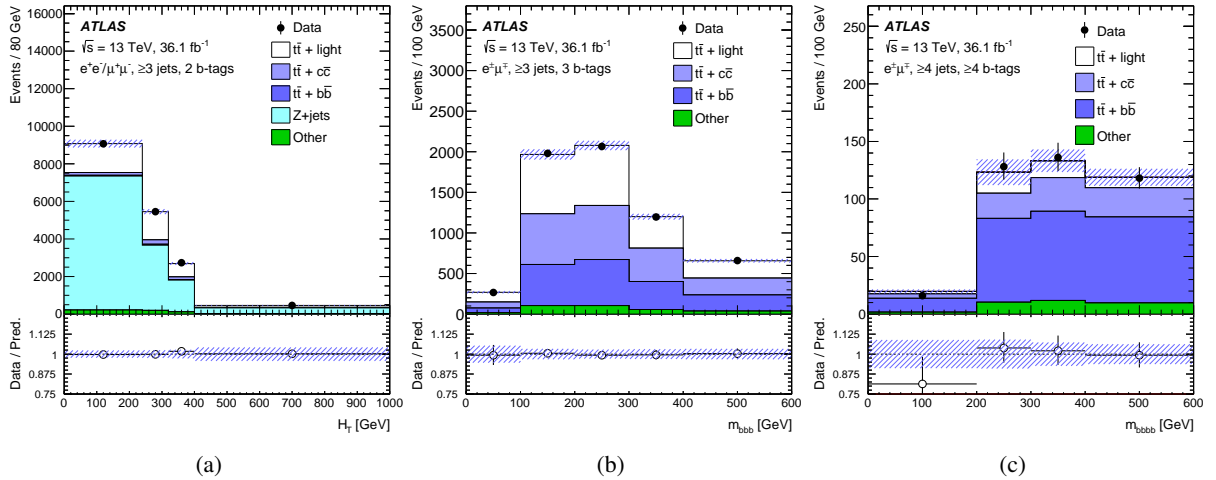


Figure 7: Comparison between data and prediction in the dilepton control regions of (a) the H_T variable for same-flavour dilepton events with (2ℓ , $3j$, $2b$) and the invariant mass of b -tagged jets for different-flavour dilepton events with (b) (2ℓ , $\geq 3j$, $3b$) and (c) (2ℓ , $\geq 4j$, $\geq 4b$), after the combined single-lepton and dilepton fit to the data. The last bin contains the overflow.

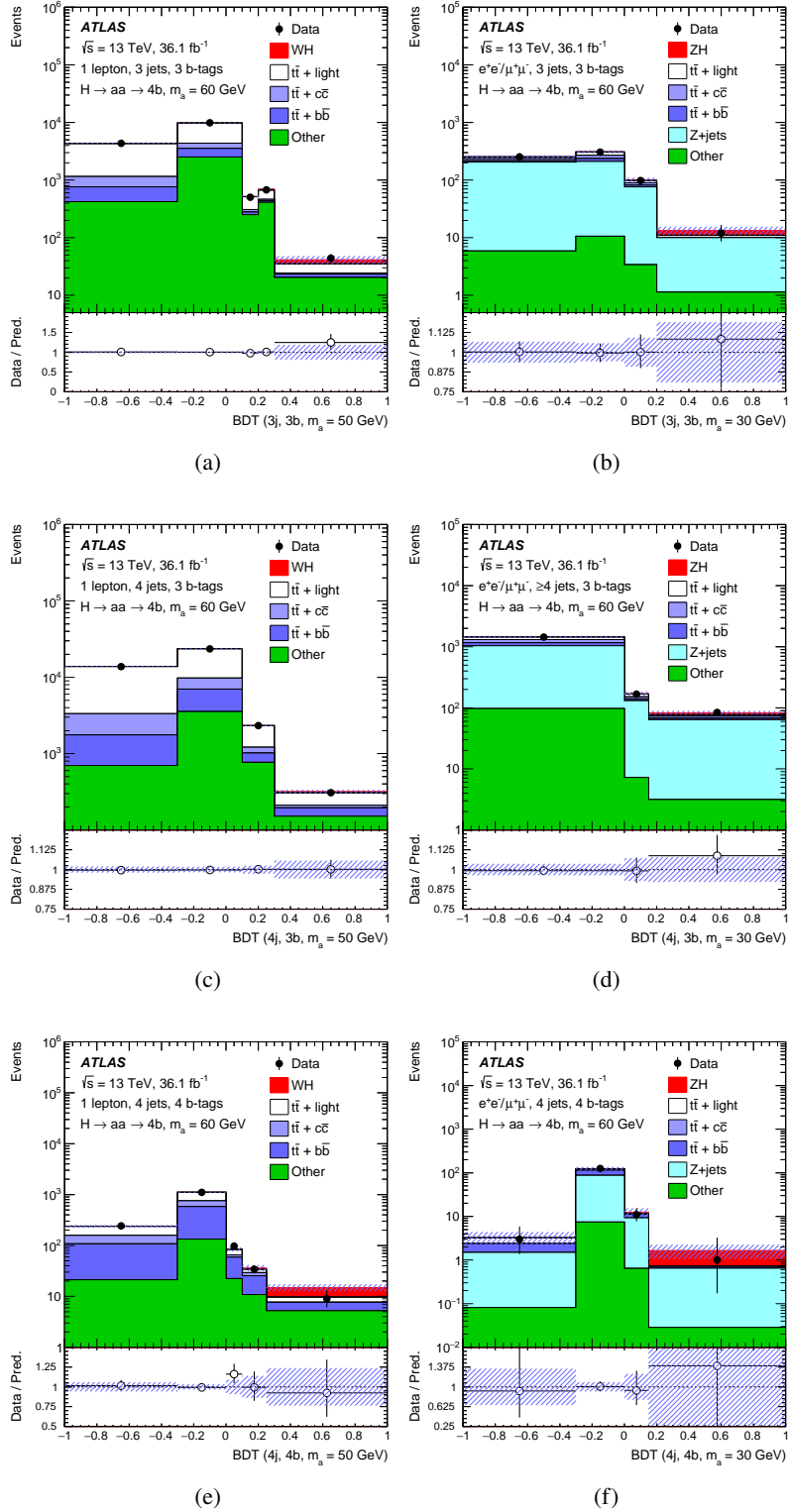


Figure 8: Comparison between data and prediction for the BDT discriminants in the (left) single-lepton signal regions trained with a signal with $m_a = 50$ GeV: (a) (1ℓ , 3j, 3b), (c) (1ℓ , 4j, 3b) and (e) (1ℓ , 4j, 4b) and in the (right) same-flavour dilepton signal regions trained with a signal with $m_a = 30$ GeV: (b) (2ℓ , 3j, 3b), (d) (2ℓ , $\geq 4j$, 3b) and (f) (2ℓ , $\geq 4j$, $\geq 4b$), after performing the combined single-lepton and dilepton fit of the predictions in all SRs and CRs to the data. The signal yield (solid red) is normalized to $\hat{\mu}$ after the fit for a signal with $m_a = 60$ GeV.

Table 5: Expected event yields of the post-fit background estimates and observed data in three signal regions for the single-lepton and dilepton channels after the combined single-lepton and dilepton fit to the data. The expected number of signal events for a few representative values of m_a are indicated, assuming the SM $pp \rightarrow WH$ and ZH cross-sections, $\sigma_{\text{SM}}(WH) = 1.37$ pb and $\sigma_{\text{SM}}(ZH) = 0.88$ pb [102], respectively, and $\mathcal{B}(H \rightarrow aa \rightarrow 4b) = 1$. The uncertainties include statistical and systematic components. The total uncertainty can differ from the sum in quadrature of individual sources due to correlations.

Process	(1 ℓ , 3j, 3b)	(1 ℓ , 4j, 3b)	(1 ℓ , 4j, 4b)	(2 ℓ , 3j, 3b)	(2 ℓ , ≥ 4 j, 3b)	(2 ℓ , ≥ 4 j, ≥ 4 b)
$t\bar{t}$ + light	9040 \pm 490	25600 \pm 1300	469 \pm 76	65 \pm 25	161 \pm 48	5 \pm 4
$t\bar{t}$ + $c\bar{c}$	1240 \pm 570	4500 \pm 1500	240 \pm 100	60 \pm 32	165 \pm 66	6 \pm 6
$t\bar{t}$ + $b\bar{b}$	1470 \pm 690	4900 \pm 1100	580 \pm 150	41 \pm 16	137 \pm 43	30 \pm 9
$t\bar{t}$ + $\gamma/W/Z$	18 \pm 2	88 \pm 7	16 \pm 2	1.2 \pm 0.4	45 \pm 6	7 \pm 1
Z + jets	137 \pm 75	205 \pm 67	8 \pm 6	483 \pm 42	1123 \pm 73	91 \pm 17
W + jets	1400 \pm 380	1550 \pm 490	53 \pm 20	-	-	-
Single top quark	1360 \pm 160	2210 \pm 320	57 \pm 31	4 \pm 2	10 \pm 3	1 \pm 1
Dibosons	-	-	-	12 \pm 7	45 \pm 22	1 \pm 1
Fakes	860 \pm 280	1130 \pm 370	68 \pm 20	3 \pm 1	8 \pm 2	0.3 \pm 0.1
Total	15520 \pm 470	40190 \pm 880	1485 \pm 88	670 \pm 31	1693 \pm 60	140 \pm 12
Data	15428	40045	1488	670	1689	140
$H \rightarrow aa \rightarrow 4b$	WH			ZH		
$m_a = 60$ GeV	103 \pm 24	100 \pm 21	27 \pm 9	28 \pm 6	55 \pm 10	12 \pm 4
$m_a = 40$ GeV	120 \pm 25	100 \pm 19	24 \pm 7	32 \pm 7	55 \pm 10	11 \pm 3
$m_a = 20$ GeV	65 \pm 15	52 \pm 11	9 \pm 3	18 \pm 4	25 \pm 5	4 \pm 1

to ZH cross-sections follows the SM prediction. The observed (expected) 95% CL upper limits on μ range from 3.0 (2.2) pb, for $m_a = 20$ GeV, to 1.3 (0.74) pb, for $m_a = 60$ GeV. The combined result excludes branching ratios as low as 0.45 in the mass range m_a between about 25 GeV and 60 GeV, assuming the SM WH and ZH cross-sections. The reduced sensitivity for the lighter a -boson hypotheses, where it is not possible to set limits on the branching ratio, is due to a lower acceptance caused by overlapping b -jets.

Lifetime-dependent 95% CL upper limits on the cross-section times $\mathcal{B}(H \rightarrow aa \rightarrow 4b)$ for the combination of single-lepton and dilepton channels are shown in figure 10. For a -boson mean proper lifetimes up to ~ 0.5 mm, the increased displacement of the b -jets leads to an enhanced b -tagging efficiency, and the limits improve slightly. For longer a -boson lifetimes, the b -jets become sufficiently displaced such that the jet reconstruction and b -tagging efficiencies are diminished and the limits decrease rapidly.

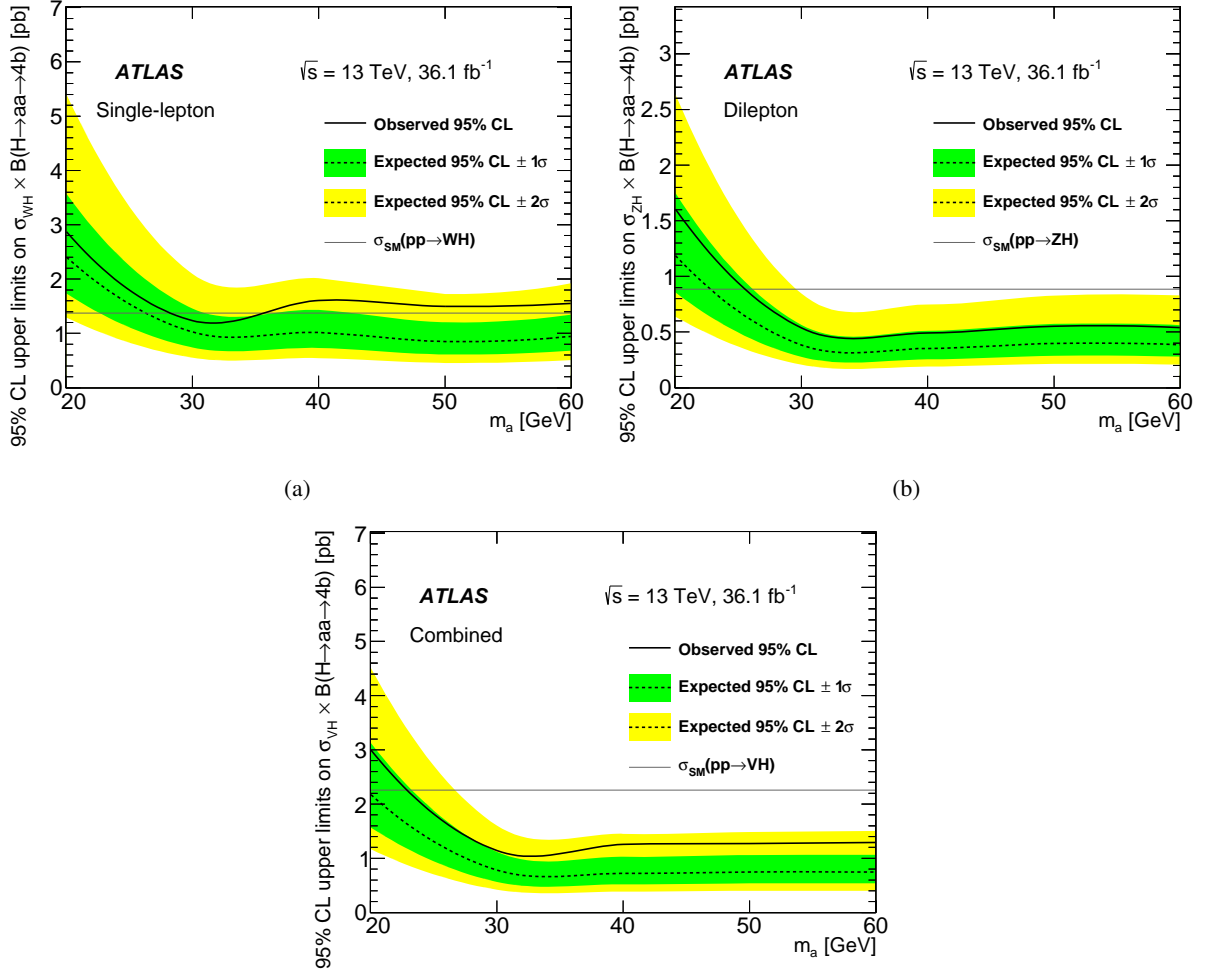


Figure 9: Summary of the 95% CL upper limits on $\sigma \times \mathcal{B}(H \rightarrow aa \rightarrow 4b)$ for (a) the single-lepton channel and (b) the dilepton channel, and (c) the combination of both channels. The observed limits are shown, together with the expected limits (dotted black lines). In the case of the expected limits, one- and two-standard-deviation uncertainty bands are also displayed.

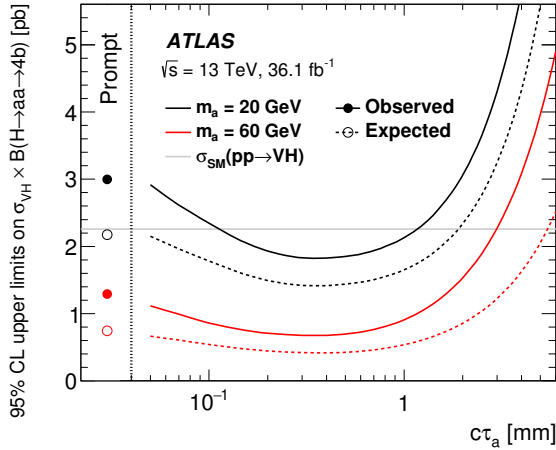


Figure 10: Summary of the expected and observed combined 95% CL upper limits on $\sigma \times \mathcal{B}(H \rightarrow aa \rightarrow 4b)$ with prompt and long-lived a -bosons. Expected (observed) limits for prompt a -bosons are shown as empty (filled) circles. Expected (observed) limits for long-lived signals are shown as dashed (solid) lines for two signal scenarios: $m_a = 20$ and 60 GeV.

9 Conclusion

This paper presents a search for exotic decays of the Higgs boson into a pair of spin-zero particles, $H \rightarrow aa$, where the a -boson decays into two b -quarks. The search focuses on processes in which the Higgs boson is produced in association with a W or Z boson that decays leptonically. The analysis uses the pp collision dataset at $\sqrt{s} = 13$ TeV recorded by the ATLAS detector at the LHC in 2015 and 2016, corresponding to an integrated luminosity of $36.1 \pm 0.8 \text{ fb}^{-1}$. The search for $H \rightarrow aa \rightarrow 4b$ is performed in the mass range $20 \text{ GeV} \leq m_a \leq 60 \text{ GeV}$, considering prompt as well as long-lived a -bosons with mean proper lifetimes $c\tau_a$ up to 6 mm. The analysis uses several kinematic variables combined in a multivariate discriminant in signal regions and uses control regions to reduce uncertainties in the background estimates. No significant excess of data is observed relative to the SM predictions. Upper limits at 95% CL are derived for the WH and ZH production cross-section times branching ratio of the decay $H \rightarrow aa \rightarrow 4b$. The combined observed upper limit for promptly decaying a -bosons ranges from 3.0 pb for $m_a = 20$ GeV to 1.3 pb for $m_a = 60$ GeV, assuming that the ratio of WH to ZH cross-sections follows the SM prediction. For a -bosons with longer proper lifetimes, the best limits are 1.8 pb and 0.68 pb, for $m_a = 20$ GeV and 60 GeV respectively, at $c\tau_a \sim 0.4$ mm.

Acknowledgements

We thank CERN for the very successful operation of the LHC, as well as the support staff from our institutions without whom ATLAS could not be operated efficiently.

We acknowledge the support of ANPCyT, Argentina; YerPhI, Armenia; ARC, Australia; BMWFW and FWF, Austria; ANAS, Azerbaijan; SSTC, Belarus; CNPq and FAPESP, Brazil; NSERC, NRC and CFI, Canada; CERN; CONICYT, Chile; CAS, MOST and NSFC, China; COLCIENCIAS, Colombia; MSMT CR, MPO CR and VSC CR, Czech Republic; DNRF and DNSRC, Denmark; IN2P3-CNRS, CEA-DRF/IRFU, France; SRNSFG, Georgia; BMBF, HGF, and MPG, Germany; GSRT, Greece; RGC, Hong Kong SAR, China; ISF, I-CORE and Benoziyo Center, Israel; INFN, Italy; MEXT and JSPS, Japan; CNRST, Morocco; NWO, Netherlands; RCN, Norway; MNiSW and NCN, Poland; FCT, Portugal; MNE/IFA, Romania; MES of Russia and NRC KI, Russian Federation; JINR; MESTD, Serbia; MSSR, Slovakia; ARRS and MIZŠ, Slovenia; DST/NRF, South Africa; MINECO, Spain; SRC and Wallenberg Foundation, Sweden; SERI, SNSF and Cantons of Bern and Geneva, Switzerland; MOST, Taiwan; TAEK, Turkey; STFC, United Kingdom; DOE and NSF, United States of America. In addition, individual groups and members have received support from BCKDF, the Canada Council, CANARIE, CRC, Compute Canada, FQRNT, and the Ontario Innovation Trust, Canada; EPLANET, ERC, ERDF, FP7, Horizon 2020 and Marie Skłodowska-Curie Actions, European Union; Investissements d’Avenir Labex and Idex, ANR, Région Auvergne and Fondation Partager le Savoir, France; DFG and AvH Foundation, Germany; Herakleitos, Thales and Aristeia programmes co-financed by EU-ESF and the Greek NSRF; BSF, GIF and Minerva, Israel; BRF, Norway; CERCA Programme Generalitat de Catalunya, Generalitat Valenciana, Spain; the Royal Society and Leverhulme Trust, United Kingdom.

The crucial computing support from all WLCG partners is acknowledged gratefully, in particular from CERN, the ATLAS Tier-1 facilities at TRIUMF (Canada), NDGF (Denmark, Norway, Sweden), CC-IN2P3 (France), KIT/GridKA (Germany), INFN-CNAF (Italy), NL-T1 (Netherlands), PIC (Spain), ASGC (Taiwan), RAL (UK) and BNL (USA), the Tier-2 facilities worldwide and large non-WLCG resource providers. Major contributors of computing resources are listed in Ref. [103].

References

- [1] ATLAS Collaboration, *Observation of a new particle in the search for the Standard Model Higgs boson with the ATLAS detector at the LHC*, *Phys. Lett. B* **716** (2012) 1, arXiv: [1207.7214 \[hep-ex\]](#).
- [2] CMS Collaboration, *Observation of a new boson at a mass of 125 GeV with the CMS experiment at the LHC*, *Phys. Lett. B* **716** (2012) 30, arXiv: [1207.7235 \[hep-ex\]](#).
- [3] ATLAS Collaboration, *Measurements of the Higgs boson production and decay rates and coupling strengths using pp collision data at $\sqrt{s} = 7$ and 8 TeV in the ATLAS experiment*, *Eur. Phys. J. C* **76** (2016) 6, arXiv: [1507.04548 \[hep-ex\]](#).
- [4] CMS Collaboration, *Precise determination of the mass of the Higgs boson and tests of compatibility of its couplings with the standard model predictions using proton collisions at 7 and 8 TeV*, *Eur. Phys. J. C* **75** (2015) 212, arXiv: [1412.8662 \[hep-ex\]](#).
- [5] ATLAS and CMS Collaborations, *Measurements of the Higgs boson production and decay rates and constraints on its couplings from a combined ATLAS and CMS analysis of the LHC pp collision data at $\sqrt{s} = 7$ and 8 TeV*, *JHEP* **08** (2016) 045, arXiv: [1606.02266 \[hep-ex\]](#).
- [6] M. J. Strassler and K. M. Zurek, *Echoes of a hidden valley at hadron colliders*, *Phys. Lett. B* **651** (2007) 374, arXiv: [hep-ph/0604261 \[hep-ph\]](#).
- [7] R. M. Schabinger and J. D. Wells, *Minimal spontaneously broken hidden sector and its impact on Higgs boson physics at the CERN Large Hadron Collider*, *Phys. Rev. D* **72** (2005) 093007, arXiv: [hep-ph/0509209 \[hep-ph\]](#).
- [8] B. Patt and F. Wilczek, *Higgs-field Portal into Hidden Sectors*, (2006), arXiv: [hep-ph/0605188 \[hep-ph\]](#).
- [9] D. Curtin et al., *Exotic Decays of the 125 GeV Higgs Boson*, *Phys. Rev. D* **90** (2014) 075004, arXiv: [1312.4992 \[hep-ph\]](#).
- [10] B. A. Dobrescu and K. T. Matchev, *Light axion within the next-to-minimal supersymmetric standard model*, *JHEP* **09** (2000) 031, arXiv: [hep-ph/0008192](#).
- [11] U. Ellwanger, J. F. Gunion, C. Hugonie and S. Moretti, *Towards a No-Lose Theorem for NMSSM Higgs Discovery at the LHC*, (2003), arXiv: [hep-ph/0305109](#).
- [12] R. Dermisek and J. F. Gunion, *Escaping the Large Fine-Tuning and Little Hierarchy Problems in the Next to Minimal Supersymmetric Model and $h \rightarrow aa$ Decays*, *Phys. Rev. Lett.* **95** (2005) 041801, arXiv: [hep-ph/0502105](#).
- [13] S. Chang, R. Dermisek, J. F. Gunion and N. Weiner, *Nonstandard Higgs Boson Decays*, *Ann. Rev. Nucl. Part. Sci.* **58** (2008) 75, arXiv: [0801.4554 \[hep-ph\]](#).
- [14] D. E. Morrissey and A. Pierce, *Modified Higgs boson phenomenology from gauge or gaugino mediation in the next-to-minimal supersymmetric standard model*, *Phys. Rev. D* **78** (2008) 075029, arXiv: [0807.2259 \[hep-ph\]](#).

- [15] S. Profumo, M. J. Ramsey-Musolf and G. Shaughnessy, *Singlet Higgs phenomenology and the electroweak phase transition*, **JHEP** **08** (2007) 010, arXiv: [0705.2425 \[hep-ph\]](#).
- [16] N. Blinov, J. Kozaczuk, D. E. Morrissey and C. Tamarit, *Electroweak baryogenesis from exotic electroweak symmetry breaking*, **Phys. Rev. D** **92** (2015) 035012, arXiv: [1504.05195 \[hep-ph\]](#).
- [17] G. Burdman, Z. Chacko, H.-S. Goh and R. Harnik, *Folded supersymmetry and the LEP paradox*, **JHEP** **02** (2007) 009, arXiv: [hep-ph/0609152](#).
- [18] N. Craig, A. Katz, M. Strassler and R. Sundrum, *Naturalness in the dark at the LHC*, **JHEP** **07** (2015) 105, arXiv: [1501.05310 \[hep-ph\]](#).
- [19] D. Curtin and C. B. Verhaaren, *Discovering uncolored naturalness in exotic higgs decays*, **JHEP** **12** (2015) 072, arXiv: [1506.06141 \[hep-ph\]](#).
- [20] V. Silveira and A. Zee, *Scalar Phantoms*, **Phys. Lett. B** **161** (1985) 136.
- [21] M. Pospelov, A. Ritz and M. B. Voloshin, *Secluded WIMP dark matter*, **Phys. Lett. B** **662** (2008) 53, arXiv: [0711.4866 \[hep-ph\]](#).
- [22] P. Draper, T. Liu, C. E. M. Wagner, L.-T. Wang and H. Zhang, *Dark Light-Higgs Bosons*, **Phys. Rev. Lett.** **106** (2011) 121805, arXiv: [1009.3963 \[hep-ph\]](#).
- [23] S. Ipek, D. McKeen and A. E. Nelson, *A renormalizable model for the Galactic Center gamma ray excess from dark matter annihilation*, **Phys. Rev. D** **90** (2014) 055021, arXiv: [1404.3716 \[hep-ph\]](#).
- [24] A. Martin, J. Shelton and J. Unwin, *Fitting the Galactic Center gamma-ray excess with cascade annihilations*, **Phys. Rev. D** **90** (2014) 103513, arXiv: [1405.0272 \[hep-ph\]](#).
- [25] M. Ajello et al., *Fermi-LAT Observations of High-Energy γ -Ray Emission Toward the Galactic Center*, **Astrophys. J.** **819** (2016) 44, arXiv: [1511.02938 \[astro-ph.HE\]](#).
- [26] C. Boehm, M. J. Dolan, C. McCabe, M. Spannowsky and C. J. Wallace, *Extended gamma-ray emission from Coy Dark Matter*, **JCAP** **1405** (2014) 009, arXiv: [1401.6458 \[hep-ph\]](#).
- [27] ATLAS Collaboration, *Search for the Higgs boson produced in association with a W boson and decaying to four b-quarks via two spin-zero particles in pp collisions at 13 TeV with the ATLAS detector*, **Eur. Phys. J. C** **76** (2016) 605, arXiv: [1606.08391 \[hep-ex\]](#).
- [28] ATLAS Collaboration, *Search for the Standard Model Higgs boson produced in association with top quarks and decaying into a $b\bar{b}$ pair in pp collisions at $\sqrt{s} = 13$ TeV with the ATLAS detector*, **Phys. Rev. D** **97** (2018) 072016, arXiv: [1712.08895 \[hep-ex\]](#).
- [29] ATLAS Collaboration, *Search for the Standard Model Higgs boson produced in association with top quarks and decaying into $b\bar{b}$ in pp collisions at $\sqrt{s} = 8$ TeV with the ATLAS detector*, **Eur. Phys. J. C** **75** (2015) 349, arXiv: [1503.05066 \[hep-ex\]](#).
- [30] ATLAS Collaboration, *Search for production of vector-like quark pairs and of four top quarks in the lepton-plus-jets final state in pp collisions at $\sqrt{s} = 8$ TeV with the ATLAS detector*, **JHEP** **08** (2015) 105, arXiv: [1505.04306 \[hep-ex\]](#).

- [31] ATLAS Collaboration, *Search for flavour-changing neutral current top quark decays $t \rightarrow Hq$ in pp collisions at $\sqrt{s} = 8$ TeV with the ATLAS detector*, *JHEP* **12** (2015) 061, arXiv: [1509.06047 \[hep-ex\]](#).
- [32] ATLAS Collaboration, *Search for charged Higgs bosons in the $H^\pm \rightarrow tb$ decay channel in pp collisions at $\sqrt{s} = 8$ TeV using the ATLAS detector*, *JHEP* **03** (2016) 127, arXiv: [1512.03704 \[hep-ex\]](#).
- [33] ATLAS Collaboration, *The ATLAS Experiment at the CERN Large Hadron Collider*, *JINST* **3** (2008) S08003.
- [34] ATLAS Collaboration, *ATLAS Insertable B-Layer Technical Design Report*, ATLAS-TDR-19 (2010), URL: <http://cdsweb.cern.ch/record/1291633>.
- [35] ATLAS Collaboration, *Luminosity determination in pp collisions at $\sqrt{s} = 8$ TeV using the ATLAS detector at the LHC*, *Eur. Phys. J. C* **76** (2016) 653, arXiv: [1608.03953 \[hep-ex\]](#).
- [36] ATLAS Collaboration, *Performance of the ATLAS Trigger System in 2015*, *Eur. Phys. J. C* **77** (2017) 317, arXiv: [1611.09661 \[hep-ex\]](#).
- [37] ATLAS Collaboration, *Electron reconstruction and identification efficiency measurements with the ATLAS detector using the 2011 LHC proton-proton collision data*, *Eur. Phys. J. C* **74** (2014) 2941, arXiv: [1404.2240 \[hep-ex\]](#).
- [38] ATLAS Collaboration, *Electron efficiency measurements with the ATLAS detector using the 2015 LHC proton-proton collision data*, ATLAS-CONF-2016-024 (2016), URL: <https://cds.cern.ch/record/2157687>.
- [39] ATLAS Collaboration, *Muon reconstruction performance of the ATLAS detector in proton-proton collision data at $\sqrt{s} = 13$ TeV*, *Eur. Phys. J. C* **76** (2016) 292, arXiv: [1603.05598 \[hep-ex\]](#).
- [40] ATLAS Collaboration, *Topological cell clustering in the ATLAS calorimeters and its performance in LHC Run 1*, *Eur. Phys. J. C* **77** (2017) 490, arXiv: [1603.02934 \[hep-ex\]](#).
- [41] M. Cacciari, G. P. Salam and G. Soyez, *The anti- k_t jet clustering algorithm*, *JHEP* **04** (2008) 063, arXiv: [0802.1189 \[hep-ph\]](#).
- [42] M. Cacciari, G. P. Salam and G. Soyez, *FastJet user manual*, *Eur. Phys. J. C* **72** (2012) 1896, arXiv: [1111.6097 \[hep-ph\]](#).
- [43] ATLAS Collaboration, *Jet energy scale measurements and their systematic uncertainties in proton-proton collisions at $\sqrt{s} = 13$ TeV with the ATLAS detector*, *Phys. Rev. D* **96** (2017) 072002, arXiv: [1703.09665 \[hep-ex\]](#).
- [44] ATLAS Collaboration, *Selection of jets produced in 13 TeV proton-proton collisions with the ATLAS detector*, ATLAS-CONF-2015-029, 2015, URL: <https://cds.cern.ch/record/2037702>.
- [45] ATLAS Collaboration, *Tagging and suppression of pileup jets with the ATLAS detector*, ATLAS-CONF-2014-018 (2014), URL: <https://cds.cern.ch/record/1700870>.
- [46] ATLAS Collaboration, *Performance of b -jet identification in the ATLAS experiment*, *JINST* **11** (2016) P04008, arXiv: [1512.01094 \[hep-ex\]](#).

- [47] ATLAS Collaboration, *Optimisation of the ATLAS b-tagging performance for the 2016 LHC Run*, ATL-PHYS-PUB-2016-012 (2016), URL: <https://cds.cern.ch/record/2160731>.
- [48] ATLAS Collaboration, *Performance of missing transverse momentum reconstruction with the ATLAS detector using proton-proton collisions at $\sqrt{s} = 13$ TeV*, (2018), arXiv: [1802.08168](https://arxiv.org/abs/1802.08168) [hep-ex].
- [49] ATLAS Collaboration, *The ATLAS Simulation Infrastructure*, *Eur. Phys. J. C* **70** (2010) 823, arXiv: [1005.4568](https://arxiv.org/abs/1005.4568) [physics.ins-det].
- [50] S. Agostinelli et al., *GEANT4 – a simulation toolkit*, *Nucl. Instrum. Meth. A* **506** (2003) 250.
- [51] ATLAS Collaboration, *The simulation principle and performance of the ATLAS fast calorimeter simulation FastCaloSim*, ATL-PHYS-PUB-2010-013, 2010, URL: <https://cds.cern.ch/record/1300517>.
- [52] T. Sjöstrand, S. Mrenna and P. Z. Skands, *A brief introduction to PYTHIA 8.1*, *Comput. Phys. Commun.* **178** (2008) 852, arXiv: [0710.3820](https://arxiv.org/abs/0710.3820) [hep-ph].
- [53] ATLAS Collaboration, *Summary of ATLAS Pythia 8 tunes*, ATL-PHYS-PUB-2012-003 (2012), URL: <https://cds.cern.ch/record/1474107>.
- [54] A. D. Martin, W. J. Stirling, R. S. Thorne and G. Watt, *Parton distributions for the LHC*, *Eur. Phys. J. C* **63** (2009) 189, arXiv: [0901.0002](https://arxiv.org/abs/0901.0002) [hep-ph].
- [55] D. J. Lange, *The EvtGen particle decay simulation package*, *Nucl. Instrum. Meth. A* **462** (2001) 152.
- [56] T. Gleisberg et al., *Event generation with SHERPA 1.1*, *JHEP* **02** (2009) 007, arXiv: [0811.4622](https://arxiv.org/abs/0811.4622) [hep-ph].
- [57] P. Nason, *A new method for combining NLO QCD with shower Monte Carlo algorithms*, *JHEP* **11** (2004) 040, arXiv: [hep-ph/0409146](https://arxiv.org/abs/hep-ph/0409146).
- [58] S. Frixione, P. Nason and G. Ridolfi, *A Positive-weight next-to-leading-order Monte Carlo for heavy flavour hadroproduction*, *JHEP* **09** (2007) 126, arXiv: [0707.3088](https://arxiv.org/abs/0707.3088) [hep-ph].
- [59] S. Frixione, P. Nason and C. Oleari, *Matching NLO QCD computations with parton shower simulations: the POWHEG method*, *JHEP* **11** (2007) 070, arXiv: [0709.2092](https://arxiv.org/abs/0709.2092) [hep-ph].
- [60] S. Alioli, P. Nason, C. Oleari and E. Re, *A general framework for implementing NLO calculations in shower Monte Carlo programs: the POWHEG BOX*, *JHEP* **06** (2010) 043, arXiv: [1002.2581](https://arxiv.org/abs/1002.2581) [hep-ph].
- [61] H.-L. Lai, M. Guzzi, J. Huston, Z. Li, P. M. Nadolsky et al., *New parton distributions for collider physics*, *Phys. Rev. D* **82** (2010) 074024, arXiv: [1007.2241](https://arxiv.org/abs/1007.2241) [hep-ph].
- [62] ATLAS Collaboration, *ATLAS Run 1 Pythia 8 tunes*, ATL-PHYS-PUB-2014-021 (2014), URL: <http://cdsweb.cern.ch/record/1966419>.
- [63] J. Alwall et al., *The automated computation of tree-level and next-to-leading order differential cross sections, and their matching to parton shower simulations*, *JHEP* **07** (2014) 079, arXiv: [1405.0301](https://arxiv.org/abs/1405.0301) [hep-ph].

- [64] R. D. Ball et al., *Parton distributions for the LHC Run II*, **JHEP** **04** (2015) 040, arXiv: [1410.8849 \[hep-ph\]](#).
- [65] D. Curtin, R. Essig, S. Gori and J. Shelton, *Illuminating dark photons with high-energy colliders*, **JHEP** **02** (2015) 157, arXiv: [1412.0018 \[hep-ph\]](#).
- [66] D. de Florian et al., *Handbook of LHC Higgs Cross Sections: 4. Deciphering the Nature of the Higgs Sector*, 2016, arXiv: [1610.07922 \[hep-ph\]](#).
- [67] J. M. Campbell, R. K. Ellis, P. Nason and E. Re, *Top-pair production and decay at NLO matched with parton showers*, **JHEP** **04** (2015) 114, arXiv: [1412.1828 \[hep-ph\]](#).
- [68] ATLAS Collaboration, *Studies on top-quark Monte Carlo modelling for Top2016*, ATL-PHYS-PUB-2016-020 (2016), URL: <https://cds.cern.ch/record/2216168>.
- [69] T. Sjöstrand et al., *An introduction to PYTHIA 8.2*, **Comput. Phys. Commun.** **191** (2015) 159, arXiv: [1410.3012 \[hep-ph\]](#).
- [70] M. Czakon and A. Mitov, *Top++: A program for the calculation of the top-pair cross-section at hadron colliders*, **Comput. Phys. Commun.** **185** (2014) 2930, arXiv: [1112.5675 \[hep-ph\]](#).
- [71] F. Cascioli, P. Maierhofer, N. Moretti, S. Pozzorini and F. Siegert, *NLO matching for $t\bar{t}b\bar{b}$ production with massive b -quarks*, **Phys. Lett. B** **734** (2014) 210, arXiv: [1309.5912 \[hep-ph\]](#).
- [72] F. Cascioli, P. Maierhofer and S. Pozzorini, *Scattering Amplitudes with Open Loops*, **Phys. Rev. Lett.** **108** (2012) 111601, arXiv: [1111.5206 \[hep-ph\]](#).
- [73] E. Re, *Single-top Wt -channel production matched with parton showers using the POWHEG method*, **Eur. Phys. J. C** **71** (2011) 1547, arXiv: [1009.2450 \[hep-ph\]](#).
- [74] S. Alioli, P. Nason, C. Oleari and E. Re, *NLO single-top production matched with shower in POWHEG: s - and t -channel contributions*, **JHEP** **09** (2009) 111, [Erratum: **JHEP** **02** (2010) 011], arXiv: [0907.4076 \[hep-ph\]](#).
- [75] S. Schumann and F. Krauss, *A Parton shower algorithm based on Catani-Seymour dipole factorisation*, **JHEP** **03** (2008) 038, arXiv: [0709.1027 \[hep-ph\]](#).
- [76] T. Gleisberg and S. Höche, *Comix, a new matrix element generator*, **JHEP** **12** (2008) 039, arXiv: [0808.3674 \[hep-ph\]](#).
- [77] S. Höche, F. Krauss, M. Schönherr and F. Siegert, *QCD matrix elements + parton showers: The NLO case*, **JHEP** **04** (2013) 027, arXiv: [1207.5030 \[hep-ph\]](#).
- [78] K. Melnikov and F. Petriello, *Electroweak gauge boson production at hadron colliders through $O(\alpha_S^2)$* , **Phys. Rev. D** **74** (2006) 114017, arXiv: [hep-ph/0609070](#).
- [79] ATLAS Collaboration, *Measurement of W^\pm and Z Boson Production Cross Sections in pp Collisions at $\sqrt{s} = 13$ TeV with the ATLAS Detector*, ATLAS-CONF-2015-039, 2015, URL: <https://cds.cern.ch/record/2045487>.

- [80] ATLAS Collaboration, *Multi-boson simulation for 13 TeV ATLAS analyses*, ATL-PHYS-PUB-2016-002 (2016), URL: <https://cds.cern.ch/record/2119986>.
- [81] S. Frixione, E. Laenen, P. Motylinski, B. R. Webber and C. D. White, *Single-top hadroproduction in association with a W boson*, *JHEP* **07** (2008) 029, arXiv: [0805.3067](https://arxiv.org/abs/0805.3067) [[hep-ph](#)].
- [82] T. Sjöstrand, S. Mrenna and P. Z. Skands, *PYTHIA 6.4 physics and manual*, *JHEP* **05** (2006) 026, arXiv: [hep-ph/0603175](https://arxiv.org/abs/hep-ph/0603175).
- [83] P. Z. Skands, *Tuning Monte Carlo generators: The Perugia tunes*, *Phys. Rev. D* **82** (2010) 074018, arXiv: [1005.3457](https://arxiv.org/abs/1005.3457) [[hep-ph](#)].
- [84] M. Aliev et al., *HATHOR: HAdronic Top and Heavy quarks crOss section calculatoR*, *Comput. Phys. Commun.* **182** (2011) 1034, arXiv: [1007.1327](https://arxiv.org/abs/1007.1327) [[hep-ph](#)].
- [85] P. Kant et al., *HATHOR for single top-quark production: Updated predictions and uncertainty estimates for single top-quark production in hadronic collisions*, *Comput. Phys. Commun.* **191** (2015) 74, arXiv: [1406.4403](https://arxiv.org/abs/1406.4403) [[hep-ph](#)].
- [86] N. Kidonakis, *Two-loop soft anomalous dimensions for single top quark associated production with a W^- or H^-* , *Phys. Rev. D* **82** (2010) 054018, arXiv: [1005.4451](https://arxiv.org/abs/1005.4451) [[hep-ph](#)].
- [87] N. Kidonakis, *Top Quark Production*, *Proceedings, Helmholtz International Summer School on Physics of Heavy Quarks and Hadrons (HQ 2013): JINR, Dubna, Russia, July 15-28, 2013*, 2014 139, arXiv: [1311.0283](https://arxiv.org/abs/1311.0283) [[hep-ph](#)].
- [88] M. Bahr et al., *Herwig++ physics and manual*, *Eur. Phys. J. C* **58** (2008) 639, arXiv: [0803.0883](https://arxiv.org/abs/0803.0883) [[hep-ph](#)].
- [89] ATLAS Collaboration, *Estimation of non-prompt and fake lepton backgrounds in final states with top quarks produced in proton–proton collisions at $\sqrt{s} = 8$ TeV with the ATLAS Detector*, ATLAS-CONF-2014-058, 2014, URL: <https://cds.cern.ch/record/1951336>.
- [90] A. Hoecker et al., *TMVA - Toolkit for Multivariate Data Analysis*, 2007, arXiv: [physics/0703039](https://arxiv.org/abs/physics/0703039) [[physics.data-an](#)].
- [91] M. Burns, K. Kong, K. T. Matchev and M. Park, *Using subsystem MT2 for complete mass determinations in decay chains with missing energy at hadron colliders*, *JHEP* **03** (2009) 143, arXiv: [0810.5576](https://arxiv.org/abs/0810.5576) [[hep-ph](#)].
- [92] ATLAS Collaboration, *Measurement of the Inelastic Proton–Proton Cross Section at $\sqrt{s} = 13$ TeV with the ATLAS Detector at the LHC*, *Phys. Rev. Lett.* **117** (2016) 182002, arXiv: [1606.02625](https://arxiv.org/abs/1606.02625) [[hep-ex](#)].
- [93] ATLAS Collaboration, *Measurements of b-jet tagging efficiency with the ATLAS detector using $t\bar{t}$ events at $\sqrt{s} = 13$ TeV*, (2018), arXiv: [1805.01845](https://arxiv.org/abs/1805.01845) [[hep-ex](#)].
- [94] ATLAS Collaboration, *Calibration of light-flavour jet b-tagging rates on ATLAS proton-proton collision data at $\sqrt{s} = 13$ TeV*, ATLAS-CONF-2018-006 (2018), URL: <https://cds.cern.ch/record/2314418>.
- [95] J. Bellm et al., *Herwig 7.0/Herwig++ 3.0 release note*, *Eur. Phys. J. C* **76** (2016) 196, arXiv: [1512.01178](https://arxiv.org/abs/1512.01178) [[hep-ph](#)].
- [96] N. Kidonakis, *Next-to-next-to-leading-order collinear and soft gluon corrections for t-channel single top quark production*, *Phys. Rev. D* **83** (2011) 091503, arXiv: [1103.2792](https://arxiv.org/abs/1103.2792) [[hep-ph](#)].

- [97] N. Kidonakis, *NNLL resummation for s-channel single top quark production*, *Phys. Rev. D* **81** (2010) 054028, arXiv: [1001.5034 \[hep-ph\]](#).
- [98] J. M. Campbell and R. K. Ellis, *$t\bar{t}W^\pm$ production and decay at NLO*, *JHEP* **07** (2012) 052, arXiv: [1204.5678 \[hep-ph\]](#).
- [99] G. Cowan, K. Cranmer, E. Gross and O. Vitells, *Asymptotic formulae for likelihood-based tests of new physics*, *Eur. Phys. J. C* **71** (2011) 1554, [Erratum: *Eur. Phys. J. C* **73** (2013) 2501], arXiv: [1007.1727 \[physics.data-an\]](#).
- [100] A. L. Read, *Presentation of search results: The CL_S technique*, *J. Phys. G* **28** (2002) 2693.
- [101] T. Junk, *Confidence level computation for combining searches with small statistics*, *Nucl. Instrum. Meth. A* **434** (1999) 435, arXiv: [hep-ex/9902006](#).
- [102] J. R. Andersen et al., *Handbook of LHC Higgs Cross Sections: 3. Higgs Properties*, (2013), ed. by S. Heinemeyer, C. Mariotti, G. Passarino and R. Tanaka, arXiv: [1307.1347 \[hep-ph\]](#).
- [103] ATLAS Collaboration, *ATLAS Computing Acknowledgements*, ATL-GEN-PUB-2016-002, URL: <https://cds.cern.ch/record/2202407>.

The ATLAS Collaboration

M. Aaboud^{34d}, G. Aad⁹⁹, B. Abbott¹²⁴, O. Abdinov^{13,*}, B. Abeloos¹²⁸, D.K. Abhayasinghe⁹¹, S.H. Abidi¹⁶⁴, O.S. AbouZeid³⁹, N.L. Abraham¹⁵³, H. Abramowicz¹⁵⁸, H. Abreu¹⁵⁷, Y. Abulaiti⁶, B.S. Acharya^{64a,64b,o}, S. Adachi¹⁶⁰, L. Adamczyk^{81a}, J. Adelman¹¹⁹, M. Adersberger¹¹², A. Adiguzel^{12c,ah}, T. Adye¹⁴¹, A.A. Affolder¹⁴³, Y. Afik¹⁵⁷, C. Agheorghiesei^{27c}, J.A. Aguilar-Saavedra^{136f,136a}, F. Ahmadov^{77,af}, G. Aielli^{71a,71b}, S. Akatsuka⁸³, T.P.A. Åkesson⁹⁴, E. Akilli⁵², A.V. Akimov¹⁰⁸, G.L. Alberghi^{23b,23a}, J. Albert¹⁷³, P. Albicocco⁴⁹, M.J. Alconada Verzini⁸⁶, S. Alderweireldt¹¹⁷, M. Aleksa³⁵, I.N. Aleksandrov⁷⁷, C. Alexa^{27b}, T. Alexopoulos¹⁰, M. Alhroob¹²⁴, B. Ali¹³⁸, G. Alimonti^{66a}, J. Alison³⁶, S.P. Alkire¹⁴⁵, C. Allaire¹²⁸, B.M.M. Allbrooke¹⁵³, B.W. Allen¹²⁷, P.P. Allport²¹, A. Aloisio^{67a,67b}, A. Alonso³⁹, F. Alonso⁸⁶, C. Alpigiani¹⁴⁵, A.A. Alshehri⁵⁵, M.I. Alstady⁹⁹, B. Alvarez Gonzalez³⁵, D. Álvarez Piqueras¹⁷¹, M.G. Alviggi^{67a,67b}, B.T. Amadio¹⁸, Y. Amaral Coutinho^{78b}, L. Ambroz¹³¹, C. Amelung²⁶, D. Amidei¹⁰³, S.P. Amor Dos Santos^{136a,136c}, S. Amoroso⁴⁴, C.S. Amrouche⁵², C. Anastopoulos¹⁴⁶, L.S. Ancu⁵², N. Andari²¹, T. Andeen¹¹, C.F. Anders^{59b}, J.K. Anders²⁰, K.J. Anderson³⁶, A. Andreazza^{66a,66b}, V. Andrei^{59a}, C.R. Anelli¹⁷³, S. Angelidakis³⁷, I. Angelozzi¹¹⁸, A. Angerami³⁸, A.V. Anisenkov^{120b,120a}, A. Annovi^{69a}, C. Antel^{59a}, M.T. Anthony¹⁴⁶, M. Antonelli⁴⁹, D.J.A. Antrim¹⁶⁸, F. Anulli^{70a}, M. Aoki⁷⁹, J.A. Aparisi Pozo¹⁷¹, L. Aperio Bella³⁵, G. Arabidze¹⁰⁴, J.P. Araque^{136a}, V. Araujo Ferraz^{78b}, R. Araujo Pereira^{78b}, A.T.H. Arce⁴⁷, R.E. Ardell⁹¹, F.A. Arduh⁸⁶, J-F. Arguin¹⁰⁷, S. Argyropoulos⁷⁵, A.J. Armbruster³⁵, L.J. Armitage⁹⁰, A. Armstrong¹⁶⁸, O. Arnaez¹⁶⁴, H. Arnold¹¹⁸, M. Arratia³¹, O. Arslan²⁴, A. Artamonov^{109,*}, G. Artoni¹³¹, S. Artz⁹⁷, S. Asai¹⁶⁰, N. Asbah⁴⁴, A. Ashkenazi¹⁵⁸, E.M. Asimakopoulou¹⁶⁹, L. Asquith¹⁵³, K. Assamagan²⁹, R. Astalos^{28a}, R.J. Atkin^{32a}, M. Atkinson¹⁷⁰, N.B. Atlay¹⁴⁸, K. Augsten¹³⁸, G. Avolio³⁵, R. Avramidou^{58a}, M.K. Ayoub^{15a}, G. Azuelos^{107,au}, A.E. Baas^{59a}, M.J. Baca²¹, H. Bachacou¹⁴², K. Bachas^{65a,65b}, M. Backes¹³¹, P. Bagnaia^{70a,70b}, M. Bahmani⁸², H. Bahrasemani¹⁴⁹, A.J. Bailey¹⁷¹, J.T. Baines¹⁴¹, M. Bajic³⁹, C. Bakalis¹⁰, O.K. Baker¹⁸⁰, P.J. Bakker¹¹⁸, D. Bakshi Gupta⁹³, E.M. Baldin^{120b,120a}, P. Balek¹⁷⁷, F. Balli¹⁴², W.K. Balunas¹³³, J. Balz⁹⁷, E. Banas⁸², A. Bandyopadhyay²⁴, S. Banerjee^{178,k}, A.A.E. Bannoura¹⁷⁹, L. Barak¹⁵⁸, W.M. Barbe³⁷, E.L. Barberio¹⁰², D. Barberis^{53b,53a}, M. Barbero⁹⁹, T. Barillari¹¹³, M-S. Barisits³⁵, J. Barkeloo¹²⁷, T. Barklow¹⁵⁰, N. Barlow³¹, R. Barnea¹⁵⁷, S.L. Barnes^{58c}, B.M. Barnett¹⁴¹, R.M. Barnett¹⁸, Z. Barnovska-Blenessy^{58a}, A. Baroncelli^{72a}, G. Barone²⁶, A.J. Barr¹³¹, L. Barranco Navarro¹⁷¹, F. Barreiro⁹⁶, J. Barreiro Guimarães da Costa^{15a}, R. Bartoldus¹⁵⁰, A.E. Barton⁸⁷, P. Bartos^{28a}, A. Basalae¹³⁴, A. Bassalat¹²⁸, R.L. Bates⁵⁵, S.J. Batista¹⁶⁴, S. Batlamous^{34e}, J.R. Batley³¹, M. Battaglia¹⁴³, M. Bauce^{70a,70b}, F. Bauer¹⁴², K.T. Bauer¹⁶⁸, H.S. Bawa^{150,m}, J.B. Beacham¹²², M.D. Beattie⁸⁷, T. Beau¹³², P.H. Beauchemin¹⁶⁷, P. Bechtel²⁴, H.C. Beck⁵¹, H.P. Beck^{20,r}, K. Becker⁵⁰, M. Becker⁹⁷, C. Becot⁴⁴, A. Beddall^{12d}, A.J. Beddall^{12a}, V.A. Bednyakov⁷⁷, M. Bedognetti¹¹⁸, C.P. Bee¹⁵², T.A. Beermann³⁵, M. Begalli^{78b}, M. Beger²⁹, A. Behera¹⁵², J.K. Behr⁴⁴, A.S. Bell⁹², G. Bella¹⁵⁸, L. Bellagamba^{23b}, A. Bellerive³³, M. Bellomo¹⁵⁷, P. Bellos⁹, K. Belotskiy¹¹⁰, N.L. Belyaev¹¹⁰, O. Benary^{158,*}, D. Benchekroun^{34a}, M. Bender¹¹², N. Benekos¹⁰, Y. Benhammou¹⁵⁸, E. Benhar Noccioli¹⁸⁰, J. Benitez⁷⁵, D.P. Benjamin⁴⁷, M. Benoit⁵², J.R. Bensinger²⁶, S. Bentvelsen¹¹⁸, L. Beresford¹³¹, M. Beretta⁴⁹, D. Berge⁴⁴, E. Bergeaas Kuutmann¹⁶⁹, N. Berger⁵, L.J. Bergsten²⁶, J. Beringer¹⁸, S. Berlendis⁷, N.R. Bernard¹⁰⁰, G. Bernardi¹³², C. Bernius¹⁵⁰, F.U. Bernlochner²⁴, T. Berry⁹¹, P. Berta⁹⁷, C. Bertella^{15a}, G. Bertoli^{43a,43b}, I.A. Bertram⁸⁷, G.J. Besjes³⁹, O. Bessidskaia Bylund^{43a,43b}, M. Bessner⁴⁴, N. Besson¹⁴², A. Bethani⁹⁸, S. Bethke¹¹³, A. Betti²⁴, A.J. Bevan⁹⁰, J. Beyer¹¹³, R.M. Bianchi¹³⁵, O. Biebel¹¹², D. Biedermann¹⁹, R. Bielski⁹⁸, K. Bierwagen⁹⁷, N.V. Biesuz^{69a,69b}, M. Biglietti^{72a}, T.R.V. Billoud¹⁰⁷, M. Bindi⁵¹, A. Bingul^{12d}, C. Bini^{70a,70b}, S. Biondi^{23b,23a}, M. Birman¹⁷⁷, T. Bisanz⁵¹, J.P. Biswal¹⁵⁸, C. Bittrich⁴⁶,

D.M. Bjergaard⁴⁷, J.E. Black¹⁵⁰, K.M. Black²⁵, T. Blazek^{28a}, I. Bloch⁴⁴, C. Blocker²⁶, A. Blue⁵⁵,
 U. Blumenschein⁹⁰, Dr. Blunier^{144a}, G.J. Bobbink¹¹⁸, V.S. Bobrovnikov^{120b,120a}, S.S. Bocchetta⁹⁴,
 A. Bocci⁴⁷, D. Boerner¹⁷⁹, D. Bogavac¹¹², A.G. Bogdanchikov^{120b,120a}, C. Bohm^{43a}, V. Boisvert⁹¹,
 P. Bokan¹⁶⁹, T. Bold^{81a}, A.S. Boldyrev¹¹¹, A.E. Bolz^{59b}, M. Bomben¹³², M. Bona⁹⁰, J.S. Bonilla¹²⁷,
 M. Boonekamp¹⁴², A. Borisov¹⁴⁰, G. Borissov⁸⁷, J. Bortfeldt³⁵, D. Bortoletto¹³¹,
 V. Bortolotto^{71a,61b,61c,71b}, D. Boscherini^{23b}, M. Bosman¹⁴, J.D. Bossio Sola³⁰, K. Bouaouda^{34a},
 J. Boudreau¹³⁵, E.V. Bouhova-Thacker⁸⁷, D. Boumediene³⁷, C. Bourdarios¹²⁸, S.K. Boutle⁵⁵,
 A. Boveia¹²², J. Boyd³⁵, I.R. Boyko⁷⁷, A.J. Bozson⁹¹, J. Bracinik²¹, N. Brahimy⁹⁹, A. Brandt⁸,
 G. Brandt¹⁷⁹, O. Brandt^{59a}, F. Braren⁴⁴, U. Bratzler¹⁶¹, B. Brau¹⁰⁰, J.E. Brau¹²⁷,
 W.D. Breaden Madden⁵⁵, K. Brendlinger⁴⁴, A.J. Brennan¹⁰², L. Brenner⁴⁴, R. Brenner¹⁶⁹, S. Bressler¹⁷⁷,
 B. Brickwedde⁹⁷, D.L. Briglin²¹, D. Britton⁵⁵, D. Britzger^{59b}, I. Brock²⁴, R. Brock¹⁰⁴, G. Brooijmans³⁸,
 T. Brooks⁹¹, W.K. Brooks^{144b}, E. Brost¹¹⁹, J.H. Broughton²¹, P.A. Bruckman de Renstrom⁸²,
 D. Bruncko^{28b}, A. Bruni^{23b}, G. Bruni^{23b}, L.S. Bruni¹¹⁸, S. Bruno^{71a,71b}, B.H. Brunt³¹, M. Bruschi^{23b},
 N. Bruscano¹³⁵, P. Bryant³⁶, L. Bryngemark⁴⁴, T. Buanes¹⁷, Q. Buat³⁵, P. Buchholz¹⁴⁸, A.G. Buckley⁵⁵,
 I.A. Budagov⁷⁷, M.K. Bugge¹³⁰, F. Bühner⁵⁰, O. Bulekov¹¹⁰, D. Bullock⁸, T.J. Burch¹¹⁹, S. Burdin⁸⁸,
 C.D. Burgard¹¹⁸, A.M. Burger⁵, B. Burghgrave¹¹⁹, K. Burka⁸², S. Burke¹⁴¹, I. Burmeister⁴⁵,
 J.T.P. Burr¹³¹, D. Büscher⁵⁰, V. Büscher⁹⁷, E. Buschmann⁵¹, P. Bussey⁵⁵, J.M. Butler²⁵, C.M. Buttar⁵⁵,
 J.M. Butterworth⁹², P. Butti³⁵, W. Buttinger³⁵, A. Buzatu¹⁵⁵, A.R. Buzykaev^{120b,120a}, G. Cabras^{23b,23a},
 S. Cabrera Urbán¹⁷¹, D. Caforio¹³⁸, H. Cai¹⁷⁰, V.M.M. Cairo², O. Cakir^{4a}, N. Calace⁵², P. Calafiura¹⁸,
 A. Calandri⁹⁹, G. Calderini¹³², P. Calfayan⁶³, G. Callea^{40b,40a}, L.P. Caloba^{78b}, S. Calvente Lopez⁹⁶,
 D. Calvet³⁷, S. Calvet³⁷, T.P. Calvet¹⁵², M. Calvetti^{69a,69b}, R. Camacho Toro¹³², S. Camarda³⁵,
 P. Camarri^{71a,71b}, D. Cameron¹³⁰, R. Caminal Armadans¹⁰⁰, C. Camincher³⁵, S. Campana³⁵,
 M. Campanelli⁹², A. Camplani³⁹, A. Campoverde¹⁴⁸, V. Canale^{67a,67b}, M. Cano Bret^{58c}, J. Cantero¹²⁵,
 T. Cao¹⁵⁸, Y. Cao¹⁷⁰, M.D.M. Capeans Garrido³⁵, I. Caprini^{27b}, M. Caprini^{27b}, M. Capua^{40b,40a},
 R.M. Carbone³⁸, R. Cardarelli^{71a}, F.C. Cardillo⁵⁰, I. Carli¹³⁹, T. Carli³⁵, G. Carlino^{67a}, B.T. Carlson¹³⁵,
 L. Carminati^{66a,66b}, R.M.D. Carney^{43a,43b}, S. Caron¹¹⁷, E. Carquin^{144b}, S. Carrá^{66a,66b},
 G.D. Carrillo-Montoya³⁵, D. Casadei^{32b}, M.P. Casado^{14,g}, A.F. Casha¹⁶⁴, M. Casolino¹⁴,
 D.W. Casper¹⁶⁸, R. Castelijin¹¹⁸, F.L. Castillo¹⁷¹, V. Castillo Gimenez¹⁷¹, N.F. Castro^{136a,136e},
 A. Catinaccio³⁵, J.R. Catmore¹³⁰, A. Cattai³⁵, J. Caudron²⁴, V. Cavaliere²⁹, E. Cavallaro¹⁴, D. Cavalli^{66a},
 M. Cavalli-Sforza¹⁴, V. Cavasinni^{69a,69b}, E. Celebi^{12b}, F. Ceradini^{72a,72b}, L. Cerda Alberich¹⁷¹,
 A.S. Cerqueira^{78a}, A. Cerri¹⁵³, L. Cerrito^{71a,71b}, F. Cerutti¹⁸, A. Cervelli^{23b,23a}, S.A. Cetin^{12b},
 A. Chafaq^{34a}, D. Chakraborty¹¹⁹, S.K. Chan⁵⁷, W.S. Chan¹¹⁸, Y.L. Chan^{61a}, J.D. Chapman³¹,
 D.G. Charlton²¹, C.C. Chau³³, C.A. Chavez Barajas¹⁵³, S. Che¹²², A. Chegwiddden¹⁰⁴, S. Chekanov⁶,
 S.V. Chekulaev^{165a}, G.A. Chelkov^{77,at}, M.A. Chelstowska³⁵, C. Chen^{58a}, C.H. Chen⁷⁶, H. Chen²⁹,
 J. Chen^{58a}, J. Chen³⁸, S. Chen¹³³, S.J. Chen^{15c}, X. Chen^{15b,as}, Y. Chen⁸⁰, Y-H. Chen⁴⁴, H.C. Cheng¹⁰³,
 H.J. Cheng^{15d}, A. Cheplakov⁷⁷, E. Cheremushkina¹⁴⁰, R. Cherkaoui El Moursli^{34e}, E. Cheu⁷,
 K. Cheung⁶², L. Chevalier¹⁴², V. Chiarella⁴⁹, G. Chiarelli^{69a}, G. Chiodini^{65a}, A.S. Chisholm³⁵,
 A. Chitan^{27b}, I. Chiu¹⁶⁰, Y.H. Chiu¹⁷³, M.V. Chizhov⁷⁷, K. Choi⁶³, A.R. Chomont¹²⁸, S. Chouridou¹⁵⁹,
 Y.S. Chow¹¹⁸, V. Christodoulou⁹², M.C. Chu^{61a}, J. Chudoba¹³⁷, A.J. Chuinard¹⁰¹, J.J. Chwastowski⁸²,
 L. Chytka¹²⁶, D. Cinca⁴⁵, V. Cindro⁸⁹, I.A. Cioară²⁴, A. Ciocio¹⁸, F. Ciroto^{67a,67b}, Z.H. Citron¹⁷⁷,
 M. Citterio^{66a}, A. Clark⁵², M.R. Clark³⁸, P.J. Clark⁴⁸, C. Clement^{43a,43b}, Y. Coadou⁹⁹, M. Cobal^{64a,64c},
 A. Coccaro^{53b,53a}, J. Cochran⁷⁶, A.E.C. Coimbra¹⁷⁷, L. Colasurdo¹¹⁷, B. Cole³⁸, A.P. Colijn¹¹⁸,
 J. Collot⁵⁶, P. Conde Muiño^{136a,136b}, E. Coniavitis⁵⁰, S.H. Connell^{32b}, I.A. Connelly⁹⁸,
 S. Constantinescu^{27b}, F. Conventi^{67a,av}, A.M. Cooper-Sarkar¹³¹, F. Cormier¹⁷², K.J.R. Cormier¹⁶⁴,
 M. Corradi^{70a,70b}, E.E. Corrigan⁹⁴, F. Corriveau^{101,ad}, A. Cortes-Gonzalez³⁵, M.J. Costa¹⁷¹,
 D. Costanzo¹⁴⁶, G. Cottin³¹, G. Cowan⁹¹, B.E. Cox⁹⁸, J. Crane⁹⁸, K. Cranmer¹²¹, S.J. Crawley⁵⁵,
 R.A. Creager¹³³, G. Cree³³, S. Crépe-Renaudin⁵⁶, F. Crescioli¹³², M. Cristinziani²⁴, V. Croft¹²¹,

G. Crosetti^{40b,40a}, A. Cueto⁹⁶, T. Cuhadar Donszelmann¹⁴⁶, A.R. Cukierman¹⁵⁰, J. Cúth⁹⁷, S. Czekierda⁸², P. Czodrowski³⁵, M.J. Da Cunha Sargedas De Sousa^{58b}, C. Da Via⁹⁸, W. Dabrowski^{81a}, T. Dado^{28a,y}, S. Dahbi^{34e}, T. Dai¹⁰³, F. Dallaire¹⁰⁷, C. Dallapiccola¹⁰⁰, M. Dam³⁹, G. D'amen^{23b,23a}, J. Damp⁹⁷, J.R. Dandoy¹³³, M.F. Daneri³⁰, N.P. Dang^{178,k}, N.D. Dann⁹⁸, M. Danninger¹⁷², V. Dao³⁵, G. Darbo^{53b}, S. Darmora⁸, O. Dartsis⁵, A. Dattagupta¹²⁷, T. Daubney⁴⁴, S. D'Auria⁵⁵, W. Davey²⁴, C. David⁴⁴, T. Davidek¹³⁹, D.R. Davis⁴⁷, E. Dawe¹⁰², I. Dawson¹⁴⁶, K. De⁸, R. De Asmundis^{67a}, A. De Benedetti¹²⁴, M. De Beurs¹¹⁸, S. De Castro^{23b,23a}, S. De Cecco^{70a,70b}, N. De Groot¹¹⁷, P. de Jong¹¹⁸, H. De la Torre¹⁰⁴, F. De Lorenzi⁷⁶, A. De Maria^{51,t}, D. De Pedis^{70a}, A. De Salvo^{70a}, U. De Sanctis^{71a,71b}, A. De Santo¹⁵³, K. De Vasconcelos Corga⁹⁹, J.B. De Vivie De Regie¹²⁸, C. Debenedetti¹⁴³, D.V. Dedovich⁷⁷, N. Dehghanian³, M. Del Gaudio^{40b,40a}, J. Del Peso⁹⁶, Y. Delabat Diaz⁴⁴, D. Delgove¹²⁸, F. Deliot¹⁴², C.M. Delitzsch⁷, M. Della Pietra^{67a,67b}, D. Della Volpe⁵², A. Dell'Acqua³⁵, L. Dell'Asta²⁵, M. Delmastro⁵, C. Delporte¹²⁸, P.A. Delsart⁵⁶, D.A. DeMarco¹⁶⁴, S. Demers¹⁸⁰, M. Demichev⁷⁷, S.P. Denisov¹⁴⁰, D. Denysiuk¹¹⁸, L. D'Eramo¹³², D. Derendarz⁸², J.E. Derkaoui^{34d}, F. Derue¹³², P. Dervan⁸⁸, K. Desch²⁴, C. Deterre⁴⁴, K. Dette¹⁶⁴, M.R. Devesa³⁰, P.O. Deviveiros³⁵, A. Dewhurst¹⁴¹, S. Dhaliwal²⁶, F.A. Di Bello⁵², A. Di Ciaccio^{71a,71b}, L. Di Ciaccio⁵, W.K. Di Clemente¹³³, C. Di Donato^{67a,67b}, A. Di Girolamo³⁵, B. Di Micco^{72a,72b}, R. Di Nardo¹⁰⁰, K.F. Di Petrillo⁵⁷, A. Di Simone⁵⁰, R. Di Sipio¹⁶⁴, D. Di Valentino³³, C. Diaconu⁹⁹, M. Diamond¹⁶⁴, F.A. Dias³⁹, T. Dias Do Vale^{136a}, M.A. Diaz^{144a}, J. Dickinson¹⁸, E.B. Diehl¹⁰³, J. Dietrich¹⁹, S. Díez Cornell⁴⁴, A. Dimitrievska¹⁸, J. Dingfelder²⁴, F. Dittus³⁵, F. Djama⁹⁹, T. Djobava^{156b}, J.I. Djuvsland^{59a}, M.A.B. Do Vale^{78c}, M. Dobre^{27b}, D. Dodsworth²⁶, C. Doglioni⁹⁴, J. Dolejsi¹³⁹, Z. Dolezal¹³⁹, M. Donadelli^{78d}, J. Donini³⁷, A. D'onofrio⁹⁰, M. D'Onofrio⁸⁸, J. Dopke¹⁴¹, A. Doria^{67a}, M.T. Dova⁸⁶, A.T. Doyle⁵⁵, E. Drechsler⁵¹, E. Dreyer¹⁴⁹, T. Dreyer⁵¹, Y. Du^{58b}, J. Duarte-Campderros¹⁵⁸, F. Dubinin¹⁰⁸, M. Dubovsky^{28a}, A. Dubreuil⁵², E. Duchovni¹⁷⁷, G. Duckeck¹¹², A. Ducourthial¹³², O.A. Ducu^{107,x}, D. Duda¹¹³, A. Dudarev³⁵, A.C. Dudder⁹⁷, E.M. Duffield¹⁸, L. Dufлот¹²⁸, M. Dührssen³⁵, C. Dülsen¹⁷⁹, M. Dumancic¹⁷⁷, A.E. Dumitriu^{27b,e}, A.K. Duncan⁵⁵, M. Dunford^{59a}, A. Duperrin⁹⁹, H. Duran Yildiz^{4a}, M. Düren⁵⁴, A. Durglishvili^{156b}, D. Duschinger⁴⁶, B. Dutta⁴⁴, D. Duvnjak¹, M. Dyndal⁴⁴, S. Dysch⁹⁸, B.S. Dziedzic⁸², C. Eckardt⁴⁴, K.M. Ecker¹¹³, R.C. Edgar¹⁰³, T. Eifert³⁵, G. Eigen¹⁷, K. Einsweiler¹⁸, T. Ekelof¹⁶⁹, M. El Kacimi^{34c}, R. El Kosseifi⁹⁹, V. Ellajosyula⁹⁹, M. Ellert¹⁶⁹, F. Ellinghaus¹⁷⁹, A.A. Elliot⁹⁰, N. Ellis³⁵, J. Elmsheuser²⁹, M. Elsing³⁵, D. Emelianov¹⁴¹, Y. Enari¹⁶⁰, J.S. Ennis¹⁷⁵, M.B. Epland⁴⁷, J. Erdmann⁴⁵, A. Ereditato²⁰, S. Errede¹⁷⁰, M. Escalier¹²⁸, C. Escobar¹⁷¹, O. Estrada Pastor¹⁷¹, A.I. Etienvre¹⁴², E. Etzion¹⁵⁸, H. Evans⁶³, A. Ezhilov¹³⁴, M. Ezzi^{34e}, F. Fabbri⁵⁵, L. Fabbri^{23b,23a}, V. Fabiani¹¹⁷, G. Facini⁹², R.M. Faisca Rodrigues Pereira^{136a}, R.M. Fakhruddinov¹⁴⁰, S. Falciano^{70a}, P.J. Falke⁵, S. Falke⁵, J. Faltova¹³⁹, Y. Fang^{15a}, M. Fanti^{66a,66b}, A. Farbin⁸, A. Farilla^{72a}, E.M. Farina^{68a,68b}, T. Farooque¹⁰⁴, S. Farrell¹⁸, S.M. Farrington¹⁷⁵, P. Farthouat³⁵, F. Fassi^{34e}, P. Fassnacht³⁵, D. Fassouliotis⁹, M. Fauci Giannelli⁴⁸, A. Favareto^{53b,53a}, W.J. Fawcett⁵², L. Fayard¹²⁸, O.L. Fedin^{134,p}, W. Fedorko¹⁷², M. Feickert⁴¹, S. Feigl¹³⁰, L. Feligioni⁹⁹, C. Feng^{58b}, E.J. Feng³⁵, M. Feng⁴⁷, M.J. Fenton⁵⁵, A.B. Fenyuk¹⁴⁰, L. Feremenga⁸, J. Ferrando⁴⁴, A. Ferrari¹⁶⁹, P. Ferrari¹¹⁸, R. Ferrari^{68a}, D.E. Ferreira de Lima^{59b}, A. Ferrer¹⁷¹, D. Ferrere⁵², C. Ferretti¹⁰³, F. Fiedler⁹⁷, A. Filipčić⁸⁹, F. Filthaut¹¹⁷, K.D. Finelli²⁵, M.C.N. Fiolhais^{136a,136c,a}, L. Fiorini¹⁷¹, C. Fischer¹⁴, W.C. Fisher¹⁰⁴, N. Flaschel⁴⁴, I. Fleck¹⁴⁸, P. Fleischmann¹⁰³, R.R.M. Fletcher¹³³, T. Flick¹⁷⁹, B.M. Flierl¹¹², L.M. Flores¹³³, L.R. Flores Castillo^{61a}, N. Fomin¹⁷, G.T. Forcolin⁹⁸, A. Formica¹⁴², F.A. Förster¹⁴, A.C. Forti⁹⁸, A.G. Foster²¹, D. Fournier¹²⁸, H. Fox⁸⁷, S. Fracchia¹⁴⁶, P. Francavilla^{69a,69b}, M. Franchini^{23b,23a}, S. Franchino^{59a}, D. Francis³⁵, L. Franconi¹³⁰, M. Franklin⁵⁷, M. Frate¹⁶⁸, M. Fraternali^{68a,68b}, D. Freeborn⁹², S.M. Fressard-Batraneanu³⁵, B. Freund¹⁰⁷, W.S. Freund^{78b}, D. Froidevaux³⁵, J.A. Frost¹³¹, C. Fukunaga¹⁶¹, E. Fullana Torregrosa¹⁷¹, T. Fusayasu¹¹⁴, J. Fuster¹⁷¹, O. Gabizon¹⁵⁷, A. Gabrielli^{23b,23a}, A. Gabrielli¹⁸, G.P. Gach^{81a}, S. Gadatsch⁵², P. Gadow¹¹³,

G. Gagliardi^{53b,53a}, L.G. Gagnon¹⁰⁷, C. Galea^{27b}, B. Galhardo^{136a,136c}, E.J. Gallas¹³¹, B.J. Gallop¹⁴¹, P. Gallus¹³⁸, G. Galster³⁹, R. Gamboa Goni⁹⁰, K.K. Gan¹²², S. Ganguly¹⁷⁷, J. Gao^{58a}, Y. Gao⁸⁸, Y.S. Gao^{150,m}, C. García¹⁷¹, J.E. García Navarro¹⁷¹, J.A. García Pascual^{15a}, M. Garcia-Sciveres¹⁸, R.W. Gardner³⁶, N. Garelli¹⁵⁰, V. Garonne¹³⁰, K. Gasnikova⁴⁴, A. Gaudiello^{53b,53a}, G. Gaudio^{68a}, I.L. Gavrilenko¹⁰⁸, A. Gavrilyuk¹⁰⁹, C. Gay¹⁷², G. Gaycken²⁴, E.N. Gazis¹⁰, C.N.P. Gee¹⁴¹, J. Geisen⁵¹, M. Geisen⁹⁷, M.P. Geisler^{59a}, K. Gellerstedt^{43a,43b}, C. Gemme^{53b}, M.H. Genest⁵⁶, C. Geng¹⁰³, S. Gentile^{70a,70b}, S. George⁹¹, D. Gerbaudo¹⁴, G. Gessner⁴⁵, S. Ghasemi¹⁴⁸, M. Ghasemi Bostanabad¹⁷³, M. Ghneimat²⁴, B. Giacobbe^{23b}, S. Giagu^{70a,70b}, N. Giangiacomi^{23b,23a}, P. Giannetti^{69a}, A. Giannini^{67a,67b}, S.M. Gibson⁹¹, M. Gignac¹⁴³, D. Gillberg³³, G. Gilles¹⁷⁹, D.M. Gingrich^{3,au}, M.P. Giordani^{64a,64c}, F.M. Giorgi^{23b}, P.F. Giraud¹⁴², P. Giromini⁵⁷, G. Giugliarelli^{64a,64c}, D. Giugni^{66a}, F. Giuli¹³¹, M. Giulini^{59b}, S. Gkaitatzis¹⁵⁹, I. Gkialas^{9,j}, E.L. Gkoukousis¹⁴, P. Gkountoumis¹⁰, L.K. Gladilin¹¹¹, C. Glasman⁹⁶, J. Glatzer¹⁴, P.C.F. Glaysher⁴⁴, A. Glazov⁴⁴, M. Goblirsch-Kolb²⁶, J. Godlewski⁸², S. Goldfarb¹⁰², T. Golling⁵², D. Golubkov¹⁴⁰, A. Gomes^{136a,136b,136d}, R. Goncalves Gama^{78a}, R. Gonçalo^{136a}, G. Gonella⁵⁰, L. Gonella²¹, A. Gongadze⁷⁷, F. Gonnella²¹, J.L. Gonski⁵⁷, S. González de la Hoz¹⁷¹, S. Gonzalez-Sevilla⁵², L. Goossens³⁵, P.A. Gorbounov¹⁰⁹, H.A. Gordon²⁹, B. Gorini³⁵, E. Gorini^{65a,65b}, A. Gorišek⁸⁹, A.T. Goshaw⁴⁷, C. Gössling⁴⁵, M.I. Gostkin⁷⁷, C.A. Gottardo²⁴, C.R. Goudet¹²⁸, D. Goujdami^{34c}, A.G. Goussiou¹⁴⁵, N. Govender^{32b,c}, C. Goy⁵, E. Gozani¹⁵⁷, I. Grabowska-Bold^{81a}, P.O.J. Gradin¹⁶⁹, E.C. Graham⁸⁸, J. Gramling¹⁶⁸, E. Gramstad¹³⁰, S. Grancagnolo¹⁹, V. Gratchev¹³⁴, P.M. Gravila^{27f}, F.G. Gravili^{65a,65b}, C. Gray⁵⁵, H.M. Gray¹⁸, Z.D. Greenwood^{93,aj}, C. Grefe²⁴, K. Gregersen⁹², I.M. Gregor⁴⁴, P. Grenier¹⁵⁰, K. Grevtsov⁴⁴, J. Griffiths⁸, A.A. Grillo¹⁴³, K. Grimm^{150,b}, S. Grinstein^{14,z}, Ph. Gris³⁷, J.-F. Grivaz¹²⁸, S. Groh⁹⁷, E. Gross¹⁷⁷, J. Grosse-Knetter⁵¹, G.C. Grossi⁹³, Z.J. Grout⁹², C. Grud¹⁰³, A. Grummer¹¹⁶, L. Guan¹⁰³, W. Guan¹⁷⁸, J. Guenther³⁵, A. Guerguichon¹²⁸, F. Guescini^{165a}, D. Guest¹⁶⁸, R. Gugel⁵⁰, B. Gui¹²², T. Guillemin⁵, S. Guindon³⁵, U. Gul⁵⁵, C. Gumpert³⁵, J. Guo^{58c}, W. Guo¹⁰³, Y. Guo^{58a,s}, Z. Guo⁹⁹, R. Gupta⁴¹, S. Gurbuz^{12c}, G. Gustavino¹²⁴, B.J. Gutelman¹⁵⁷, P. Gutierrez¹²⁴, C. Gutschow⁹², C. Guyot¹⁴², M.P. Guzik^{81a}, C. Gwenlan¹³¹, C.B. Gwilliam⁸⁸, A. Haas¹²¹, C. Haber¹⁸, H.K. Hadavand⁸, N. Haddad^{34e}, A. Hader^{58a}, S. Hageböck²⁴, M. Hagihara¹⁶⁶, H. Hakobyan^{181,*}, M. Haleem¹⁷⁴, J. Haley¹²⁵, G. Halladjian¹⁰⁴, G.D. Hallewell⁹⁹, K. Hamacher¹⁷⁹, P. Hamal¹²⁶, K. Hamano¹⁷³, A. Hamilton^{32a}, G.N. Hamity¹⁴⁶, K. Han^{58a,ai}, L. Han^{58a}, S. Han^{15d}, K. Hanagaki^{79,v}, M. Hance¹⁴³, D.M. Handl¹¹², B. Haney¹³³, R. Hankache¹³², P. Hanke^{59a}, E. Hansen⁹⁴, J.B. Hansen³⁹, J.D. Hansen³⁹, M.C. Hansen²⁴, P.H. Hansen³⁹, K. Hara¹⁶⁶, A.S. Hard¹⁷⁸, T. Harenberg¹⁷⁹, S. Harkusha¹⁰⁵, P.F. Harrison¹⁷⁵, N.M. Hartmann¹¹², Y. Hasegawa¹⁴⁷, A. Hasib⁴⁸, S. Hassani¹⁴², S. Haug²⁰, R. Hauser¹⁰⁴, L. Hauswald⁴⁶, L.B. Havener³⁸, M. Havranek¹³⁸, C.M. Hawkes²¹, R.J. Hawkings³⁵, D. Hayden¹⁰⁴, C. Hayes¹⁵², C.P. Hays¹³¹, J.M. Hays⁹⁰, H.S. Hayward⁸⁸, S.J. Haywood¹⁴¹, M.P. Heath⁴⁸, V. Hedberg⁹⁴, L. Heelan⁸, S. Heer²⁴, K.K. Heidegger⁵⁰, J. Heilman³³, S. Heim⁴⁴, T. Heim¹⁸, B. Heinemann^{44,ap}, J.J. Heinrich¹¹², L. Heinrich¹²¹, C. Heinz⁵⁴, J. Hejbal¹³⁷, L. Helary³⁵, A. Held¹⁷², S. Hellesund¹³⁰, S. Hellman^{43a,43b}, C. Helsen³⁵, R.C.W. Henderson⁸⁷, Y. Heng¹⁷⁸, S. Henkelmann¹⁷², A.M. Henriques Correia³⁵, G.H. Herbert¹⁹, H. Herde²⁶, V. Herget¹⁷⁴, Y. Hernández Jiménez^{32c}, H. Herr⁹⁷, M.G. Herrmann¹¹², G. Herten⁵⁰, R. Hertenberger¹¹², L. Hervas³⁵, T.C. Herwig¹³³, G.G. Hesketh⁹², N.P. Hesse^{165a}, J.W. Hetherly⁴¹, S. Higashino⁷⁹, E. Higón-Rodríguez¹⁷¹, K. Hildebrand³⁶, E. Hill¹⁷³, J.C. Hill³¹, K.K. Hill²⁹, K.H. Hiller⁴⁴, S.J. Hillier²¹, M. Hils⁴⁶, I. Hinchliffe¹⁸, M. Hirose¹²⁹, D. Hirschbuehl¹⁷⁹, B. Hiti⁸⁹, O. Hladik¹³⁷, D.R. Hlaluku^{32c}, X. Hoad⁴⁸, J. Hobbs¹⁵², N. Hod^{165a}, M.C. Hodgkinson¹⁴⁶, A. Hoecker³⁵, M.R. Hoefkamp¹¹⁶, F. Hoenig¹¹², D. Hohn²⁴, D. Hohov¹²⁸, T.R. Holmes³⁶, M. Holzbock¹¹², M. Homann⁴⁵, S. Honda¹⁶⁶, T. Honda⁷⁹, T.M. Hong¹³⁵, A. Hönle¹¹³, B.H. Hooberman¹⁷⁰, W.H. Hopkins¹²⁷, Y. Horii¹¹⁵, P. Horn⁴⁶, A.J. Horton¹⁴⁹, L.A. Horyn³⁶, J.-Y. Hostachy⁵⁶, A. Hostiuc¹⁴⁵, S. Hou¹⁵⁵, A. Hoummada^{34a}, J. Howarth⁹⁸, J. Hoya⁸⁶, M. Hrabovsky¹²⁶, J. Hrdinka³⁵, I. Hristova¹⁹, J. Hrivnac¹²⁸, A. Hrynevich¹⁰⁶,

T. Hryn'ova⁵, P.J. Hsu⁶², S.-C. Hsu¹⁴⁵, Q. Hu²⁹, S. Hu^{58c}, Y. Huang^{15a}, Z. Hubacek¹³⁸, F. Hubaut⁹⁹, M. Huebner²⁴, F. Huegging²⁴, T.B. Huffman¹³¹, E.W. Hughes³⁸, M. Huhtinen³⁵, R.F.H. Hunter³³, P. Huo¹⁵², A.M. Hupe³³, N. Huseynov^{77,af}, J. Huston¹⁰⁴, J. Huth⁵⁷, R. Hyneman¹⁰³, G. Iacobucci⁵², G. Iakovidis²⁹, I. Ibragimov¹⁴⁸, L. Iconomidou-Fayard¹²⁸, Z. Idrissi^{34e}, P. Iengo³⁵, R. Ignazzi³⁹, O. Igonkina^{118,ab}, R. Iguchi¹⁶⁰, T. Iizawa⁵², Y. Ikegami⁷⁹, M. Ikeno⁷⁹, D. Iliadis¹⁵⁹, N. Ilic¹⁵⁰, F. Iltzsche⁴⁶, G. Introzzi^{68a,68b}, M. Iodice^{72a}, K. Iordanidou³⁸, V. Ippolito^{70a,70b}, M.F. Isacson¹⁶⁹, N. Ishijima¹²⁹, M. Ishino¹⁶⁰, M. Ishitsuka¹⁶², W. Islam¹²⁵, C. Issever¹³¹, S. Istin^{12c,ao}, F. Ito¹⁶⁶, J.M. Iturbe Ponce^{61a}, R. Iuppa^{73a,73b}, A. Ivina¹⁷⁷, H. Iwasaki⁷⁹, J.M. Izen⁴², V. Izzo^{67a}, P. Jacka¹³⁷, P. Jackson¹, R.M. Jacobs²⁴, V. Jain², G. Jäkel¹⁷⁹, K.B. Jakobi⁹⁷, K. Jakobs⁵⁰, S. Jakobsen⁷⁴, T. Jakoubek¹³⁷, D.O. Jamin¹²⁵, D.K. Jana⁹³, R. Jansky⁵², J. Janssen²⁴, M. Janus⁵¹, P.A. Janus^{81a}, G. Jarlskog⁹⁴, N. Javadov^{77,af}, T. Javůrek⁵⁰, M. Javurkova⁵⁰, F. Jeanneau¹⁴², L. Jeanty¹⁸, J. Jejelava^{156a,ag}, A. Jelinskas¹⁷⁵, P. Jenni^{50,d}, J. Jeong⁴⁴, S. Jézéquel⁵, H. Ji¹⁷⁸, J. Jia¹⁵², H. Jiang⁷⁶, Y. Jiang^{58a}, Z. Jiang^{150,q}, S. Jiggins⁵⁰, F.A. Jimenez Morales³⁷, J. Jimenez Pena¹⁷¹, S. Jin^{15c}, A. Jinaru^{27b}, O. Jinnouchi¹⁶², H. Jivan^{32c}, P. Johansson¹⁴⁶, K.A. Johns⁷, C.A. Johnson⁶³, W.J. Johnson¹⁴⁵, K. Jon-And^{43a,43b}, R.W.L. Jones⁸⁷, S.D. Jones¹⁵³, S. Jones⁷, T.J. Jones⁸⁸, J. Jongmanns^{59a}, P.M. Jorge^{136a,136b}, J. Jovicevic^{165a}, X. Ju¹⁷⁸, J.J. Junggeburth¹¹³, A. Juste Rozas^{14,z}, A. Kaczmarska⁸², M. Kado¹²⁸, H. Kagan¹²², M. Kagan¹⁵⁰, T. Kaji¹⁷⁶, E. Kajomovitz¹⁵⁷, C.W. Kalderon⁹⁴, A. Kaluza⁹⁷, S. Kama⁴¹, A. Kamenshchikov¹⁴⁰, L. Kanjir⁸⁹, Y. Kano¹⁶⁰, V.A. Kantserov¹¹⁰, J. Kanzaki⁷⁹, B. Kaplan¹²¹, L.S. Kaplan¹⁷⁸, D. Kar^{32c}, M.J. Kareem^{165b}, E. Karentzos¹⁰, S.N. Karpov⁷⁷, Z.M. Karpova⁷⁷, V. Kartvelishvili⁸⁷, A.N. Karyukhin¹⁴⁰, K. Kasahara¹⁶⁶, L. Kashif¹⁷⁸, R.D. Kass¹²², A. Kastanas¹⁵¹, Y. Kataoka¹⁶⁰, C. Kato¹⁶⁰, J. Katzy⁴⁴, K. Kawade⁸⁰, K. Kawagoe⁸⁵, T. Kawamoto¹⁶⁰, G. Kawamura⁵¹, E.F. Kay⁸⁸, V.F. Kazanin^{120b,120a}, R. Keeler¹⁷³, R. Kehoe⁴¹, J.S. Keller³³, E. Kellermann⁹⁴, J.J. Kempster²¹, J. Kendrick²¹, O. Kepka¹³⁷, S. Kersten¹⁷⁹, B.P. Kerševan⁸⁹, R.A. Keyes¹⁰¹, M. Khader¹⁷⁰, F. Khalil-Zada¹³, A. Khanov¹²⁵, A.G. Kharlamov^{120b,120a}, T. Kharlamova^{120b,120a}, A. Khodinov¹⁶³, T.J. Khoo⁵², E. Khramov⁷⁷, J. Khubua^{156b}, S. Kido⁸⁰, M. Kiehn⁵², C.R. Kilby⁹¹, S.H. Kim¹⁶⁶, Y.K. Kim³⁶, N. Kimura^{64a,64c}, O.M. Kind¹⁹, B.T. King⁸⁸, D. Kirchmeier⁴⁶, J. Kirk¹⁴¹, A.E. Kiryunin¹¹³, T. Kishimoto¹⁶⁰, D. Kisielewska^{81a}, V. Kitali⁴⁴, O. Kiverny⁵, E. Kladiva^{28b,*}, T. Klapdor-Kleingrothaus⁵⁰, M.H. Klein¹⁰³, M. Klein⁸⁸, U. Klein⁸⁸, K. Kleinknecht⁹⁷, P. Klimek¹¹⁹, A. Klimentov²⁹, R. Klingenberg^{45,*}, T. Klingl²⁴, T. Klioutchnikova³⁵, F.F. Klitzner¹¹², P. Kluit¹¹⁸, S. Kluth¹¹³, E. Kneringer⁷⁴, E.B.F.G. Knoops⁹⁹, A. Knue⁵⁰, A. Kobayashi¹⁶⁰, D. Kobayashi⁸⁵, T. Kobayashi¹⁶⁰, M. Kobel⁴⁶, M. Kocian¹⁵⁰, P. Kodys¹³⁹, T. Koffas³³, E. Koffeman¹¹⁸, N.M. Köhler¹¹³, T. Koi¹⁵⁰, M. Kolb^{59b}, I. Koletsou⁵, T. Kondo⁷⁹, N. Kondrashova^{58c}, K. Köneke⁵⁰, A.C. König¹¹⁷, T. Kono⁷⁹, R. Konoplich^{121,al}, V. Konstantinides⁹², N. Konstantinidis⁹², B. Konya⁹⁴, R. Kopeliansky⁶³, S. Koperny^{81a}, K. Korcyl⁸², K. Kordas¹⁵⁹, A. Korn⁹², I. Korolkov¹⁴, E.V. Korolkova¹⁴⁶, O. Kortner¹¹³, S. Kortner¹¹³, T. Kosek¹³⁹, V.V. Kostyukhin²⁴, A. Kotwal⁴⁷, A. Koulouris¹⁰, A. Kourkouveli-Charalampidi^{68a,68b}, C. Kourkouvelis⁹, E. Kourlitis¹⁴⁶, V. Kouskoura²⁹, A.B. Kowalewska⁸², R. Kowalewski¹⁷³, T.Z. Kowalski^{81a}, C. Kozakai¹⁶⁰, W. Kozanecki¹⁴², A.S. Kozhin¹⁴⁰, V.A. Kramarenko¹¹¹, G. Kramberger⁸⁹, D. Krasnopevtsev¹¹⁰, M.W. Krasny¹³², A. Krasznahorkay³⁵, D. Krauss¹¹³, J.A. Kremer^{81a}, J. Kretzschmar⁸⁸, P. Krieger¹⁶⁴, K. Krizka¹⁸, K. Kroeninger⁴⁵, H. Kroha¹¹³, J. Kroll¹³⁷, J. Kroll¹³³, J. Krstic¹⁶, U. Kruchonak⁷⁷, H. Krüger²⁴, N. Krumnack⁷⁶, M.C. Kruse⁴⁷, T. Kubota¹⁰², S. Kuday^{4b}, J.T. Kuechler¹⁷⁹, S. Kuehn³⁵, A. Kugel^{59a}, F. Kuger¹⁷⁴, T. Kuhl⁴⁴, V. Kukhtin⁷⁷, R. Kukla⁹⁹, Y. Kulchitsky¹⁰⁵, S. Kuleshov^{144b}, Y.P. Kulinich¹⁷⁰, M. Kuna⁵⁶, T. Kunigo⁸³, A. Kupco¹³⁷, T. Kupfer⁴⁵, O. Kuprash¹⁵⁸, H. Kurashige⁸⁰, L.L. Kurchaninov^{165a}, Y.A. Kurochkin¹⁰⁵, M.G. Kurth^{15d}, E.S. Kuwertz¹⁷³, M. Kuze¹⁶², J. Kvita¹²⁶, T. Kwan¹⁰¹, A. La Rosa¹¹³, J.L. La Rosa Navarro^{78d}, L. La Rotonda^{40b,40a}, F. La Ruffa^{40b,40a}, C. Lacasta¹⁷¹, F. Lacava^{70a,70b}, J. Lacey⁴⁴, D.P.J. Lack⁹⁸, H. Lacker¹⁹, D. Lacour¹³², E. Ladygin⁷⁷, R. Lafaye⁵, B. Laforge¹³², T. Lagouri^{32c}, S. Lai⁵¹, S. Lammers⁶³, W. Lampl⁷, E. Lançon²⁹,

U. Landgraf⁵⁰, M.P.J. Landon⁹⁰, M.C. Lanfermann⁵², V.S. Lang⁴⁴, J.C. Lange¹⁴, R.J. Langenberg³⁵,
 A.J. Lankford¹⁶⁸, F. Lanni²⁹, K. Lantsch²⁴, A. Lanza^{68a}, A. Lapertosa^{53b,53a}, S. Laplace¹³²,
 J.F. Laporte¹⁴², T. Lari^{66a}, F. Lasagni Manghi^{23b,23a}, M. Lassnig³⁵, T.S. Lau^{61a}, A. Laudrain¹²⁸,
 M. Lavorgna^{67a,67b}, A.T. Law¹⁴³, P. Laycock⁸⁸, M. Lazzaroni^{66a,66b}, B. Le¹⁰², O. Le Dortz¹³²,
 E. Le Guirriec⁹⁹, E.P. Le Quilleuc¹⁴², M. LeBlanc⁷, T. LeCompte⁶, F. Ledroit-Guillon⁵⁶, C.A. Lee²⁹,
 G.R. Lee^{144a}, L. Lee⁵⁷, S.C. Lee¹⁵⁵, B. Lefebvre¹⁰¹, M. Lefebvre¹⁷³, F. Legger¹¹², C. Leggett¹⁸,
 N. Lehmann¹⁷⁹, G. Lehmann Miotto³⁵, W.A. Leight⁴⁴, A. Leisos^{159,w}, M.A.L. Leite^{78d}, R. Leitner¹³⁹,
 D. Lellouch¹⁷⁷, B. Lemmer⁵¹, K.J.C. Leney⁹², T. Lenz²⁴, B. Lenzi³⁵, R. Leone⁷, S. Leone^{69a},
 C. Leonidopoulos⁴⁸, G. Lerner¹⁵³, C. Leroy¹⁰⁷, R. Les¹⁶⁴, A.A.J. Lesage¹⁴², C.G. Lester³¹,
 M. Levchenko¹³⁴, J. Levêque⁵, D. Levin¹⁰³, L.J. Levinson¹⁷⁷, D. Lewis⁹⁰, B. Li¹⁰³, C-Q. Li^{58a,ak},
 H. Li^{58b}, L. Li^{58c}, Q. Li^{15d}, Q.Y. Li^{58a}, S. Li^{58d,58c}, X. Li^{58c}, Y. Li¹⁴⁸, Z. Liang^{15a}, B. Liberti^{71a},
 A. Liblong¹⁶⁴, K. Lie^{61c}, S. Liem¹¹⁸, A. Limosani¹⁵⁴, C.Y. Lin³¹, K. Lin¹⁰⁴, T.H. Lin⁹⁷, R.A. Linck⁶³,
 B.E. Lindquist¹⁵², A.L. Lioni⁵², E. Lipeles¹³³, A. Lipniacka¹⁷, M. Lisovyi^{59b}, T.M. Liss^{170,ar},
 A. Lister¹⁷², A.M. Litke¹⁴³, J.D. Little⁸, B. Liu⁷⁶, B.L. Liu⁶, H.B. Liu²⁹, H. Liu¹⁰³, J.B. Liu^{58a},
 J.K.K. Liu¹³¹, K. Liu¹³², M. Liu^{58a}, P. Liu¹⁸, Y. Liu^{15a}, Y.L. Liu^{58a}, Y.W. Liu^{58a}, M. Livan^{68a,68b},
 A. Lleres⁵⁶, J. Llorente Merino^{15a}, S.L. Lloyd⁹⁰, C.Y. Lo^{61b}, F. Lo Sterzo⁴¹, E.M. Lobodzinska⁴⁴,
 P. Loch⁷, K.M. Loew²⁶, T. Lohse¹⁹, K. Lohwasser¹⁴⁶, M. Lokajicek¹³⁷, B.A. Long²⁵, J.D. Long¹⁷⁰,
 R.E. Long⁸⁷, L. Longo^{65a,65b}, K.A. Looper¹²², J.A. Lopez^{144b}, I. Lopez Paz¹⁴, A. Lopez Solis¹⁴⁶,
 J. Lorenz¹¹², N. Lorenzo Martinez⁵, M. Losada²², P.J. Lösel¹¹², A. Lösle⁵⁰, X. Lou⁴⁴, X. Lou^{15a},
 A. Lounis¹²⁸, J. Love⁶, P.A. Love⁸⁷, J.J. Lozano Bahilo¹⁷¹, H. Lu^{61a}, M. Lu^{58a}, N. Lu¹⁰³, Y.J. Lu⁶²,
 H.J. Lubatti¹⁴⁵, C. Luci^{70a,70b}, A. Lucotte⁵⁶, C. Luedtke⁵⁰, F. Luehring⁶³, I. Luise¹³², W. Lukas⁷⁴,
 L. Luminari^{70a}, B. Lund-Jensen¹⁵¹, M.S. Lutz¹⁰⁰, P.M. Luzi¹³², D. Lynn²⁹, R. Lysak¹³⁷, E. Lytken⁹⁴,
 F. Lyu^{15a}, V. Lyubushkin⁷⁷, H. Ma²⁹, L.L. Ma^{58b}, Y. Ma^{58b}, G. Maccarrone⁴⁹, A. Macchiolo¹¹³,
 C.M. Macdonald¹⁴⁶, J. Machado Miguens^{133,136b}, D. Madaffari¹⁷¹, R. Madar³⁷, W.F. Mader⁴⁶,
 A. Madsen⁴⁴, N. Madysa⁴⁶, J. Maeda⁸⁰, K. Maekawa¹⁶⁰, S. Maeland¹⁷, T. Maeno²⁹, A.S. Maevskiy¹¹¹,
 V. Magerl⁵⁰, C. Maidantchik^{78b}, T. Maier¹¹², A. Maio^{136a,136b,136d}, O. Majersky^{28a}, S. Majewski¹²⁷,
 Y. Makida⁷⁹, N. Makovec¹²⁸, B. Malaescu¹³², Pa. Malecki⁸², V.P. Maleev¹³⁴, F. Malek⁵⁶, U. Mallik⁷⁵,
 D. Malon⁶, C. Malone³¹, S. Maltezos¹⁰, S. Malyukov³⁵, J. Mamuzic¹⁷¹, G. Mancini⁴⁹, I. Mandić⁸⁹,
 J. Maneira^{136a}, L. Manhaes de Andrade Filho^{78a}, J. Manjarres Ramos⁴⁶, K.H. Mankinen⁹⁴, A. Mann¹¹²,
 A. Manousos⁷⁴, B. Mansoulie¹⁴², J.D. Mansour^{15a}, M. Mantoani⁵¹, S. Manzoni^{66a,66b}, G. Marceca³⁰,
 L. March⁵², L. Marchese¹³¹, G. Marchiori¹³², M. Marcisovsky¹³⁷, C.A. Marin Tobon³⁵,
 M. Marjanovic³⁷, D.E. Marley¹⁰³, F. Marroquin^{78b}, Z. Marshall¹⁸, M.U.F. Martensson¹⁶⁹,
 S. Marti-Garcia¹⁷¹, C.B. Martin¹²², T.A. Martin¹⁷⁵, V.J. Martin⁴⁸, B. Martin dit Latour¹⁷,
 M. Martinez^{14,z}, V.I. Martinez Outschoorn¹⁰⁰, S. Martin-Haugh¹⁴¹, V.S. Martoiu^{27b}, A.C. Martyniuk⁹²,
 A. Marzin³⁵, L. Masetti⁹⁷, T. Mashimo¹⁶⁰, R. Mashinistov¹⁰⁸, J. Masik⁹⁸, A.L. Maslennikov^{120b,120a},
 L.H. Mason¹⁰², L. Massa^{71a,71b}, P. Massarotti^{67a,67b}, P. Mastrandrea⁵, A. Mastroberardino^{40b,40a},
 T. Masubuchi¹⁶⁰, P. Mättig¹⁷⁹, J. Maurer^{27b}, B. Maček⁸⁹, S.J. Maxfield⁸⁸, D.A. Maximov^{120b,120a},
 R. Mazini¹⁵⁵, I. Maznas¹⁵⁹, S.M. Mazza¹⁴³, N.C. Mc Fadden¹¹⁶, G. Mc Goldrick¹⁶⁴, S.P. Mc Kee¹⁰³,
 A. McCarn¹⁰³, T.G. McCarthy¹¹³, L.I. McClymont⁹², E.F. McDonald¹⁰², J.A. Mcfayden³⁵,
 G. Mchedlidze⁵¹, M.A. McKay⁴¹, K.D. McLean¹⁷³, S.J. McMahon¹⁴¹, P.C. McNamara¹⁰²,
 C.J. McNicol¹⁷⁵, R.A. McPherson^{173,ad}, J.E. Mdhlu^{32c}, Z.A. Meadows¹⁰⁰, S. Meehan¹⁴⁵, T.M. Megy⁵⁰,
 S. Mehlhase¹¹², A. Mehta⁸⁸, T. Meideck⁵⁶, B. Meirose⁴², D. Melini^{171,h}, B.R. Mellado Garcia^{32c},
 J.D. Mellenthin⁵¹, M. Melo^{28a}, F. Meloni⁴⁴, A. Melzer²⁴, S.B. Menary⁹⁸, E.D. Mendes Gouveia^{136a},
 L. Meng⁸⁸, X.T. Meng¹⁰³, A. Mengarelli^{23b,23a}, S. Menke¹¹³, E. Meoni^{40b,40a}, S. Mergelmeyer¹⁹,
 C. Merlassino²⁰, P. Mermod⁵², L. Merola^{67a,67b}, C. Meroni^{66a}, F.S. Merritt³⁶, A. Messina^{70a,70b},
 J. Metcalfe⁶, A.S. Mete¹⁶⁸, C. Meyer¹³³, J. Meyer¹⁵⁷, J-P. Meyer¹⁴², H. Meyer Zu Theenhausen^{59a},
 F. Miano¹⁵³, R.P. Middleton¹⁴¹, L. Mijović⁴⁸, G. Mikenberg¹⁷⁷, M. Mikestikova¹³⁷, M. Mikuž⁸⁹,

M. Milesi¹⁰², A. Milic¹⁶⁴, D.A. Millar⁹⁰, D.W. Miller³⁶, A. Milov¹⁷⁷, D.A. Milstead^{43a,43b}, A.A. Minaenko¹⁴⁰, M. Miñano Moya¹⁷¹, I.A. Minashvili^{156b}, A.I. Mincer¹²¹, B. Mindur^{81a}, M. Mineev⁷⁷, Y. Minegishi¹⁶⁰, Y. Ming¹⁷⁸, L.M. Mir¹⁴, A. Mirto^{65a,65b}, K.P. Mistry¹³³, T. Mitani¹⁷⁶, J. Mitrevski¹¹², V.A. Mitsou¹⁷¹, A. Miucci²⁰, P.S. Miyagawa¹⁴⁶, A. Mizukami⁷⁹, J.U. Mjörnmark⁹⁴, T. Mkrtychyan¹⁸¹, M. Mlynarikova¹³⁹, T. Moa^{43a,43b}, K. Mochizuki¹⁰⁷, P. Mogg⁵⁰, S. Mohapatra³⁸, S. Molander^{43a,43b}, R. Moles-Valls²⁴, M.C. Mondragon¹⁰⁴, K. Mönig⁴⁴, J. Monk³⁹, E. Monnier⁹⁹, A. Montalbano¹⁴⁹, J. Montejo Berlingen³⁵, F. Monticelli⁸⁶, S. Monzani^{66a}, R.W. Moore³, N. Morange¹²⁸, D. Moreno²², M. Moreno Llácer³⁵, P. Morettini^{53b}, M. Morgenstern¹¹⁸, S. Morgenstern⁴⁶, D. Mori¹⁴⁹, T. Mori¹⁶⁰, M. Morii⁵⁷, M. Morinaga¹⁷⁶, V. Morisbak¹³⁰, A.K. Morley³⁵, G. Mornacchi³⁵, A.P. Morris⁹², J.D. Morris⁹⁰, L. Morvaj¹⁵², P. Moschovakos¹⁰, M. Mosidze^{156b}, H.J. Moss¹⁴⁶, J. Moss^{150,n}, K. Motohashi¹⁶², R. Mount¹⁵⁰, E. Mountricha³⁵, E.J.W. Moyse¹⁰⁰, S. Muanza⁹⁹, F. Mueller¹¹³, J. Mueller¹³⁵, R.S.P. Mueller¹¹², D. Muenstermann⁸⁷, P. Mullen⁵⁵, G.A. Mullier²⁰, F.J. Munoz Sanchez⁹⁸, P. Murin^{28b}, W.J. Murray^{175,141}, A. Murrone^{66a,66b}, M. Muškinja⁸⁹, C. Mwewa^{32a}, A.G. Myagkov^{140,am}, J. Myers¹²⁷, M. Myska¹³⁸, B.P. Nachman¹⁸, O. Nackenhorst⁴⁵, K. Nagai¹³¹, K. Nagano⁷⁹, Y. Nagasaka⁶⁰, K. Nagata¹⁶⁶, M. Nagel⁵⁰, E. Nagy⁹⁹, A.M. Nairz³⁵, Y. Nakahama¹¹⁵, K. Nakamura⁷⁹, T. Nakamura¹⁶⁰, I. Nakano¹²³, H. Nanjo¹²⁹, F. Napolitano^{59a}, R.F. Naranjo Garcia⁴⁴, R. Narayan¹¹, D.I. Narrias Villar^{59a}, I. Naryshkin¹³⁴, T. Naumann⁴⁴, G. Navarro²², R. Nayyar⁷, H.A. Neal^{103,*}, P.Y. Nechaeva¹⁰⁸, T.J. Neep¹⁴², A. Negri^{68a,68b}, M. Negrini^{23b}, S. Nektarijevic¹¹⁷, C. Nellist⁵¹, M.E. Nelson¹³¹, S. Nemecek¹³⁷, P. Nemethy¹²¹, M. Nessi^{35,f}, M.S. Neubauer¹⁷⁰, M. Neumann¹⁷⁹, P.R. Newman²¹, T.Y. Ng^{61c}, Y.S. Ng¹⁹, H.D.N. Nguyen⁹⁹, T. Nguyen Manh¹⁰⁷, E. Nibigira³⁷, R.B. Nickerson¹³¹, R. Nicolaidou¹⁴², J. Nielsen¹⁴³, N. Nikiforou¹¹, V. Nikolaenko^{140,am}, I. Nikolic-Audit¹³², K. Nikolopoulos²¹, P. Nilsson²⁹, Y. Ninomiya⁷⁹, A. Nisati^{70a}, N. Nishu^{58c}, R. Nisius¹¹³, I. Nitsche⁴⁵, T. Nitta¹⁷⁶, T. Nobe¹⁶⁰, Y. Noguchi⁸³, M. Nomachi¹²⁹, I. Nomidis¹³², M.A. Nomura²⁹, T. Nooney⁹⁰, M. Nordberg³⁵, N. Norjoharuddeen¹³¹, T. Novak⁸⁹, O. Novgorodova⁴⁶, R. Novotny¹³⁸, L. Nozka¹²⁶, K. Ntekas¹⁶⁸, E. Nurse⁹², F. Nuti¹⁰², F.G. Oakham^{33,au}, H. Oberlack¹¹³, T. Obermann²⁴, J. Ocariz¹³², A. Ochi⁸⁰, I. Ochoa³⁸, J.P. Ochoa-Ricoux^{144a}, K. O'Connor²⁶, S. Oda⁸⁵, S. Odaka⁷⁹, S. Oerdek⁵¹, A. Oh⁹⁸, S.H. Oh⁴⁷, C.C. Ohm¹⁵¹, H. Oide^{53b,53a}, H. Okawa¹⁶⁶, Y. Okazaki⁸³, Y. Okumura¹⁶⁰, T. Okuyama⁷⁹, A. Olariu^{27b}, L.F. Oleiro Seabra^{136a}, S.A. Olivares Pino^{144a}, D. Oliveira Damazio²⁹, J.L. Oliver¹, M.J.R. Olsson³⁶, A. Olszewski⁸², J. Olszowska⁸², D.C. O'Neil¹⁴⁹, A. Onofre^{136a,136e}, K. Onogi¹¹⁵, P.U.E. Onyisi¹¹, H. Oppen¹³⁰, M.J. Oreglia³⁶, Y. Oren¹⁵⁸, D. Orestano^{72a,72b}, E.C. Orgill⁹⁸, N. Orlando^{61b}, A.A. O'Rourke⁴⁴, R.S. Orr¹⁶⁴, B. Osculati^{53b,53a,*}, V. O'Shea⁵⁵, R. Ospanov^{58a}, G. Otero y Garzon³⁰, H. Otono⁸⁵, M. Ouchrif^{34d}, F. Ould-Saada¹³⁰, A. Ouraou¹⁴², Q. Ouyang^{15a}, M. Owen⁵⁵, R.E. Owen²¹, V.E. Ozcan^{12c}, N. Ozturk⁸, J. Pacalt¹²⁶, H.A. Pacey³¹, K. Pachal¹⁴⁹, A. Pacheco Pages¹⁴, L. Pacheco Rodriguez¹⁴², C. Padilla Aranda¹⁴, S. Pagan Griso¹⁸, M. Paganini¹⁸⁰, G. Palacino⁶³, S. Palazzo^{40b,40a}, S. Palestini³⁵, M. Palka^{81b}, D. Pallin³⁷, I. Panagoulas¹⁰, C.E. Pandini³⁵, J.G. Panduro Vazquez⁹¹, P. Pani³⁵, G. Panizzo^{64a,64c}, L. Paolozzi⁵², T.D. Papadopoulou¹⁰, K. Papageorgiou^{9j}, A. Paramonov⁶, D. Paredes Hernandez^{61b}, S.R. Paredes Saenz¹³¹, B. Parida^{58c}, A.J. Parker⁸⁷, K.A. Parker⁴⁴, M.A. Parker³¹, F. Parodi^{53b,53a}, J.A. Parsons³⁸, U. Parzefall⁵⁰, V.R. Pascuzzi¹⁶⁴, J.M.P. Pasner¹⁴³, E. Pasqualucci^{70a}, S. Passaggio^{53b}, F. Pastore⁹¹, P. Pasuwan^{43a,43b}, S. Patariaia⁹⁷, J.R. Pater⁹⁸, A. Pathak^{178,k}, T. Pauly³⁵, B. Pearson¹¹³, M. Pedersen¹³⁰, L. Pedraza Diaz¹¹⁷, R. Pedro^{136a,136b}, S.V. Peleganchuk^{120b,120a}, O. Penc¹³⁷, C. Peng^{15d}, H. Peng^{58a}, B.S. Peralva^{78a}, M.M. Perego¹⁴², A.P. Pereira Peixoto^{136a}, D.V. Perepelitsa²⁹, F. Peri¹⁹, L. Perini^{66a,66b}, H. Pernegger³⁵, S. Perrella^{67a,67b}, V.D. Peshekhonov^{77,*}, K. Peters⁴⁴, R.F.Y. Peters⁹⁸, B.A. Petersen³⁵, T.C. Petersen³⁹, E. Petit⁵⁶, A. Petridis¹, C. Petridou¹⁵⁹, P. Petroff¹²⁸, E. Petrolo^{70a}, M. Petrov¹³¹, F. Petrucci^{72a,72b}, M. Pettee¹⁸⁰, N.E. Pettersson¹⁰⁰, A. Peyaud¹⁴², R. Pezoa^{144b}, T. Pham¹⁰², F.H. Phillips¹⁰⁴, P.W. Phillips¹⁴¹, G. Piacquadio¹⁵², E. Pianori¹⁸, A. Picazio¹⁰⁰, M.A. Pickering¹³¹, R. Piegaia³⁰, J.E. Pilcher³⁶, A.D. Pilkington⁹⁸, M. Pinamonti^{71a,71b}, J.L. Pinfeld³, M. Pitt¹⁷⁷,

M.-A. Pleier²⁹, V. Pleskot¹³⁹, E. Plotnikova⁷⁷, D. Pluth⁷⁶, P. Podberezko^{120b,120a}, R. Poettgen⁹⁴,
R. Poggi⁵², L. Poggioli¹²⁸, I. Pogrebnyak¹⁰⁴, D. Pohl²⁴, I. Pokharel⁵¹, G. Polesello^{68a}, A. Poley⁴⁴,
A. Policicchio^{70a,70b}, R. Polifka³⁵, A. Polini^{23b}, C.S. Pollard⁴⁴, V. Polychronakos²⁹, D. Ponomarenko¹¹⁰,
L. Pontecorvo³⁵, G.A. Popeneciu^{27d}, D.M. Portillo Quintero¹³², S. Pospisil¹³⁸, K. Potamianos⁴⁴,
I.N. Potrap⁷⁷, C.J. Potter³¹, H. Potti¹¹, T. Poulsen⁹⁴, J. Poveda³⁵, T.D. Powell¹⁴⁶,
M.E. Pozo Astigarraga³⁵, P. Pralavorio⁹⁹, S. Prell⁷⁶, D. Price⁹⁸, M. Primavera^{65a}, S. Prince¹⁰¹,
N. Proklova¹¹⁰, K. Prokofiev^{61c}, F. Prokoshin^{144b}, S. Protopopescu²⁹, J. Proudfoot⁶, M. Przybycien^{81a},
A. Puri¹⁷⁰, P. Puzo¹²⁸, J. Qian¹⁰³, Y. Qin⁹⁸, A. Quadt⁵¹, M. Queitsch-Maitland⁴⁴, A. Qureshi¹,
P. Rados¹⁰², F. Ragusa^{66a,66b}, G. Rahal⁹⁵, J.A. Raine⁹⁸, S. Rajagopalan²⁹, A. Ramirez Morales⁹⁰,
T. Rashid¹²⁸, S. Raspopov⁵, M.G. Ratti^{66a,66b}, D.M. Rauch⁴⁴, F. Rauscher¹¹², S. Rave⁹⁷, B. Ravina¹⁴⁶,
I. Ravinovich¹⁷⁷, J.H. Rawling⁹⁸, M. Raymond³⁵, A.L. Read¹³⁰, N.P. Readioff⁵⁶, M. Reale^{65a,65b},
D.M. Rebuzzi^{68a,68b}, A. Redelbach¹⁷⁴, G. Redlinger²⁹, R. Reece¹⁴³, R.G. Reed^{32c}, K. Reeves⁴²,
L. Rehnisch¹⁹, J. Reichert¹³³, A. Reiss⁹⁷, C. Rembser³⁵, H. Ren^{15d}, M. Rescigno^{70a}, S. Resconi^{66a},
E.D. Resseguie¹³³, S. Rettie¹⁷², E. Reynolds²¹, O.L. Rezanova^{120b,120a}, P. Reznicek¹³⁹, E. Ricci^{73a,73b},
R. Richter¹¹³, S. Richter⁹², E. Richter-Was^{81b}, O. Ricken²⁴, M. Ridel¹³², P. Rieck¹¹³, C.J. Riegel¹⁷⁹,
O. Rifki⁴⁴, M. Rijssenbeek¹⁵², A. Rimoldi^{68a,68b}, M. Rimoldi²⁰, L. Rinaldi^{23b}, G. Ripellino¹⁵¹,
B. Ristić⁸⁷, E. Ritsch³⁵, I. Riu¹⁴, J.C. Rivera Vergara^{144a}, F. Rizatdinova¹²⁵, E. Rizvi⁹⁰, C. Rizzi¹⁴,
R.T. Roberts⁹⁸, S.H. Robertson^{101,ad}, A. Robichaud-Veronneau¹⁰¹, D. Robinson³¹, J.E.M. Robinson⁴⁴,
A. Robson⁵⁵, E. Rocco⁹⁷, C. Roda^{69a,69b}, Y. Rodina⁹⁹, S. Rodriguez Bosca¹⁷¹, A. Rodriguez Perez¹⁴,
D. Rodriguez Rodriguez¹⁷¹, A.M. Rodríguez Vera^{165b}, S. Roe³⁵, C.S. Rogan⁵⁷, O. Røhne¹³⁰,
R. Röhrig¹¹³, C.P.A. Roland⁶³, J. Roloff⁵⁷, A. Romaniouk¹¹⁰, M. Romano^{23b,23a}, N. Rompotis⁸⁸,
M. Ronzani¹²¹, L. Roos¹³², S. Rosati^{70a}, K. Rosbach⁵⁰, P. Rose¹⁴³, N-A. Rosien⁵¹, E. Rossi⁴⁴,
E. Rossi^{67a,67b}, L.P. Rossi^{53b}, L. Rossini^{66a,66b}, J.H.N. Rosten³¹, R. Rosten¹⁴, M. Rotaru^{27b},
J. Rothberg¹⁴⁵, D. Rousseau¹²⁸, D. Roy^{32c}, A. Rozanov⁹⁹, Y. Rozen¹⁵⁷, X. Ruan^{32c}, F. Rubbo¹⁵⁰,
F. Rühr⁵⁰, A. Ruiz-Martinez¹⁷¹, Z. Rurikova⁵⁰, N.A. Rusakovich⁷⁷, H.L. Russell¹⁰¹, J.P. Rutherford⁷,
E.M. Rüttinger^{44,1}, Y.F. Ryabov¹³⁴, M. Rybar¹⁷⁰, G. Rybkin¹²⁸, S. Ryu⁶, A. Ryzhov¹⁴⁰, G.F. Rzehorz⁵¹,
P. Sabatini⁵¹, G. Sabato¹¹⁸, S. Sacerdoti¹²⁸, H.F.W. Sadrozinski¹⁴³, R. Sadykov⁷⁷, F. Safai Tehrani^{70a},
P. Saha¹¹⁹, M. Sahinsoy^{59a}, A. Sahu¹⁷⁹, M. Saimpert⁴⁴, M. Saito¹⁶⁰, T. Saito¹⁶⁰, H. Sakamoto¹⁶⁰,
A. Sakharov^{121,al}, D. Salamani⁵², G. Salamanna^{72a,72b}, J.E. Salazar Loyola^{144b}, D. Salek¹¹⁸,
P.H. Sales De Bruin¹⁶⁹, D. Salihagic¹¹³, A. Salnikov¹⁵⁰, J. Salt¹⁷¹, D. Salvatore^{40b,40a}, F. Salvatore¹⁵³,
A. Salvucci^{61a,61b,61c}, A. Salzburger³⁵, J. Samarati³⁵, D. Sammel⁵⁰, D. Sampsonidis¹⁵⁹,
D. Sampsonidou¹⁵⁹, J. Sánchez¹⁷¹, A. Sanchez Pineda^{64a,64c}, H. Sandaker¹³⁰, C.O. Sander⁴⁴,
M. Sandhoff¹⁷⁹, C. Sandoval²², D.P.C. Sankey¹⁴¹, M. Sannino^{53b,53a}, Y. Sano¹¹⁵, A. Sansoni⁴⁹,
C. Santoni³⁷, H. Santos^{136a}, I. Santoyo Castillo¹⁵³, A. Saproinov⁷⁷, J.G. Saraiva^{136a,136d}, O. Sasaki⁷⁹,
K. Sato¹⁶⁶, E. Sauvan⁵, P. Savard^{164,au}, N. Savic¹¹³, R. Sawada¹⁶⁰, C. Sawyer¹⁴¹, L. Sawyer^{93,aj},
C. Sbarra^{23b}, A. Sbrizzi^{23b,23a}, T. Scanlon⁹², J. Schaarschmidt¹⁴⁵, P. Schacht¹¹³, B.M. Schachtner¹¹²,
D. Schaefer³⁶, L. Schaefer¹³³, J. Schaeffer⁹⁷, S. Schaepe³⁵, U. Schäfer⁹⁷, A.C. Schaffer¹²⁸, D. Schaile¹¹²,
R.D. Schamberger¹⁵², N. Scharmberg⁹⁸, V.A. Schegelsky¹³⁴, D. Scheirich¹³⁹, F. Schenck¹⁹,
M. Schernau¹⁶⁸, C. Schiavi^{53b,53a}, S. Schier¹⁴³, L.K. Schildgen²⁴, Z.M. Schillaci²⁶, E.J. Schioppa³⁵,
M. Schioppa^{40b,40a}, K.E. Schleicher⁵⁰, S. Schlenker³⁵, K.R. Schmidt-Sommerfeld¹¹³, K. Schmieden³⁵,
C. Schmitt⁹⁷, S. Schmitt⁴⁴, S. Schmitz⁹⁷, U. Schnoor⁵⁰, L. Schoeffel¹⁴², A. Schoening^{59b}, E. Schopf²⁴,
M. Schott⁹⁷, J.F.P. Schouwenberg¹¹⁷, J. Schovancova³⁵, S. Schramm⁵², A. Schulte⁹⁷,
H-C. Schultz-Coulon^{59a}, M. Schumacher⁵⁰, B.A. Schumm¹⁴³, Ph. Schune¹⁴², A. Schwartzman¹⁵⁰,
T.A. Schwarz¹⁰³, H. Schweiger⁹⁸, Ph. Schwemling¹⁴², R. Schwienhorst¹⁰⁴, A. Sciandra²⁴, G. Sciolla²⁶,
M. Scornajenghi^{40b,40a}, F. Scuri^{69a}, F. Scutti¹⁰², L.M. Scyboz¹¹³, J. Searcy¹⁰³, C.D. Sebastiani^{70a,70b},
P. Seema²⁴, S.C. Seidel¹¹⁶, A. Seiden¹⁴³, T. Seiss³⁶, J.M. Seixas^{78b}, G. Sekhniaidze^{67a}, K. Sekhon¹⁰³,
S.J. Sekula⁴¹, N. Semprini-Cesari^{23b,23a}, S. Sen⁴⁷, S. Senkin³⁷, C. Serfon¹³⁰, L. Serin¹²⁸, L. Serkin^{64a,64b},

M. Sessa^{72a,72b}, H. Severini¹²⁴, F. Sforza¹⁶⁷, A. Sfyrila⁵², E. Shabalina⁵¹, J.D. Shahinian¹⁴³,
N.W. Shaikh^{43a,43b}, L.Y. Shan^{15a}, R. Shang¹⁷⁰, J.T. Shank²⁵, M. Shapiro¹⁸, A.S. Sharma¹, A. Sharma¹³¹,
P.B. Shatalov¹⁰⁹, K. Shaw¹⁵³, S.M. Shaw⁹⁸, A. Shcherbakova¹³⁴, Y. Shen¹²⁴, N. Sherafati³³,
A.D. Sherman²⁵, P. Sherwood⁹², L. Shi^{155,aq}, S. Shimizu⁸⁰, C.O. Shimmin¹⁸⁰, M. Shimojima¹¹⁴,
I.P.J. Shipsey¹³¹, S. Shirabe⁸⁵, M. Shiyakova⁷⁷, J. Shlomi¹⁷⁷, A. Shmeleva¹⁰⁸, D. Shoaleh Saadi¹⁰⁷,
M.J. Shochet³⁶, S. Shojaii¹⁰², D.R. Shope¹²⁴, S. Shrestha¹²², E. Shulga¹¹⁰, P. Sicho¹³⁷, A.M. Sickles¹⁷⁰,
P.E. Sidebo¹⁵¹, E. Sideras Haddad^{32c}, O. Sidiropoulou¹⁷⁴, A. Sidoti^{23b,23a}, F. Siegert⁴⁶, Dj. Sijacki¹⁶,
J. Silva^{136a}, M. Silva Jr.¹⁷⁸, M.V. Silva Oliveira^{78a}, S.B. Silverstein^{43a}, L. Simic⁷⁷, S. Simion¹²⁸,
E. Simioni⁹⁷, M. Simon⁹⁷, R. Simoniello⁹⁷, P. Sinervo¹⁶⁴, N.B. Sinev¹²⁷, M. Sioli^{23b,23a}, G. Siragusa¹⁷⁴,
I. Siral¹⁰³, S.Yu. Sivoklov¹¹¹, J. Sjölin^{43a,43b}, M.B. Skinner⁸⁷, P. Skubic¹²⁴, M. Slater²¹, T. Slavicek¹³⁸,
M. Slawinska⁸², K. Sliwa¹⁶⁷, R. Slovak¹³⁹, V. Smakhtin¹⁷⁷, B.H. Smart⁵, J. Smiesko^{28a}, N. Smirnov¹¹⁰,
S.Yu. Smirnov¹¹⁰, Y. Smirnov¹¹⁰, L.N. Smirnova¹¹¹, O. Smirnova⁹⁴, J.W. Smith⁵¹, M.N.K. Smith³⁸,
R.W. Smith³⁸, M. Smizanska⁸⁷, K. Smolek¹³⁸, A. Smykiewicz⁸², A.A. Snasarev¹⁰⁸, I.M. Snyder¹²⁷,
S. Snyder²⁹, R. Sobie^{173,ad}, A.M. Soffa¹⁶⁸, A. Soffer¹⁵⁸, A. Søggaard⁴⁸, D.A. Soh¹⁵⁵, G. Sokhrannyi⁸⁹,
C.A. Solans Sanchez³⁵, M. Solar¹³⁸, E.Yu. Soldatov¹¹⁰, U. Soldevila¹⁷¹, A.A. Solodkov¹⁴⁰,
A. Soloshenko⁷⁷, O.V. Solovyanov¹⁴⁰, V. Solovyev¹³⁴, P. Sommer¹⁴⁶, H. Son¹⁶⁷, W. Song¹⁴¹,
A. Sopczak¹³⁸, F. Sopkova^{28b}, D. Sosa^{59b}, C.L. Sotiropoulou^{69a,69b}, S. Sottocornola^{68a,68b},
R. Soualah^{64a,64c,i}, A.M. Soukharev^{120b,120a}, D. South⁴⁴, B.C. Sowden⁹¹, S. Spagnolo^{65a,65b},
M. Spalla¹¹³, M. Spangenberg¹⁷⁵, F. Spanò⁹¹, D. Sperlich¹⁹, F. Spettel¹¹³, T.M. Spieker^{59a}, R. Spighi^{23b},
G. Spigo³⁵, L.A. Spiller¹⁰², D.P. Spiteri⁵⁵, M. Spousta¹³⁹, A. Stabile^{66a,66b}, R. Stamen^{59a}, S. Stamm¹⁹,
E. Stanecka⁸², R.W. Stanek⁶, C. Stanescu^{72a}, B. Stanislaus¹³¹, M.M. Stanitzki⁴⁴, B. Stapf¹¹⁸,
S. Stapnes¹³⁰, E.A. Starchenko¹⁴⁰, G.H. Stark³⁶, J. Stark⁵⁶, S.H. Stark³⁹, P. Staroba¹³⁷, P. Starovoitov^{59a},
S. Stärz³⁵, R. Staszewski⁸², M. Stegler⁴⁴, P. Steinberg²⁹, B. Stelzer¹⁴⁹, H.J. Stelzer³⁵,
O. Stelzer-Chilton^{165a}, H. Stenzel⁵⁴, T.J. Stevenson⁹⁰, G.A. Stewart⁵⁵, M.C. Stockton¹²⁷, G. Stoicea^{27b},
P. Stolte⁵¹, S. Stonjek¹¹³, A. Straessner⁴⁶, J. Strandberg¹⁵¹, S. Strandberg^{43a,43b}, M. Strauss¹²⁴,
P. Striznec^{28b}, R. Ströhmer¹⁷⁴, D.M. Strom¹²⁷, R. Stroynowski⁴¹, A. Strubig⁴⁸, S.A. Stucci²⁹,
B. Stugu¹⁷, J. Stupak¹²⁴, N.A. Styles⁴⁴, D. Su¹⁵⁰, J. Su¹³⁵, S. Suchek^{59a}, Y. Sugaya¹²⁹, M. Suk¹³⁸,
V.V. Sulin¹⁰⁸, D.M.S. Sultan⁵², S. Sultansoy^{4c}, T. Sumida⁸³, S. Sun¹⁰³, X. Sun³, K. Suruliz¹⁵³,
C.J.E. Suster¹⁵⁴, M.R. Sutton¹⁵³, S. Suzuki⁷⁹, M. Svatos¹³⁷, M. Swiatlowski³⁶, S.P. Swift²,
A. Sydorenko⁹⁷, I. Sykora^{28a}, T. Sykora¹³⁹, D. Ta⁹⁷, K. Tackmann^{44,aa}, J. Taenzer¹⁵⁸, A. Taffard¹⁶⁸,
R. Tafirout^{165a}, E. Tahirovic⁹⁰, N. Taiblum¹⁵⁸, H. Takai²⁹, R. Takashima⁸⁴, E.H. Takasugi¹¹³,
K. Takeda⁸⁰, T. Takeshita¹⁴⁷, Y. Takubo⁷⁹, M. Talby⁹⁹, A.A. Talyshev^{120b,120a}, J. Tanaka¹⁶⁰,
M. Tanaka¹⁶², R. Tanaka¹²⁸, R. Tanioka⁸⁰, B.B. Tannenwald¹²², S. Tapia Araya^{144b}, S. Tapprogge⁹⁷,
A. Tarek Abouelfadl Mohamed¹³², S. Tarem¹⁵⁷, G. Tarna^{27b,e}, G.F. Tartarelli^{66a}, P. Tas¹³⁹,
M. Tasevsky¹³⁷, T. Tashiro⁸³, E. Tassi^{40b,40a}, A. Tavares Delgado^{136a,136b}, Y. Tayalati^{34e}, A.C. Taylor¹¹⁶,
A.J. Taylor⁴⁸, G.N. Taylor¹⁰², P.T.E. Taylor¹⁰², W. Taylor^{165b}, A.S. Tee⁸⁷, P. Teixeira-Dias⁹¹,
H. Ten Kate³⁵, P.K. Teng¹⁵⁵, J.J. Teoh¹¹⁸, F. Tepel¹⁷⁹, S. Terada⁷⁹, K. Terashi¹⁶⁰, J. Terron⁹⁶, S. Terzo¹⁴,
M. Testa⁴⁹, R.J. Teuscher^{164,ad}, S.J. Thais¹⁸⁰, T. Thevenaux-Pelzer⁴⁴, F. Thiele³⁹, D.W. Thomas⁹¹,
J.P. Thomas²¹, A.S. Thompson⁵⁵, P.D. Thompson²¹, L.A. Thomsen¹⁸⁰, E. Thomson¹³³, Y. Tian³⁸,
R.E. Ticse Torres⁵¹, V.O. Tikhomirov^{108,an}, Yu.A. Tikhonov^{120b,120a}, S. Timoshenko¹¹⁰, P. Tipton¹⁸⁰,
S. Tisserant⁹⁹, K. Todome¹⁶², S. Todorova-Nova⁵, S. Todt⁴⁶, J. Tojo⁸⁵, S. Tokár^{28a}, K. Tokushuku⁷⁹,
E. Tolley¹²², K.G. Tomiwa^{32c}, M. Tomoto¹¹⁵, L. Tompkins^{150,q}, K. Toms¹¹⁶, B. Tong⁵⁷, P. Tornambe⁵⁰,
E. Torrence¹²⁷, H. Torres⁴⁶, E. Torró Pastor¹⁴⁵, C. Toscirri¹³¹, J. Toth^{99,ac}, F. Touchard⁹⁹, D.R. Tovey¹⁴⁶,
C.J. Treado¹²¹, T. Trefzger¹⁷⁴, F. Tresoldi¹⁵³, A. Tricoli²⁹, I.M. Trigger^{165a}, S. Trincaz-Duvoid¹³²,
M.F. Tripiana¹⁴, W. Trischuk¹⁶⁴, B. Trocme⁵⁶, A. Trofymov¹²⁸, C. Troncon^{66a}, M. Trovatelli¹⁷³,
F. Trovato¹⁵³, L. Truong^{32b}, M. Trzebinski⁸², A. Trzupek⁸², F. Tsai⁴⁴, J.C-L. Tseng¹³¹,
P.V. Tsiareshka¹⁰⁵, N. Tsirintanis⁹, V. Tsiskaridze¹⁵², E.G. Tskhadadze^{156a}, I.I. Tsukerman¹⁰⁹,

V. Tsulaia¹⁸, S. Tsuno⁷⁹, D. Tsybychev¹⁵², Y. Tu^{61b}, A. Tudorache^{27b}, V. Tudorache^{27b}, T.T. Tulbure^{27a}, A.N. Tuna⁵⁷, S. Turchikhin⁷⁷, D. Turgeman¹⁷⁷, I. Turk Cakir^{4b,u}, R. Turra^{66a}, P.M. Tuts³⁸, E. Tzovara⁹⁷, G. Uccielli^{23b,23a}, I. Ueda⁷⁹, M. Ughetto^{43a,43b}, F. Ukegawa¹⁶⁶, G. Unal³⁵, A. Undrus²⁹, G. Unel¹⁶⁸, F.C. Ungaro¹⁰², Y. Unno⁷⁹, K. Uno¹⁶⁰, J. Urban^{28b}, P. Urquijo¹⁰², P. Urrejola⁹⁷, G. Usai⁸, J. Usui⁷⁹, L. Vacavant⁹⁹, V. Vacek¹³⁸, B. Vachon¹⁰¹, K.O.H. Vadla¹³⁰, A. Vaidya⁹², C. Valderanis¹¹², E. Valdes Santurio^{43a,43b}, M. Valente⁵², S. Valentinetti^{23b,23a}, A. Valero¹⁷¹, L. Valéry⁴⁴, R.A. Vallance²¹, A. Vallier⁵, J.A. Valls Ferrer¹⁷¹, T.R. Van Daalen¹⁴, W. Van Den Wollenberg¹¹⁸, H. Van der Graaf¹¹⁸, P. Van Gemmeren⁶, J. Van Nieuwkoop¹⁴⁹, I. Van Vulpen¹¹⁸, M. Vanadia^{71a,71b}, W. Vandelli³⁵, A. Vaniachine¹⁶³, P. Vankov¹¹⁸, R. Vari^{70a}, E.W. Varnes⁷, C. Varni^{53b,53a}, T. Varol⁴¹, D. Varouchas¹²⁸, K.E. Varvell¹⁵⁴, G.A. Vasquez^{144b}, J.G. Vasquez¹⁸⁰, F. Vazeille³⁷, D. Vazquez Furelos¹⁴, T. Vazquez Schroeder¹⁰¹, J. Veatch⁵¹, V. Vecchio^{72a,72b}, L.M. Veloce¹⁶⁴, F. Veloso^{136a,136c}, S. Veneziano^{70a}, A. Ventura^{65a,65b}, M. Venturi¹⁷³, N. Venturi³⁵, V. Vercesi^{68a}, M. Verducci^{72a,72b}, C.M. Vergel Infante⁷⁶, W. Verkerke¹¹⁸, A.T. Vermeulen¹¹⁸, J.C. Vermeulen¹¹⁸, M.C. Vetterli^{149,au}, N. Viaux Maira^{144b}, M. Vicente Barreto Pinto⁵², I. Vichou^{170,*}, T. Vickey¹⁴⁶, O.E. Vickey Boeriu¹⁴⁶, G.H.A. Viehhauser¹³¹, S. Viel¹⁸, L. Vigani¹³¹, M. Villa^{23b,23a}, M. Villaplana Perez^{66a,66b}, E. Vilucchi⁴⁹, M.G. Vincter³³, V.B. Vinogradov⁷⁷, A. Vishwakarma⁴⁴, C. Vittori^{23b,23a}, I. Vivarelli¹⁵³, S. Vlachos¹⁰, M. Vogel¹⁷⁹, P. Vokac¹³⁸, G. Volpi¹⁴, S.E. von Buddenbrock^{32c}, E. Von Toerne²⁴, V. Vorobel¹³⁹, K. Vorobev¹¹⁰, M. Vos¹⁷¹, J.H. Vosseveld⁸⁸, N. Vranjes¹⁶, M. Vranjes Milosavljevic¹⁶, V. Vrba¹³⁸, M. Vreeswijk¹¹⁸, T. Šfiligoj⁸⁹, R. Vuillermet³⁵, I. Vukotic³⁶, T. Ženiš^{28a}, L. Živković¹⁶, P. Wagner²⁴, W. Wagner¹⁷⁹, J. Wagner-Kuhr¹¹², H. Wahlberg⁸⁶, S. Wahrmund⁴⁶, K. Wakamiya⁸⁰, V.M. Walbrecht¹¹³, J. Walder⁸⁷, R. Walker¹¹², S.D. Walker⁹¹, W. Walkowiak¹⁴⁸, V. Wallangen^{43a,43b}, A.M. Wang⁵⁷, C. Wang^{58b,e}, F. Wang¹⁷⁸, H. Wang¹⁸, H. Wang³, J. Wang¹⁵⁴, J. Wang^{59b}, P. Wang⁴¹, Q. Wang¹²⁴, R.-J. Wang¹³², R. Wang^{58a}, R. Wang⁶, S.M. Wang¹⁵⁵, W.T. Wang^{58a}, W. Wang^{15c,ae}, W.X. Wang^{58a,ae}, Y. Wang^{58a,ak}, Z. Wang^{58c}, C. Wanotayaroj⁴⁴, A. Warburton¹⁰¹, C.P. Ward³¹, D.R. Wardrope⁹², A. Washbrook⁴⁸, P.M. Watkins²¹, A.T. Watson²¹, M.F. Watson²¹, G. Watts¹⁴⁵, S. Watts⁹⁸, B.M. Waugh⁹², A.F. Webb¹¹, S. Webb⁹⁷, C. Weber¹⁸⁰, M.S. Weber²⁰, S.A. Weber³³, S.M. Weber^{59a}, A.R. Weidberg¹³¹, B. Weinert⁶³, J. Weingarten⁵¹, M. Weirich⁹⁷, C. Weiser⁵⁰, P.S. Wells³⁵, T. Wenaus²⁹, T. Wengler³⁵, S. Wenig³⁵, N. Wermes²⁴, M.D. Werner⁷⁶, P. Werner³⁵, M. Wessels^{59a}, T.D. Weston²⁰, K. Whalen¹²⁷, N.L. Whallon¹⁴⁵, A.M. Wharton⁸⁷, A.S. White¹⁰³, A. White⁸, M.J. White¹, R. White^{144b}, D. Whiteson¹⁶⁸, B.W. Whitmore⁸⁷, F.J. Wickens¹⁴¹, W. Wiedenmann¹⁷⁸, M. Wielers¹⁴¹, C. Wiglesworth³⁹, L.A.M. Wiik-Fuchs⁵⁰, A. Wildauer¹¹³, F. Wilk⁹⁸, H.G. Wilkens³⁵, L.J. Wilkins⁹¹, H.H. Williams¹³³, S. Williams³¹, C. Willis¹⁰⁴, S. Willocq¹⁰⁰, J.A. Wilson²¹, I. Wingerter-Seez⁵, E. Winkels¹⁵³, F. Winklmeier¹²⁷, O.J. Winston¹⁵³, B.T. Winter²⁴, M. Wittgen¹⁵⁰, M. Wobisch⁹³, A. Wolf⁹⁷, T.M.H. Wolf¹¹⁸, R. Wolff⁹⁹, M.W. Wolter⁸², H. Wolters^{136a,136c}, V.W.S. Wong¹⁷², N.L. Woods¹⁴³, S.D. Worm²¹, B.K. Wosiek⁸², K.W. Woźniak⁸², K. Wraight⁵⁵, M. Wu³⁶, S.L. Wu¹⁷⁸, X. Wu⁵², Y. Wu^{58a}, T.R. Wyatt⁹⁸, B.M. Wynne⁴⁸, S. Xella³⁹, Z. Xi¹⁰³, L. Xia¹⁷⁵, D. Xu^{15a}, H. Xu^{58a,e}, L. Xu²⁹, T. Xu¹⁴², W. Xu¹⁰³, B. Yabsley¹⁵⁴, S. Yacoub^{32a}, K. Yajima¹²⁹, D.P. Yallup⁹², D. Yamaguchi¹⁶², Y. Yamaguchi¹⁶², A. Yamamoto⁷⁹, T. Yamanaka¹⁶⁰, F. Yamane⁸⁰, M. Yamatani¹⁶⁰, T. Yamazaki¹⁶⁰, Y. Yamazaki⁸⁰, Z. Yan²⁵, H.J. Yang^{58c,58d}, H.T. Yang¹⁸, S. Yang⁷⁵, Y. Yang¹⁶⁰, Z. Yang¹⁷, W.-M. Yao¹⁸, Y.C. Yap⁴⁴, Y. Yasu⁷⁹, E. Yatsenko^{58c,58d}, J. Ye⁴¹, S. Ye²⁹, I. Yeletsikh⁷⁷, E. Yigitbasi²⁵, E. Yildirim⁹⁷, K. Yorita¹⁷⁶, K. Yoshihara¹³³, C.J.S. Young³⁵, C. Young¹⁵⁰, J. Yu⁸, J. Yu⁷⁶, X. Yue^{59a}, S.P.Y. Yuen²⁴, B. Zabinski⁸², G. Zacharis¹⁰, E. Zaffaroni⁵², R. Zaidan¹⁴, A.M. Zaitsev^{140,am}, N. Zakharchuk⁴⁴, J. Zalieckas¹⁷, S. Zambito⁵⁷, D. Zanzi³⁵, D.R. Zaripovas⁵⁵, S.V. Zeiβner⁴⁵, C. Zeitnitz¹⁷⁹, G. Zemaityte¹³¹, J.C. Zeng¹⁷⁰, Q. Zeng¹⁵⁰, O. Zenin¹⁴⁰, D. Zerwas¹²⁸, M. Zgubic¹³¹, D.F. Zhang^{58b}, D. Zhang¹⁰³, F. Zhang¹⁷⁸, G. Zhang^{58a}, H. Zhang^{15c}, J. Zhang⁶, L. Zhang^{15c}, L. Zhang^{58a}, M. Zhang¹⁷⁰, P. Zhang^{15c}, R. Zhang^{58a}, R. Zhang²⁴, X. Zhang^{58b}, Y. Zhang^{15d}, Z. Zhang¹²⁸, P. Zhao⁴⁷, X. Zhao⁴¹, Y. Zhao^{58b,128,ai}, Z. Zhao^{58a}, A. Zhemchugov⁷⁷, B. Zhou¹⁰³, C. Zhou¹⁷⁸, L. Zhou⁴¹, M.S. Zhou^{15d},

M. Zhou¹⁵², N. Zhou^{58c}, Y. Zhou⁷, C.G. Zhu^{58b}, H.L. Zhu^{58a}, H. Zhu^{15a}, J. Zhu¹⁰³, Y. Zhu^{58a}, X. Zhuang^{15a}, K. Zhukov¹⁰⁸, V. Zhulanov^{120b,120a}, A. Zibell¹⁷⁴, D. Zieminska⁶³, N.I. Zimine⁷⁷, S. Zimmermann⁵⁰, Z. Zinonos¹¹³, M. Zinser⁹⁷, M. Ziolkowski¹⁴⁸, G. Zobernig¹⁷⁸, A. Zoccoli^{23b,23a}, K. Zoch⁵¹, T.G. Zorbas¹⁴⁶, R. Zou³⁶, M. Zur Nedden¹⁹, L. Zwalinski³⁵.

¹Department of Physics, University of Adelaide, Adelaide; Australia.

²Physics Department, SUNY Albany, Albany NY; United States of America.

³Department of Physics, University of Alberta, Edmonton AB; Canada.

⁴(^a)Department of Physics, Ankara University, Ankara; (^b)Istanbul Aydin University, Istanbul; (^c)Division of Physics, TOBB University of Economics and Technology, Ankara; Turkey.

⁵LAPP, Université Grenoble Alpes, Université Savoie Mont Blanc, CNRS/IN2P3, Annecy; France.

⁶High Energy Physics Division, Argonne National Laboratory, Argonne IL; United States of America.

⁷Department of Physics, University of Arizona, Tucson AZ; United States of America.

⁸Department of Physics, University of Texas at Arlington, Arlington TX; United States of America.

⁹Physics Department, National and Kapodistrian University of Athens, Athens; Greece.

¹⁰Physics Department, National Technical University of Athens, Zografou; Greece.

¹¹Department of Physics, University of Texas at Austin, Austin TX; United States of America.

¹²(^a)Bahcesehir University, Faculty of Engineering and Natural Sciences, Istanbul; (^b)Istanbul Bilgi University, Faculty of Engineering and Natural Sciences, Istanbul; (^c)Department of Physics, Bogazici University, Istanbul; (^d)Department of Physics Engineering, Gaziantep University, Gaziantep; Turkey.

¹³Institute of Physics, Azerbaijan Academy of Sciences, Baku; Azerbaijan.

¹⁴Institut de Física d'Altes Energies (IFAE), Barcelona Institute of Science and Technology, Barcelona; Spain.

¹⁵(^a)Institute of High Energy Physics, Chinese Academy of Sciences, Beijing; (^b)Physics Department, Tsinghua University, Beijing; (^c)Department of Physics, Nanjing University, Nanjing; (^d)University of Chinese Academy of Science (UCAS), Beijing; China.

¹⁶Institute of Physics, University of Belgrade, Belgrade; Serbia.

¹⁷Department for Physics and Technology, University of Bergen, Bergen; Norway.

¹⁸Physics Division, Lawrence Berkeley National Laboratory and University of California, Berkeley CA; United States of America.

¹⁹Institut für Physik, Humboldt Universität zu Berlin, Berlin; Germany.

²⁰Albert Einstein Center for Fundamental Physics and Laboratory for High Energy Physics, University of Bern, Bern; Switzerland.

²¹School of Physics and Astronomy, University of Birmingham, Birmingham; United Kingdom.

²²Centro de Investigaciones, Universidad Antonio Nariño, Bogota; Colombia.

²³(^a)Dipartimento di Fisica e Astronomia, Università di Bologna, Bologna; (^b)INFN Sezione di Bologna; Italy.

²⁴Physikalisches Institut, Universität Bonn, Bonn; Germany.

²⁵Department of Physics, Boston University, Boston MA; United States of America.

²⁶Department of Physics, Brandeis University, Waltham MA; United States of America.

²⁷(^a)Transilvania University of Brasov, Brasov; (^b)Horia Hulubei National Institute of Physics and Nuclear Engineering, Bucharest; (^c)Department of Physics, Alexandru Ioan Cuza University of Iasi, Iasi; (^d)National Institute for Research and Development of Isotopic and Molecular Technologies, Physics Department, Cluj-Napoca; (^e)University Politehnica Bucharest, Bucharest; (^f)West University in Timisoara, Timisoara; Romania.

²⁸(^a)Faculty of Mathematics, Physics and Informatics, Comenius University, Bratislava; (^b)Department of Subnuclear Physics, Institute of Experimental Physics of the Slovak Academy of Sciences, Kosice;

Slovak Republic.

²⁹Physics Department, Brookhaven National Laboratory, Upton NY; United States of America.

³⁰Departamento de Física, Universidad de Buenos Aires, Buenos Aires; Argentina.

³¹Cavendish Laboratory, University of Cambridge, Cambridge; United Kingdom.

^{32(a)}Department of Physics, University of Cape Town, Cape Town;^(b)Department of Mechanical Engineering Science, University of Johannesburg, Johannesburg;^(c)School of Physics, University of the Witwatersrand, Johannesburg; South Africa.

³³Department of Physics, Carleton University, Ottawa ON; Canada.

^{34(a)}Faculté des Sciences Ain Chock, Réseau Universitaire de Physique des Hautes Energies - Université Hassan II, Casablanca;^(b)Centre National de l'Energie des Sciences Techniques Nucleaires (CNESTEN), Rabat;^(c)Faculté des Sciences Semlalia, Université Cadi Ayyad, LPHEA-Marrakech;^(d)Faculté des Sciences, Université Mohamed Premier and LPTPM, Oujda;^(e)Faculté des sciences, Université Mohammed V, Rabat; Morocco.

³⁵CERN, Geneva; Switzerland.

³⁶Enrico Fermi Institute, University of Chicago, Chicago IL; United States of America.

³⁷LPC, Université Clermont Auvergne, CNRS/IN2P3, Clermont-Ferrand; France.

³⁸Nevis Laboratory, Columbia University, Irvington NY; United States of America.

³⁹Niels Bohr Institute, University of Copenhagen, Copenhagen; Denmark.

^{40(a)}Dipartimento di Fisica, Università della Calabria, Rende;^(b)INFN Gruppo Collegato di Cosenza, Laboratori Nazionali di Frascati; Italy.

⁴¹Physics Department, Southern Methodist University, Dallas TX; United States of America.

⁴²Physics Department, University of Texas at Dallas, Richardson TX; United States of America.

^{43(a)}Department of Physics, Stockholm University;^(b)Oskar Klein Centre, Stockholm; Sweden.

⁴⁴Deutsches Elektronen-Synchrotron DESY, Hamburg and Zeuthen; Germany.

⁴⁵Lehrstuhl für Experimentelle Physik IV, Technische Universität Dortmund, Dortmund; Germany.

⁴⁶Institut für Kern- und Teilchenphysik, Technische Universität Dresden, Dresden; Germany.

⁴⁷Department of Physics, Duke University, Durham NC; United States of America.

⁴⁸SUPA - School of Physics and Astronomy, University of Edinburgh, Edinburgh; United Kingdom.

⁴⁹INFN e Laboratori Nazionali di Frascati, Frascati; Italy.

⁵⁰Physikalisches Institut, Albert-Ludwigs-Universität Freiburg, Freiburg; Germany.

⁵¹II. Physikalisches Institut, Georg-August-Universität Göttingen, Göttingen; Germany.

⁵²Département de Physique Nucléaire et Corpusculaire, Université de Genève, Genève; Switzerland.

^{53(a)}Dipartimento di Fisica, Università di Genova, Genova;^(b)INFN Sezione di Genova; Italy.

⁵⁴II. Physikalisches Institut, Justus-Liebig-Universität Giessen, Giessen; Germany.

⁵⁵SUPA - School of Physics and Astronomy, University of Glasgow, Glasgow; United Kingdom.

⁵⁶LPSC, Université Grenoble Alpes, CNRS/IN2P3, Grenoble INP, Grenoble; France.

⁵⁷Laboratory for Particle Physics and Cosmology, Harvard University, Cambridge MA; United States of America.

^{58(a)}Department of Modern Physics and State Key Laboratory of Particle Detection and Electronics, University of Science and Technology of China, Hefei;^(b)Institute of Frontier and Interdisciplinary Science and Key Laboratory of Particle Physics and Particle Irradiation (MOE), Shandong University, Qingdao;^(c)School of Physics and Astronomy, Shanghai Jiao Tong University, KLPPAC-MoE, SKLPPC, Shanghai;^(d)Tsung-Dao Lee Institute, Shanghai; China.

^{59(a)}Kirchhoff-Institut für Physik, Ruprecht-Karls-Universität Heidelberg, Heidelberg;^(b)Physikalisches Institut, Ruprecht-Karls-Universität Heidelberg, Heidelberg; Germany.

⁶⁰Faculty of Applied Information Science, Hiroshima Institute of Technology, Hiroshima; Japan.

^{61(a)}Department of Physics, Chinese University of Hong Kong, Shatin, N.T., Hong Kong;^(b)Department

of Physics, University of Hong Kong, Hong Kong;^(c)Department of Physics and Institute for Advanced Study, Hong Kong University of Science and Technology, Clear Water Bay, Kowloon, Hong Kong; China.

⁶²Department of Physics, National Tsing Hua University, Hsinchu; Taiwan.

⁶³Department of Physics, Indiana University, Bloomington IN; United States of America.

^{64(a)}INFN Gruppo Collegato di Udine, Sezione di Trieste, Udine;^(b)ICTP, Trieste;^(c)Dipartimento di Chimica, Fisica e Ambiente, Università di Udine, Udine; Italy.

^{65(a)}INFN Sezione di Lecce;^(b)Dipartimento di Matematica e Fisica, Università del Salento, Lecce; Italy.

^{66(a)}INFN Sezione di Milano;^(b)Dipartimento di Fisica, Università di Milano, Milano; Italy.

^{67(a)}INFN Sezione di Napoli;^(b)Dipartimento di Fisica, Università di Napoli, Napoli; Italy.

^{68(a)}INFN Sezione di Pavia;^(b)Dipartimento di Fisica, Università di Pavia, Pavia; Italy.

^{69(a)}INFN Sezione di Pisa;^(b)Dipartimento di Fisica E. Fermi, Università di Pisa, Pisa; Italy.

^{70(a)}INFN Sezione di Roma;^(b)Dipartimento di Fisica, Sapienza Università di Roma, Roma; Italy.

^{71(a)}INFN Sezione di Roma Tor Vergata;^(b)Dipartimento di Fisica, Università di Roma Tor Vergata, Roma; Italy.

^{72(a)}INFN Sezione di Roma Tre;^(b)Dipartimento di Matematica e Fisica, Università Roma Tre, Roma; Italy.

^{73(a)}INFN-TIFPA;^(b)Università degli Studi di Trento, Trento; Italy.

⁷⁴Institut für Astro- und Teilchenphysik, Leopold-Franzens-Universität, Innsbruck; Austria.

⁷⁵University of Iowa, Iowa City IA; United States of America.

⁷⁶Department of Physics and Astronomy, Iowa State University, Ames IA; United States of America.

⁷⁷Joint Institute for Nuclear Research, Dubna; Russia.

^{78(a)}Departamento de Engenharia Elétrica, Universidade Federal de Juiz de Fora (UFJF), Juiz de Fora;^(b)Universidade Federal do Rio De Janeiro COPPE/EE/IF, Rio de Janeiro;^(c)Universidade Federal de São João del Rei (UFSJ), São João del Rei;^(d)Instituto de Física, Universidade de São Paulo, São Paulo; Brazil.

⁷⁹KEK, High Energy Accelerator Research Organization, Tsukuba; Japan.

⁸⁰Graduate School of Science, Kobe University, Kobe; Japan.

^{81(a)}AGH University of Science and Technology, Faculty of Physics and Applied Computer Science, Krakow;^(b)Marian Smoluchowski Institute of Physics, Jagiellonian University, Krakow; Poland.

⁸²Institute of Nuclear Physics Polish Academy of Sciences, Krakow; Poland.

⁸³Faculty of Science, Kyoto University, Kyoto; Japan.

⁸⁴Kyoto University of Education, Kyoto; Japan.

⁸⁵Research Center for Advanced Particle Physics and Department of Physics, Kyushu University, Fukuoka ; Japan.

⁸⁶Instituto de Física La Plata, Universidad Nacional de La Plata and CONICET, La Plata; Argentina.

⁸⁷Physics Department, Lancaster University, Lancaster; United Kingdom.

⁸⁸Oliver Lodge Laboratory, University of Liverpool, Liverpool; United Kingdom.

⁸⁹Department of Experimental Particle Physics, Jožef Stefan Institute and Department of Physics, University of Ljubljana, Ljubljana; Slovenia.

⁹⁰School of Physics and Astronomy, Queen Mary University of London, London; United Kingdom.

⁹¹Department of Physics, Royal Holloway University of London, Egham; United Kingdom.

⁹²Department of Physics and Astronomy, University College London, London; United Kingdom.

⁹³Louisiana Tech University, Ruston LA; United States of America.

⁹⁴Fysiska institutionen, Lunds universitet, Lund; Sweden.

⁹⁵Centre de Calcul de l'Institut National de Physique Nucléaire et de Physique des Particules (IN2P3), Villeurbanne; France.

- ⁹⁶Departamento de Física Teórica C-15 and CIAFF, Universidad Autónoma de Madrid, Madrid; Spain.
- ⁹⁷Institut für Physik, Universität Mainz, Mainz; Germany.
- ⁹⁸School of Physics and Astronomy, University of Manchester, Manchester; United Kingdom.
- ⁹⁹CPPM, Aix-Marseille Université, CNRS/IN2P3, Marseille; France.
- ¹⁰⁰Department of Physics, University of Massachusetts, Amherst MA; United States of America.
- ¹⁰¹Department of Physics, McGill University, Montreal QC; Canada.
- ¹⁰²School of Physics, University of Melbourne, Victoria; Australia.
- ¹⁰³Department of Physics, University of Michigan, Ann Arbor MI; United States of America.
- ¹⁰⁴Department of Physics and Astronomy, Michigan State University, East Lansing MI; United States of America.
- ¹⁰⁵B.I. Stepanov Institute of Physics, National Academy of Sciences of Belarus, Minsk; Belarus.
- ¹⁰⁶Research Institute for Nuclear Problems of Byelorussian State University, Minsk; Belarus.
- ¹⁰⁷Group of Particle Physics, University of Montreal, Montreal QC; Canada.
- ¹⁰⁸P.N. Lebedev Physical Institute of the Russian Academy of Sciences, Moscow; Russia.
- ¹⁰⁹Institute for Theoretical and Experimental Physics (ITEP), Moscow; Russia.
- ¹¹⁰National Research Nuclear University MEPhI, Moscow; Russia.
- ¹¹¹D.V. Skobel'syn Institute of Nuclear Physics, M.V. Lomonosov Moscow State University, Moscow; Russia.
- ¹¹²Fakultät für Physik, Ludwig-Maximilians-Universität München, München; Germany.
- ¹¹³Max-Planck-Institut für Physik (Werner-Heisenberg-Institut), München; Germany.
- ¹¹⁴Nagasaki Institute of Applied Science, Nagasaki; Japan.
- ¹¹⁵Graduate School of Science and Kobayashi-Maskawa Institute, Nagoya University, Nagoya; Japan.
- ¹¹⁶Department of Physics and Astronomy, University of New Mexico, Albuquerque NM; United States of America.
- ¹¹⁷Institute for Mathematics, Astrophysics and Particle Physics, Radboud University Nijmegen/Nikhef, Nijmegen; Netherlands.
- ¹¹⁸Nikhef National Institute for Subatomic Physics and University of Amsterdam, Amsterdam; Netherlands.
- ¹¹⁹Department of Physics, Northern Illinois University, DeKalb IL; United States of America.
- ^{120(a)}Budker Institute of Nuclear Physics, SB RAS, Novosibirsk; ^(b)Novosibirsk State University Novosibirsk; Russia.
- ¹²¹Department of Physics, New York University, New York NY; United States of America.
- ¹²²Ohio State University, Columbus OH; United States of America.
- ¹²³Faculty of Science, Okayama University, Okayama; Japan.
- ¹²⁴Homer L. Dodge Department of Physics and Astronomy, University of Oklahoma, Norman OK; United States of America.
- ¹²⁵Department of Physics, Oklahoma State University, Stillwater OK; United States of America.
- ¹²⁶Palacký University, RCPTM, Joint Laboratory of Optics, Olomouc; Czech Republic.
- ¹²⁷Center for High Energy Physics, University of Oregon, Eugene OR; United States of America.
- ¹²⁸LAL, Université Paris-Sud, CNRS/IN2P3, Université Paris-Saclay, Orsay; France.
- ¹²⁹Graduate School of Science, Osaka University, Osaka; Japan.
- ¹³⁰Department of Physics, University of Oslo, Oslo; Norway.
- ¹³¹Department of Physics, Oxford University, Oxford; United Kingdom.
- ¹³²LPNHE, Sorbonne Université, Paris Diderot Sorbonne Paris Cité, CNRS/IN2P3, Paris; France.
- ¹³³Department of Physics, University of Pennsylvania, Philadelphia PA; United States of America.
- ¹³⁴Konstantinov Nuclear Physics Institute of National Research Centre "Kurchatov Institute", PNPI, St. Petersburg; Russia.

- ¹³⁵Department of Physics and Astronomy, University of Pittsburgh, Pittsburgh PA; United States of America.
- ¹³⁶(^a)Laboratório de Instrumentação e Física Experimental de Partículas - LIP;(^b)Departamento de Física, Faculdade de Ciências, Universidade de Lisboa, Lisboa;(^c)Departamento de Física, Universidade de Coimbra, Coimbra;(^d)Centro de Física Nuclear da Universidade de Lisboa, Lisboa;(^e)Departamento de Física, Universidade do Minho, Braga;(^f)Departamento de Física Teórica y del Cosmos, Universidad de Granada, Granada (Spain);(^g)Dep Física and CEFITEC of Faculdade de Ciências e Tecnologia, Universidade Nova de Lisboa, Caparica; Portugal.
- ¹³⁷Institute of Physics, Academy of Sciences of the Czech Republic, Prague; Czech Republic.
- ¹³⁸Czech Technical University in Prague, Prague; Czech Republic.
- ¹³⁹Charles University, Faculty of Mathematics and Physics, Prague; Czech Republic.
- ¹⁴⁰State Research Center Institute for High Energy Physics, NRC KI, Protvino; Russia.
- ¹⁴¹Particle Physics Department, Rutherford Appleton Laboratory, Didcot; United Kingdom.
- ¹⁴²IRFU, CEA, Université Paris-Saclay, Gif-sur-Yvette; France.
- ¹⁴³Santa Cruz Institute for Particle Physics, University of California Santa Cruz, Santa Cruz CA; United States of America.
- ¹⁴⁴(^a)Departamento de Física, Pontificia Universidad Católica de Chile, Santiago;(^b)Departamento de Física, Universidad Técnica Federico Santa María, Valparaíso; Chile.
- ¹⁴⁵Department of Physics, University of Washington, Seattle WA; United States of America.
- ¹⁴⁶Department of Physics and Astronomy, University of Sheffield, Sheffield; United Kingdom.
- ¹⁴⁷Department of Physics, Shinshu University, Nagano; Japan.
- ¹⁴⁸Department Physik, Universität Siegen, Siegen; Germany.
- ¹⁴⁹Department of Physics, Simon Fraser University, Burnaby BC; Canada.
- ¹⁵⁰SLAC National Accelerator Laboratory, Stanford CA; United States of America.
- ¹⁵¹Physics Department, Royal Institute of Technology, Stockholm; Sweden.
- ¹⁵²Departments of Physics and Astronomy, Stony Brook University, Stony Brook NY; United States of America.
- ¹⁵³Department of Physics and Astronomy, University of Sussex, Brighton; United Kingdom.
- ¹⁵⁴School of Physics, University of Sydney, Sydney; Australia.
- ¹⁵⁵Institute of Physics, Academia Sinica, Taipei; Taiwan.
- ¹⁵⁶(^a)E. Andronikashvili Institute of Physics, Iv. Javakhishvili Tbilisi State University, Tbilisi;(^b)High Energy Physics Institute, Tbilisi State University, Tbilisi; Georgia.
- ¹⁵⁷Department of Physics, Technion, Israel Institute of Technology, Haifa; Israel.
- ¹⁵⁸Raymond and Beverly Sackler School of Physics and Astronomy, Tel Aviv University, Tel Aviv; Israel.
- ¹⁵⁹Department of Physics, Aristotle University of Thessaloniki, Thessaloniki; Greece.
- ¹⁶⁰International Center for Elementary Particle Physics and Department of Physics, University of Tokyo, Tokyo; Japan.
- ¹⁶¹Graduate School of Science and Technology, Tokyo Metropolitan University, Tokyo; Japan.
- ¹⁶²Department of Physics, Tokyo Institute of Technology, Tokyo; Japan.
- ¹⁶³Tomsk State University, Tomsk; Russia.
- ¹⁶⁴Department of Physics, University of Toronto, Toronto ON; Canada.
- ¹⁶⁵(^a)TRIUMF, Vancouver BC;(^b)Department of Physics and Astronomy, York University, Toronto ON; Canada.
- ¹⁶⁶Division of Physics and Tomonaga Center for the History of the Universe, Faculty of Pure and Applied Sciences, University of Tsukuba, Tsukuba; Japan.
- ¹⁶⁷Department of Physics and Astronomy, Tufts University, Medford MA; United States of America.
- ¹⁶⁸Department of Physics and Astronomy, University of California Irvine, Irvine CA; United States of

America.

¹⁶⁹Department of Physics and Astronomy, University of Uppsala, Uppsala; Sweden.

¹⁷⁰Department of Physics, University of Illinois, Urbana IL; United States of America.

¹⁷¹Instituto de Física Corpuscular (IFIC), Centro Mixto Universidad de Valencia - CSIC, Valencia; Spain.

¹⁷²Department of Physics, University of British Columbia, Vancouver BC; Canada.

¹⁷³Department of Physics and Astronomy, University of Victoria, Victoria BC; Canada.

¹⁷⁴Fakultät für Physik und Astronomie, Julius-Maximilians-Universität Würzburg, Würzburg; Germany.

¹⁷⁵Department of Physics, University of Warwick, Coventry; United Kingdom.

¹⁷⁶Waseda University, Tokyo; Japan.

¹⁷⁷Department of Particle Physics, Weizmann Institute of Science, Rehovot; Israel.

¹⁷⁸Department of Physics, University of Wisconsin, Madison WI; United States of America.

¹⁷⁹Fakultät für Mathematik und Naturwissenschaften, Fachgruppe Physik, Bergische Universität Wuppertal, Wuppertal; Germany.

¹⁸⁰Department of Physics, Yale University, New Haven CT; United States of America.

¹⁸¹Yerevan Physics Institute, Yerevan; Armenia.

^a Also at Borough of Manhattan Community College, City University of New York, NY; United States of America.

^b Also at California State University, East Bay; United States of America.

^c Also at Centre for High Performance Computing, CSIR Campus, Rosebank, Cape Town; South Africa.

^d Also at CERN, Geneva; Switzerland.

^e Also at CPPM, Aix-Marseille Université, CNRS/IN2P3, Marseille; France.

^f Also at Département de Physique Nucléaire et Corpusculaire, Université de Genève, Genève; Switzerland.

^g Also at Departament de Física de la Universitat Autònoma de Barcelona, Barcelona; Spain.

^h Also at Departamento de Física Teórica y del Cosmos, Universidad de Granada, Granada (Spain); Spain.

ⁱ Also at Department of Applied Physics and Astronomy, University of Sharjah, Sharjah; United Arab Emirates.

^j Also at Department of Financial and Management Engineering, University of the Aegean, Chios; Greece.

^k Also at Department of Physics and Astronomy, University of Louisville, Louisville, KY; United States of America.

^l Also at Department of Physics and Astronomy, University of Sheffield, Sheffield; United Kingdom.

^m Also at Department of Physics, California State University, Fresno CA; United States of America.

ⁿ Also at Department of Physics, California State University, Sacramento CA; United States of America.

^o Also at Department of Physics, King's College London, London; United Kingdom.

^p Also at Department of Physics, St. Petersburg State Polytechnical University, St. Petersburg; Russia.

^q Also at Department of Physics, Stanford University; United States of America.

^r Also at Department of Physics, University of Fribourg, Fribourg; Switzerland.

^s Also at Department of Physics, University of Michigan, Ann Arbor MI; United States of America.

^t Also at Dipartimento di Fisica E. Fermi, Università di Pisa, Pisa; Italy.

^u Also at Giresun University, Faculty of Engineering, Giresun; Turkey.

^v Also at Graduate School of Science, Osaka University, Osaka; Japan.

^w Also at Hellenic Open University, Patras; Greece.

^x Also at Horia Hulubei National Institute of Physics and Nuclear Engineering, Bucharest; Romania.

^y Also at II. Physikalisches Institut, Georg-August-Universität Göttingen, Göttingen; Germany.

^z Also at Institutio Catalana de Recerca i Estudis Avancats, ICREA, Barcelona; Spain.

- aa* Also at Institut für Experimentalphysik, Universität Hamburg, Hamburg; Germany.
- ab* Also at Institute for Mathematics, Astrophysics and Particle Physics, Radboud University Nijmegen/Nikhef, Nijmegen; Netherlands.
- ac* Also at Institute for Particle and Nuclear Physics, Wigner Research Centre for Physics, Budapest; Hungary.
- ad* Also at Institute of Particle Physics (IPP); Canada.
- ae* Also at Institute of Physics, Academia Sinica, Taipei; Taiwan.
- af* Also at Institute of Physics, Azerbaijan Academy of Sciences, Baku; Azerbaijan.
- ag* Also at Institute of Theoretical Physics, Ilia State University, Tbilisi; Georgia.
- ah* Also at Istanbul University, Dept. of Physics, Istanbul; Turkey.
- ai* Also at LAL, Université Paris-Sud, CNRS/IN2P3, Université Paris-Saclay, Orsay; France.
- aj* Also at Louisiana Tech University, Ruston LA; United States of America.
- ak* Also at LPNHE, Sorbonne Université, Paris Diderot Sorbonne Paris Cité, CNRS/IN2P3, Paris; France.
- al* Also at Manhattan College, New York NY; United States of America.
- am* Also at Moscow Institute of Physics and Technology State University, Dolgoprudny; Russia.
- an* Also at National Research Nuclear University MEPhI, Moscow; Russia.
- ao* Also at Near East University, Nicosia, North Cyprus, Mersin; Turkey.
- ap* Also at Physikalisches Institut, Albert-Ludwigs-Universität Freiburg, Freiburg; Germany.
- aq* Also at School of Physics, Sun Yat-sen University, Guangzhou; China.
- ar* Also at The City College of New York, New York NY; United States of America.
- as* Also at The Collaborative Innovation Center of Quantum Matter (CICQM), Beijing; China.
- at* Also at Tomsk State University, Tomsk, and Moscow Institute of Physics and Technology State University, Dolgoprudny; Russia.
- au* Also at TRIUMF, Vancouver BC; Canada.
- av* Also at Università di Napoli Parthenope, Napoli; Italy.
- * Deceased